**Joana Campainhas Bastos**

Licenciada em Biologia Humana

# Ionic Liquids in the Development of Novel Biomaterials

Dissertação para Obtenção do Grau de Mestre em

Bioquímica para a Saúde

**Orientador:** Ana Belén Pereiro, Investigadora Auxiliar do REQUIMTE, Faculdade de Ciências e Tecnologia da Universidade Nova de Lisboa

**Co-orientador:** João Miguel Mendes de Araújo, Investigador Auxiliar do REQUIMTE, Faculdade de Ciências e Tecnologia da Universidade Nova de Lisboa

**Novembro 2016**

**Joana Campainhas Bastos**

Licenciada em Biologia Humana

# Ionic Liquids in the Development of Novel Biomaterials

Dissertação para obtenção do Grau de Mestre em
Bioquímica para a Saúde

**Orientador:** Ana Belén Pereiro, Investigadora Auxiliar do REQUIMTE, Faculdade de Ciências e Tecnologia da Universidade Nova de Lisboa

**Co-orientador:** João Miguel Mendes de Araújo, Investigador Auxiliar do REQUIMTE, Faculdade de Ciências e Tecnologia da Universidade Nova de Lisboa

**Constituição do Júri:**

**Presidente:** Doutor Pedro Matias, Investigador Principal do Instituto de Tecnologia Química e Biológica António Xavier da Universidade Nova de Lisboa

**Arguente:** Doutora Karina Shimizu, Investigadora do Instituto Superior Técnico da Universidade de Lisboa

**Vogais:** Doutora Ana Estevéz, Investigadora Auxiliar do REQUIMTE, Faculdade de Ciências e Tecnologia da Universidade Nova de Lisboa

Doutora Margarida Archer, Investigadora Principal do Instituto de Tecnologia Química e Biológica António Xavier da Universidade Nova de Lisboa

**Instituto Tecnológico de Química e Biológica António Xavier da Universidade Nova de Lisboa (ITQB), Oeiras, Portugal**

**Novembro 2016**

**Ionic Liquids in the Development of Novel Biomaterials**

# COPYRIGHT

**Joana Campainhas Bastos**

**Instituto de Tecnologia Química e Biológica António Xavier**

**Universidade Nova de Lisboa**

*Aos meus pais, por me permitirem alcançar*

*todos os meus sonhos*

# Agradecimentos

Este espaço é dedicado a todos os que, de alguma forma contribuíram para que esta dissertação fosse realizada. Não pudendo nomeá-los a todos, há alguns a quem não posso deixar de manifestar o meu apreço e agradecimento sinceros.

Em primeiro lugar quero agradecer á minha orientadora, Doutora Ana Belén Pereiro e co-orientador Doutor João Miguel Mendes de Araújo, por me terem proporcionado esta oportunidade. Expresso ainda o meu profundo agradecimento pelo apoio e disponibilidade manifestada, confiança depositada e partilha de conhecimento que contribuíram decisivamente para que este trabalho tenha chegado a um bom termo.

Aos meus colegas do laboratório Fluídos Alternativos para a Química Verde por me terem acolhido e animado nos dias mais árduos de trabalho. À Sara Carvalho e à Fátima Moscoso pelo companheirismo e palavras amigas. Um agradecimento especial à Margarida Ferreira e à Nicole Vieira por poder sempre contar com o vosso entusiasmo, alegria e paciência nos meus dias menos bons durante este ano.

Gostaria de agradecer também à Professora Doutora Isabel Fonseca e Doutora Isabel Pacheco pela disponibilidade dos seus laboratórios para realização de algumas medidas esporádicas experimentais. Ainda, um especial obrigada à Doutora Manuela Dias pela ajuda imprescindível nesta última fase do meu trabalho.

Aos meus amigos, especialmente à Vera Moreira e à Inês Cabrita, ouvintes e atentos aos meus desânimos e sucessos, que mesmo longe sempre me ajudaram muito. Um muito obrigada pelo apoio e pela valorização sempre tão entusiasta do meu trabalho.

À minha família, uma palavra de reconhecimento muito especial pelo amor incondicional e pela forma como ao longo de todos estes anos, tão bem, me souberam ajudar. Aos meus pais o meu eterno obrigada por me proporcionarem esta oportunidade de progredir na vida profissional.

**Palavras-chave**

Líquidos Iónicos Fluorados; Biomateriais; Entrega de Fármacos; Caracterização Termofísica; Equilíbrio de Fases; Agregação; Coeficientes de Partição Octanol-Água; Ligações de Hidrogénio; Polaridade.

**Resumo**

Atualmente, a industria farmacêutica, uma das áreas cientificas em maior crescimento, tem mostrado interesse na utilização de líquidos iónicos (ILs) em diversas aplicações. Por exemplo, a utilização destes compostos no desenvolvimento de plataformas para entrega de fármacos tem recebido uma atenção especial por parte da comunidade científica. O desenvolvimento de LIs biocompatíveis que aumentem a solubilidade e a biodisponibilidade de princípios ativos farmacêuticos e de proteínas terapêuticas é também de extrema importância para a resolução de alguns dos problemas enfrentados pelas grandes indústrias farmacêuticas.

Os líquidos iónicos fluorados (LIFs), são uma família de ILs com cadeias alquílicas fluoradas com pelo menos 4 átomos de carbono. A presença das cadeias fluoradas aumenta a atividade surfatante e a capacidade de agregação em estruturas supramoleculares organizadas. Adicionalmente, devido às diversas conjugações possíveis entre aniões e catiões, as características destes líquidos são facilmente manipuláveis (hidrofobicidade, comportamento em solução, biodegradação e toxicidade) de acordo com a aplicação final desejada.

Por último, para avaliar a utilização de LIFs como novos biomateriais, o estudo das propriedades termofísicas, das propriedades de partição e o comportamento de fases foi realizado. Além destas propriedades, para avaliar a dissolução de moléculas terapêuticas nos FILs também foram determinados parâmetros solvatocrómicos, de modo a caracterizar as ligações de hidrogénio e a polaridade dos compostos em estudo.

Este trabalho está integrado nos projetos da FCT: PTDC/QEQ-EPR/5841/2014, PTDC/QEQ-FTT/3289/2014 e IF/00210/2014/CP1244/CT0003.

**Keywords**

Fluorinated Ionic Liquids; Biomaterials; Drug Delivery; Thermophysical Characterization; Phase Equilibria; Self-aggregation; Octanol-Water Partition Coefficient; Hydrogen-Bonding; Polarity

**Abstract**

An emerging research field of interest is the use of ionic liquids (ILs) in pharmaceutical applications. For example, their use as drug delivery vehicles has received increasing attention. Finding biocompatible ILs that can improve the solubility and bioavailability of active pharmaceutical ingredients and therapeutic proteins is of upmost relevance in finding solutions for today's societal challenges.

Fluorinated ionic liquids (FILs) are great candidates to be investigated as a type of tuneable materials with enhanced solubility for therapeutic molecules, including therapeutic proteins, due to their diverse and unique features such as hydrophobicity, solution behaviour, thermophysical properties, biodegradation or toxicity. These compounds are ionic liquids with a fluorinated alkyl chain of at least four carbon atoms which can be easily manipulated by choosing the nature and structure of their composing ions. The presence of a fluorinated alkyl chain increases their high surface activity and their strong tendency to self-aggregate into stable, well-organized supramolecular assemblies.

In order to evaluate the feasibility of using FILs as novel biomaterials, the study of their thermophysical properties, partition properties and aqueous solution behaviour were attained. In addition, the solvatochromic parameters were determined, characterizing the hydrogen-bonding and polarity of FILs, for assessing the dissolution of therapeutic molecules.

This work is an integral part of the FCT projects PTDC/QEQ-EPR/5841/2014, PTDC/QEQ-FTT/3289/2014 and IF/00210/2014/CP1244/CT0003.

# Contents

# List of Abbreviatures

| | |
|---|---|
| R&D | Research and Development |
| IL | Ionic Liquids |
| FILs | Fluorinated Ionic Liquids |
| PFC | Perfluorocarbons |
| C | Carbon |
| F | Fluor |
| C-F bonds | Carbon and Fluor Bonds |
| F-Chains | Fluorinated Chains |
| $O_2$ | Oxygen |
| $CO_2$ | Carbon Dioxide |
| CMC | Critical Micellar Concentrations |
| ACV | Acyclovir |
| ETO | Etodolac |
| pH | Potencial of Hydrogen |
| MMT | Montmorillonite |
| MAA | Methhacrylic Acid |
| PDA | Polydopamine |
| DOX | Doxorubicin |
| MWTT | Microwave Thermal Therapy |
| ECD | Electrochemical detector |
| CE | Capillary electrophoresis |
| UV-Vis | Ultraviolet visible |
| Abs | Absorbance |
| AFMC | Analyte Focusing by Micelle Collapse |
| DNA | Deoxyribonucleic Acid |
| LLE | Liquid-Liquid Equilibrium |
| CTAB | Cetyltrimethylammonium Bromide |
| f-AuNPs | Fluorinated Gold Nanoparticles |
| siRNA | Interfering Ribonucleic Acid |
| TEM | Transmission Electron Microscopy |
| NMR | Nuclear Magnetic Resonance |

| | |
|---|---|
| KF | Karl Fisher |
| TGA | Thermogravimetric Analysis |
| TA | Thermal Analysis |
| DSC | Differential Scanning Calorimeter |
| D | Demal (1 g equivalent of solute dissolved in 1dm3 solvent) |
| KCl | Potassium Chloride |
| API | Active Pharmaceutical Ingredients |
| ADME | Absorption, Distribution, Metabolism and Excretion |
| HPLC | High-Performance Liquid Chromatography |
| HBD | Hydrogen Bond Donation |
| HBA | Hydrogen Bond Acceptance |
| KT | Kamlet-Taft |
| DCM | Dicloromethane |
| RSD | Relative Standard Deviation |
| dsDNA | Double-strand DNA |
| ssDNA | Single-stranded |
| H-bonding | Hydrogen bonding |
| N-H | Nitrogen hydrogen bond |
| C-H | Carbon hydrogen bond |

# List of Symbols

| | |
|---|---|
| $[C_nC_1Im]^+$ | Imidazolium-based Ils (*n*, number of methylene groups) |
| $[C_2C_1py]^+$ | Pyridinium-based ILs |
| $[C_1CO_2]^-$ | Acetate anion |
| $[(CH_3O)_2PO_2]^-$ | Dimethylphosphate anion |
| $[C_1C_1Im][(CH_3O)_2PO_2]$ | Dimethylimidazole dimethylphosphate |
| $[C_4C_1Im][PF_6]$ | 1-Butyl-3-methylimidazolium hexafluorophosphate |
| $[C_{16}C_1Im]Br$ | 1-Hexadecyl-3-methyllimidazolium bromide |
| $[C_4C_1Im]Br$ | 1-Butyl-3-methylimidazolium bromide |
| $[C_8C_1Im][PF_6]$ | 1-Octyl-3-methylimidazolium hexafluorophosphate |
| $C^o$ | Celsius |
| $[C_8C_1Im]$ Br | 1-Octyl-3-methylimidazolium bromide |
| $[C_4C_1Im][PF_6]$ | 1-Butyl-3-methylimidazolium hexafluorophosphate |
| $[C_2C_1Im]$ $[(CH_3)_2PO_4)]$ | 1-Ethyl-3-methylimidazolium dimethylphosphate |
| $[C_{10}POHIM]$ Br | 1-(1,2-Dihydroxypropyl)-3-decylimidazolium bromide |
| $[C_{16}POHIM]$ Br | 1-(1,2-Dihydroxypropyl)-3-hexadecylimidazolium bromide |
| $[C_2C_1Im]$ Cl | 1-Ethyl-3-methylimidazolium chloride |
| $[C_2C_1Im][BF_4]$ | 1-Ethyl-3-methylimidazolium tetrafluoroborate |
| $[C_2C_1Im]$ $[NTf_2]$ | 1-Ethyl-3-methylimidazolium bis(trifluoromethylsulfonyl)imide |
| $[NTf_2]^-$ | Bis(trifluoromethylsulfonyl)imide anion |
| $[BF_4]^-$ | tetrafluoroborate anion |
| $[PF_6]^-$ | hexafluorophosphate anion |
| $Cl^-$ | Chloride anion |
| $[C_6C_1Im]$ Cl | 1-Hexyl-3-methylimidazolium chloride |
| $[C_4C_1Im][BF_4]$ | 1-Butyl-3methylimidazolium tetrafluoroborate |
| $[C_1C_2py][C_4F_9SO_3]$ | 1-Ethyl-3-methylpyridinium perfluorobutanesulfonate |
| $[C_4C_1Im][C_4F_9SO_3]$ | 1-butyl-3methylimidazolium perfluorobutanesulfonate |
| $[C_{10}C_1Im][C_4F_9SO_3]$ | 1-decyl-3-methylimidazolium perfluorobutanesulfonate |
| $[C_4F_9SO_3]^-$ | Perfluorobutanesulfonate anion |
| $[C_8F_{17}SO_3]^-$ | Perfluorooctanesulfonate anion |

| | |
|---|---|
| $[N_{4444}]^+$ | Tetrabutylammonium based-ILs |
| K | Kelvin |
| ppm | Parts per million |
| $T_{onset}$ | onset temperature |
| $T_{start}$ | starting temperature |
| $T_{dec}$ | decomposition temperature |
| $T_m$ | Melting temperature |
| $[C_2C_1Im][C_4F_9SO_3]$ | 1-ethyl-3-methylimidazolium perfluorobutanesulfonate |
| $[C_8C_1Im][C_4F_9SO_3]$ | 1-butyl-3-methylimidazolium perfluorobutanesulfonate |
| $[C_6C_1Im][C_4F_9SO_3]$ | 1-hexyl-3-methylimidazolium perfluorobutanesulfonate |
| $[C_{12}C_1Im][C_4F_9SO_3]$ | 1-dodecyl-3-methylimidazolium perfluorobutanesulfonate |
| $\rho$ | Density |
| $\eta$ | Viscosity |
| $\phi$ | Fluidity |
| $n_D$ | Refractive Index |
| $k$ | Ionic Conductivity |
| $T$ | Temperature |
| $\alpha_e$ | Electronic polarizability |
| $R_m$ | Molar polarizability |
| $N_A$ | Avogadro's number |
| $\varepsilon_0$ | Vacuum permittivity |
| $V_m$ | Molar free volume |
| $M_w$ | Molecular weight |
| $a_r$ | Spherical molecular radius |
| $f_m$ | Free volume |
| $\Lambda$ | Molar conductivity |
| $C$ | Constant |
| $w^1_{water}$ | Water mass fraction on FIL rich-phase |
| $w^1_{FIL}$ | FIL mass fraction on FIL rich-phase |
| $w^2_{\mathrm{water}}$ | Water mass fraction on water rich-phase |

| | |
|---|---|
| $w_{\mathrm{FIL}}^{2}$ | FIL mass fraction on water rich-phase |
| $\alpha_{\mathrm{CMC}}$ | Degree of ionization of the aggregates |
| $\beta_{\mathrm{CMC}}$ | Degree of counterion binding or counterions condensed on the micellar interface |
| $\Delta G^{0}_{\mathrm{agg}}$ | Standard free energy of the aggregation process |
| RT | Universal gas constant and absolute temperature |
| $ln\, x_{CMC}$ | Neperian logarithm for critical micellar concentration expressed in mole fraction |
| $\pi$ | Pi |
| $\lambda_{max}$ | Maximum absorption wavelength |
| $\alpha$ | Hydrogen bond acidity / hydrogen bond donation |
| $\beta$ | Hydrogen bond basicity / hydrogen bond acceptance |
| $\pi^{*}$ | Dipolarity/polarizability |
| $\nu$ | Maximum absorption wavelength for the solvatochromic dyes |
| $E_T^{30}$, | Polarity scale based only on Reichardt's dye |
| *w*t% | Weight percentage |
| $[C_2C_1Im][CF_3SO_3]$ | 1-Ethyl-3-methylimidazolium trifluoromethanesulfonate |
| $[C_4C_1Im][CF_3SO_3]$ | 1-Butyl-3-methylimidazolium trifluoromethanesulfonate |
| $[C_2C_1py][C_4F_9SO_3]$ | 1-Ethyl-3-methylpyridinium perfluorobutanesulfonate |
| $[C_2C_1Im][C_4F_9SO_3]$ | 1-Ethyl-3-methylimidazolium perfluorobutanesulfonate |
| $[C_6C_1Im][C_4F_9SO_3]$ | 1-Hexyl-3-methylimidazolium perfluorobutanesulfonate |
| $[C_8C_1Im][C_4F_9SO_3]$ | 1-Octyl-3-methylimidazolium perfluorobutanesulfonate |
| $[N_{1112OH}][C_4F_9SO_3]$ | Choline perfluorobutanesulfonate |
| $[N_{4444}][C_4F_9SO_3]$ | Tetrabutylammonium perfluorobutanesulfonate |
| $[N_{4444}][C_8F_{17}SO_3]$ | Tetrabutylammonium perfluoroctanesulfonate |
| $[C_2C_1Im][C_1CO_2]$ | 1-Ethyl-3-methylimidazolium acetate |
| $[C_2C_1py]$ Br | 1-Ethyl-3-methylpyridinium bromide |
| $[C_2C_1Im]$ Cl | 1-Ethyl-3-methylimidazolium chloride |
| $[N_{1112OH}]$ Cl | Choline chloride |
| $[N_{1112OH}]^{+}$ | Choline-based ILs |

# List of Figures

## 1.Introduction



## 2. Characterization of Fluorinated Ionic Liquids: Thermophysical, Phase Equilibria and Aggregation Behaviour

## 3. Partition Properties of Fluorinated Ionic Liquids

## 4. Kamlet-Taft Solvatochromic Parameters of Fluorinated Ionic Liquids

# List of Tables

## 2. Characterization of Fluorinated Ionic Liquids: Thermophysical, Phase Equilibria and Aggregation Behaviour



## 3. Partition Properties of Fluorinated Ionic Liquids



## 4. Kamlet-Taft Solvatochromic Parameters of Fluorinated Ionic Liquids



.

# 1. Introduction

## 1.1 General context

The pharmaceutical industry is facing a growing pressure due to environmental issues, patent expirations, lengthening of drug-development cycles and more demanding regulatory requirements (1). Thus, pharmaceutical R&D is more than ever focusing on a few new molecular compounds to enhance clinical efficacy at low cost (2). The possibility of producing innovative medicinal materials "by design" brought an increasing number of compounds possessing low aqueous solubility and limited bioavailability (1). To overcome these restraints pharmaceutical industries are pursuing new strategies, such as, development of prodrugs (3), emulsions using surfactant components (4), micellar systems (5,6), solid dispersions (7) and crystal engineering (8).

Ionic liquids (ILs) have emerged as a new class of materials that have considerable potential to provide advances in pharmaceutical applications (9–11). Their negligible vapor pressure at ambient conditions, low surface tension, high thermal, chemical and electrochemical stability, and widely tunable properties such as viscosity, density, polarity, hydrophobicity and solvent miscibility are some interesting properties of these compounds (8). These remarkable characteristics are a result of the innumerous possible combinations between ILs constitutive ions (10). Due to their surfactant behaviour, ILs can form micelles which can be used as drug-delivery devices for sparingly water-soluble drugs (12). In the past decades, attempts to use ILs to enhance bioavailability of drug molecules have been made (5,11,13,14).

Fluorinated anions such as bis(trifluoromethylsulfonyl)imide, hexafluorophosphate, or tetrafluoroborate have been frequently characterized and explored for several biomedical applications (15). However, few works have focused on the fluorinated ionic liquids (FILs) here characterized, with a anionic fluorinated alkyl chain of at least four carbons (16). One of the major interest in FILs is that they combine the best properties of perfluorocarbon compounds (PFCs) with those ones of ionic liquids (15). Then, FILs can be useful in areas were PFCs are applied such as for oxygen therapeutics to enhance oxygen transport, pulmonary drug delivery devices with dispersions of drug microparticles and microemulsions, gel microemulsions for dermal drug delivery, and also fluorinated microcontainers for general drug delivery (17,18).

The main focus of this work is the development of fluorinated ionic liquids for biomedical applications in order to resolve some of the abovementioned drawbacks of the pharmaceutical industry. To design the most suitable FILs as novel and improved materials for pharmaceutical applications, such as drug delivery systems, the thermophysical and partition properties, solution and self-aggregation behaviour were evaluated. Furthermore, the hydrogen-bonding ability and polarizability were also studied to address the relevance of designing functionalized (so-called task-specific) ILs that have been synthesized with a particular application in mind, e.g. dissolution of therapeutic molecules.

## 1.2 Ionic Liquids

Ionic liquids are salts, entirely constituted of ions where cations are organic while anions can be organic or inorganic (8). The most common families of cations and anions used for biomedical applications are shown in **Figure 1.1.** and **Figure 1.2.**, respectively (19,20).

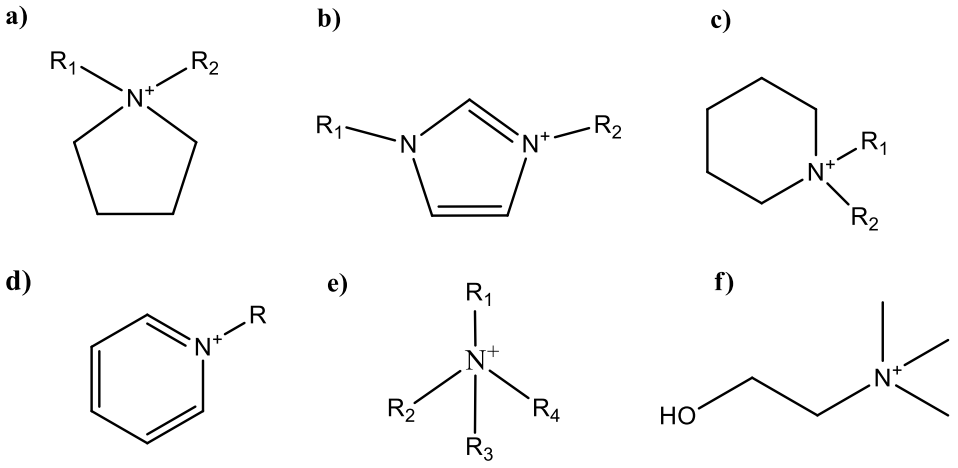


**Figure 1.1.** Most common cations structures of ILs: **a)** pyrrolidinium; **b)** imidazolium; **c)** piperidinium; **d)** pyridinium; **e)** ammonium and **f)** choline where R could be a hydrogenated chain, a fluorinated chain or a functional group.

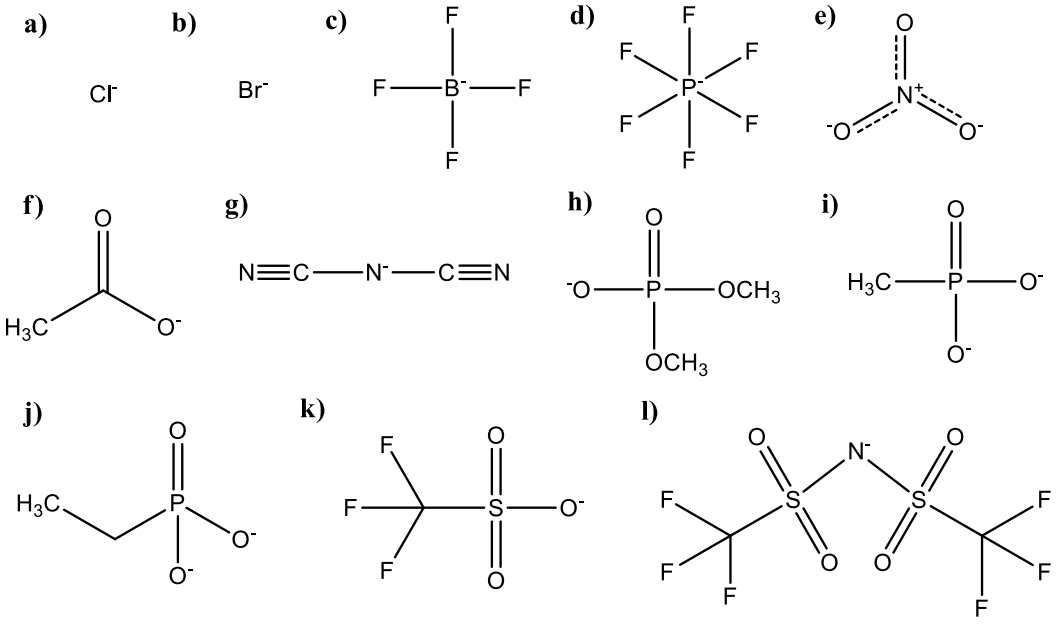


**Figure 1.2.** Most common anion structures of ILs: **a)** chloride; **b)** bromide; **c)** tetrafluoroborate; **d)** hexafluorophosphate; **e)** nitrate; **f)** acetate; **g)** dicyanamide; **h)** dimethylphosphonate **i)** methylphosphonate **j)** ethylphosphonate; **k)** trifluoromethanesulfonate and **l)** bis(trifluoromethylsulfonyl)imide.

The possibility to manage the final characteristics through the diverse combination of cations and anions make this compounds suitable for numerous applications (21). Nowadays, ILs are used as reaction media for organic transformations, separations and extractions (10) in nanotechnology, biotechnology (20) and engineering processes (22). In the biomedical field, ILs have proven to be useful as solvents to enhance solubility of poor water soluble drugs, and thus to be used as drug delivery device (8,23,24). In **Figure 1.3.** are represented some of the relevant applications where ILs have been extensively studied.

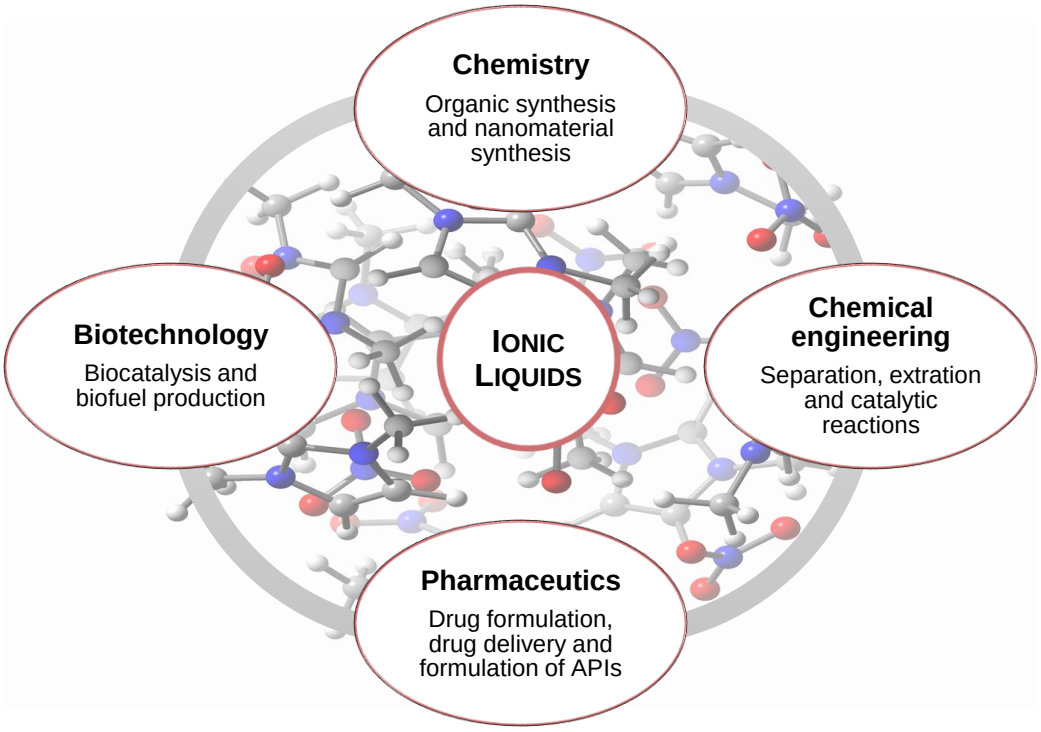


**Figure 1.3.** Relevant applications of ionic liquids as biomaterials in chemistry, chemical engineering, biotechnology and pharmaceutics industries.

## 1.2.1 Fluorinated Ionic Liquids

Fluorinated ionic liquids are defined as ionic liquids with fluorine tags equal or longer than four carbon atoms (15). The interest in these compounds is that they can combine the best properties of ILs with those ones of perfluorocarbons compounds, such as, exceptional chemical and biological inertness, low surface tension and refractive index, extreme surface activity, high density and excellent spreading characteristics (17,25).

Introducing fluorine atoms to the IL's composition can generate novel behaviour and an unmatched performance in several processes involving biomolecules (16,26–28). The high ionization potential, high electronegativity and low polarizability are some of the attributes that pointed out the element fluorine (29). The thermal and chemical stability of F-chains are due to the strength of the C-F bonds, the strongest single bond in organic chemistry (30). Additionally, resistance of F-chains to metabolism could be useful in enzymatic materials (27).

One of the most remarkable characteristics of FILs is their amphiphilic behaviour which enhance their self-aggregation (31). Due to the fluorinated components there is a more organized space (at molecular, nanometer and micrometer scales) increasing the hydrophobic segregation effect and making them suitable surfactants (32). Previous works shown that the critical micellar concentration (CMC) values of short chain fluorinated surfactants are analogous to those of hydrogenated surfactants with longer chain lengths as will be further discussed (31).

Although fluorinated compounds have been extensively investigated (18), no significant studies using FILs for biomedical applications have been carried out. Moreover, a comprehensive investigation of FILs properties is needed to evaluate the application of these remarkable ILs.

## 1.2.2. Applications of Ionic Liquids as Biomaterials

One of the most challenging problems faced by the pharmaceutical industry is the limited aqueous solubility present in 20-30% of the pharmaceutical compounds which entails a very poor bioavailability (33). Therefore, to increase drugs solubility several approaches have been described such as the use of liquid and gel microemulsions , salt formation and coating systems (8). Ionic liquids were found to play a special role in the pharmaceutical industry (10). As tunable chemicals they are ideal candidates for incorporating various functional groups, including biologically active substances (8,15).

An important series of ionic liquids based on the 1-alkyl-3-methylimidazole $[C_nC_1Im]^+$ cation, where *n* is the carbon number in the alkyl group, were extensively investigated (34). These imidazolium-based ILs can have amphiphilic behaviour depending on the alkyl side chain, such as cationic surfactants (34). Due to their hydrophobic chains and polar imidazolium groups they have been called “surfactant-like” ionic liquids (35). In the past decades, imidazolium-based ILs were explored for several pharmaceutical and industrial applications as illustrated in **Figure 1.4.**.

The first work that uses IL-based microemulsions as drug delivery devices was reported in 2010 by Moniruzzanan *et al*. (36). In this study, the solubility of acyclovir (ACV), a poor water and organic soluble antiviral, was tested in $[C_1\text{-}_4C_1Im]^+$ imidazolium-based ILs combined with several anions. It was observed that ACV was only soluble on IL with acetate ($[C_1CO_2]^-$) and dimethylphosphate ($[(CH_3O)_2PO_2]$) anions. Despite the enhanced solubility, further tests to represent transport of ACV through skin were performed and no significant results were found. Therefore, dimethylimidazole dimethylphosphate ($[C_1C_1Im][(CH_3O)_2PO_2]$) was tested as a co-solvent for AVC microemulsion together with Tween-80 and Span-20 commercial surfactants. The results show that the skin permeability was increased by several orders of magnitude compared to results obtained for the cream currently available on market (37). Since then, ionic liquids have been studied as additives in several formulations as well as enhancers of drug solubility.

Goindi *et al*. used 1-butyl-3-methylimidazolium hexafluorophosphate ([$C_4C_1$Im][$PF_6$]) together with Tween 80 and ethanol to create a type gel microemulsion for a topical delivery of etodolac (ETO) (38). ETO[1] demonstrate poor oral bioavailability in which gastrointestinal and cardiovascular side effects are noticed (39). To overcome these side effects and obtain high drug concentration at the target site, topical application of drug seems to be an ideal route of administration (38). Thus, the authors compared the results obtained from the gel-type microemulsion with the available commercial formulation (Proxym gel®) (38). The results showed a drop in granuloma tissue weight in mice up to 20 %*wt* with the IL-formulations. In addition, a decrease in the number of leukocytes on the affected area where observed (7800 for IL formulations and 8333.33 for Proxym gel®) demonstrating the anti-inflammatory effect (38). The authors justified the results on the basis of an enhanced permeation of ETO through the IL (38). In addition, Wang *et al*. reported that 1-hexadecyl-3-methyllimidazolium bromide ([$C_{16}C_1$Im] Br) presented more suitable results for preparing drug-loading nanoparticle microemulsions in comparison with conventional surfactants molecules (40). In this paper, nanoparticles were loaded with methylene blue (drug model) and the IL enhanced encapsulation and microemulsion stabilization up to 2h. Moreover, a drug release profile was conducted and methylene blue showed a release process almost up to 8 hours with an 99.9% efficiency (40).

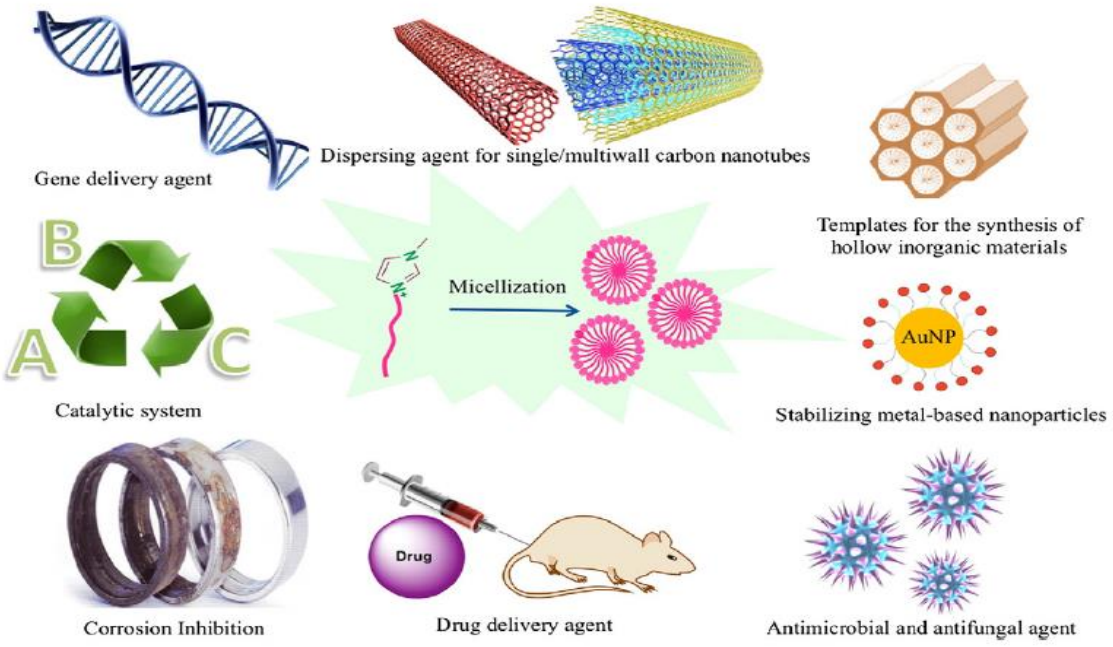


**Figure 1.4.** Application areas of imidazolium-based surfactants. Adapted from literature (35).

Taking into account the use of ILs as nanocarriers for drug delivery devices, Mahkam *et al*. prepared a novel pH-sensitive nanocarrier for colon specific drug delivery[2] (41). An imidazolium chloride based

[1] Etodolac (ETO) is a poorly water soluble nonsteroidal anti-inflammatory (NSAID) used to relieve inflammation, swelling, stiffness, and pain associated with rheumatoid arthritis and osteoarthritis (39)
[2] Colon-specific drug delivery system is a sort of pH sensitive system that protects the drugs from degradation in the acidic medium of stomach and after passing the acidic medium, they release containing drugs at the alkaline media of colon (pH 7.4) (41)

IL was placed between montmorillonite (MMT) layers and copolymerized with methacrylic acid (MAA) to encapsulate naproxen (used to treat pain or inflammation). The incorporation of positive charges into the framework of the nanocomposites ($IL^+$+MMT+MAA) promoted a controlled drug realise by changes of the pH media. By increasing the pH value (pH 7.4), diffusion of the hydrolysing agents into the carrier is increased, therefore the rate of hydrolysis increased (41).

Tang and co-workers have reported for the first time an amazing use of ILs as microwave sensitization agent (42). By loading polydopamine (PDA) nanoparticles with 1-butyl-3-methylimidazolium hexafluorophosphate ($[C_4C_1Im]$ $[PF_6]$) it was possible to enhance encapsulation of doxorubicin (DOX). Since $[C_4C_1Im][PF_6]$ is considered highly susceptible to microwave irradiation, a combined chemotherapy and microwave thermal therapy (MWTT) was proposed to improve the delivery effect of the drug to tumour sites. The results showed that IL-PDA-DOX nanoparticles can ablate DOX under microwave radiation inhibiting efficiently the tumour size without inducing any appreciable tissue toxicity (42). In **Figure 1.5** is illustrated the effect of IL-PDA-DOX nanoparticles.

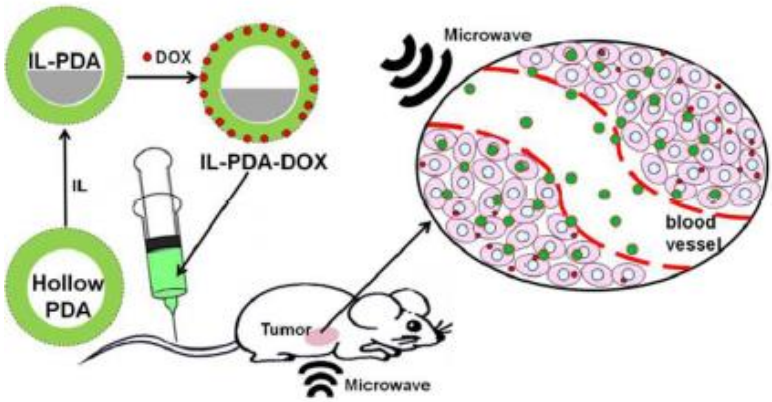


**Figure 1.5.** Schematic illustration of the use of IL-PDA-DOX nanoparticles for combined chemotherapy with MWTT. Adapted from literature (42).

Ionic liquids are powerful solvents and electrically conducting fluids (10). They can be used as biomaterials to enhance detection of biomolecules through electrophoretic techniques as described by Abd El-Hady *et al*. (43). In this work, an electrochemical detector (ECD) based on 1-octyl-3-methylimidazolium hexafluorophosphate ($[C_8C_1Im][PF_6]$) was developed to improve detection of vitamins B2, B6 and C. This device, coupled with capillary electrophoresis (CE) based on micelle collapse[3] (see **Figure 1.6**), enhanced the micellar encapsulation of vitamins and prevented vitamin degradation on the electrophoresis buffer/solution media. Thus, the sensitivity of the method was substantially improved up to 5000-fold compared to conventional CE coupled with UV-visible techniques (43).

[3] Analyte focusing technique achieved by micelle collapse. The CE/AFMC method is based on the presence of a sample zone contained the micelles-forming agent with higher conductivity at the beginning of the run. Due to concentration difference a micelle dilution zone is formed. Subsequently, micelles were collapsed and the analyte is accumulated (43).

In addition, Abd El-Hady and co-workers also tested the use of ILs to stabilize vitamins in biological samples in which 1-octyl-3-methylimidazolium bromide ($[C_8C_1Im]$ Br) showed the best result. The samples were viable up to 5 days under lab storage conditions (25ºC, light and air oxygen) without the need for lengthy and extensive pretreatment (43).

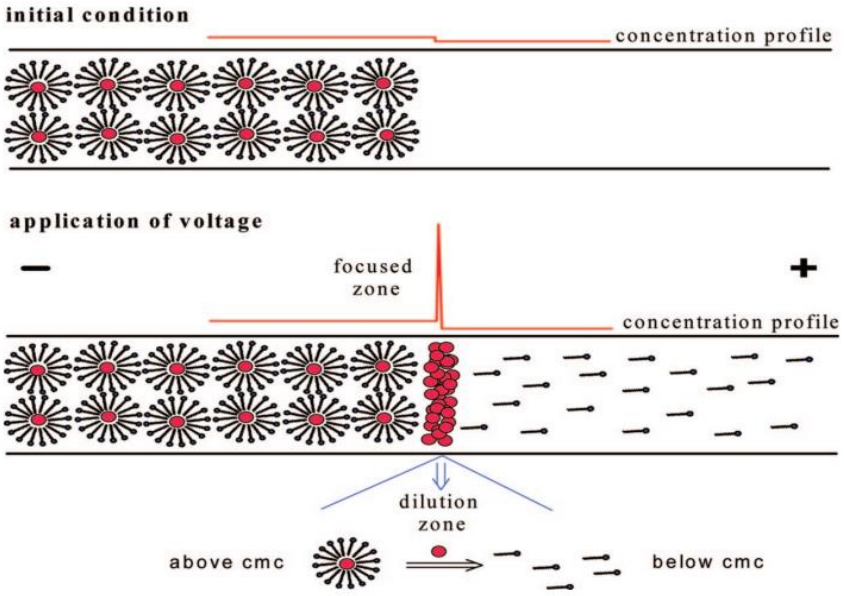


**Figure 1.6.** Transport, release, and accumulation of analytes by micelle collapse. Adapted from literature (44).

The technological utility of biomolecules can also be significantly enhanced by using ILs rather than other organic solvents or aqueous reaction media due to the IL's unique solvent characteristics (10). In **Figure 1.7.** are represented some of the advantages of using ILs for biomolecular processes in contrast with other organic solvents.

| ADVANTAGES OF USING ILS FOR BIOMOLECULAR PROCESSES |
|---|
| ♦ Opportunity to design particular bioprocesses due to tailor-made and inimitable physical, chemical and biological properties of ILs. |
| ♦ In several cases, biomolecules have become more soluble and stable (both operationally and thermally) in presence of ILs. |
| ♦ Easy recoveries of subtract, products and ILs after biocatalysts and biotransformation |
| ♦ Prevent self-aggregation of biomolecules during solubilisation process |
| ♦ Enhance solubility into insoluble/sparingly soluble subtracts in ILs promoting biomolecular reactions |
| ♦ Enhance immobilization of biomolecules in highly viscous ILs for biochemical processes |

**Figure 1.7.** Advantages of using ILs for biomolecular processes (20).

For instance, DNA can be extracted from biological samples using the phenol/chloroform method where the proteins are dissolved in the organic medium (phenol/chloroform) while DNA remains in the aqueous solution (45). However, this type of processes can involve toxic organic compounds and have several time-consuming steps (45). Recently, a number of studies reported the use of ILs for separation and extraction of nuclei acids, especially DNA (46,47). A previous study employed the 1-butyl-3-methylimidazolium hexafluorophosphate ($[C_4C_1Im][PF_6]$) IL for direct extraction of DNA from aqueous solution using the liquid-liquid extraction technique (LLE) (48). The interactions between the imidazolium cation alkyl chain and the phosphate groups of the DNA were deemed responsible for the DNA/IL binding and the efficient extraction and purification (48). García *et al*. also tested several ILs to produce a fast and efficient strategy for the extraction of DNA directly from maize (49). The results suggested that 1-ethyl-3-methylimidazolium dimethylphosphate ($[C_2C_1Im]$ $[(CH_3)_2PO_4]$) was the most efficient extraction system with a yield ranging from 696.7-721.2 μg DNA / g sample (49). These results improve the common available method based on the surfactant cetyltrimethylammonium bromide (CTAB) with a yield between 252.3 and 256.2 μg DNA / g sample. Moreover, this technique demonstrated timesavings of approximately 3h and the DNA extracted was stable when stored at room temperature for 10 days (49). The hydrogen bonding interactions between ILs and DNA were considered an important parameter when ILs are used as solvent in extraction process (49,50).

Additionally, Li *et al*. studied two specifically designed ILs, namely 1-(1,2-dihydroxypropyl)-3-decylimidazolium bromide ($[C_{10}POHIM]$ Br) and 1-(1,2-dihydroxypropyl)-3-hexadecylimidazolium bromide ($[C_{16}POHIM]$ Br) which contain two hydroxyl groups capable of forming hydrogen bonds (45). Considering the extraction efficiency, $[C_{10}POHIM]$ Br and $[C_{16}POHIM]$ Br show the most suitable yields (52.4% and 95.2%, respectively) when compared with other ILs containing similar structures but lacking hydroxyl functional groups (45). Thus, the importance of the alkyl chain of the IL for DNA biding was also proved in this work (45).

For successfully design of IL it is crucial to meet the requirements of the particular task. For instance, in IL-based extraction processes, the number of carbons present in the alkyl chain is taken into consideration since it influences the ability to form biphasic systems (51).

The activity and stability of enzymes, such as lipases, proteases, alcohol dehydrogenases and oxidoreductases, have been evaluated using ILs as media (20). The polarity, cation/anion nature, alkyl chain length, hydrophobicity and viscosity are some of the main factors that can affect the enzyme performance (52). Regarding the anion, they can have a profound effect on the stability and activity of enzymes due to their high hydrogen bond forming capabilities which strongly interact with proteins and can cause conformational changes (20). Noritomi *et al*. compared the effect of various anions on the activity of lysozyme and found that it had lower activity in $[C_2C_1Im]$ Cl rather than $[C_2C_1Im][BF_4]$ and $[C_2C_1Im]$ $[NTf_2]$ (53). In this case, it was suggested that fluorinated anions can promote stability of this

enzyme (53). In fact, some works have reported that enzymes are most active in a presence of a hydrophobic anion, such as $[BF_4]^-$ and $[PF_6]^-$. On the other hand, the most deactivating enzymatic reactions are found when are used ILs containing anions capable of breaking hydrogen bonds, such as $Cl^-$ (20). Machado and Saraiva investigated the effect of the cation chain length of alkyl-imidazolium based ILs (ethyl-, butyl-, and hexyl-imidazolium based ILs) on the enzyme activity of horseradish peroxidase(54) and found that 1-hexyl-3-methylimidazolium chloride ($[C_6C_1Im]$ Cl) lowered the peroxidase enzyme activity.

Correlating the enzyme stability and nanocarriers, Soni *et al*. reported the inherent antitumor efficiency of self-assembled phytase enzyme nanospheres (55). This efficiency can be enhanced with the use of platinum nanoparticles loaded with the anticancer drug curcumin. In this study, the 1-butyl-3-methylimidazolium tetrafluoroborate IL ($[C_4C_1Im][BF_4]$) was used to form therapeutically active phytase nanospheres (55). **Figure 1.8.** illustrates the self-assembled phytase nanospheres promoted by the IL.

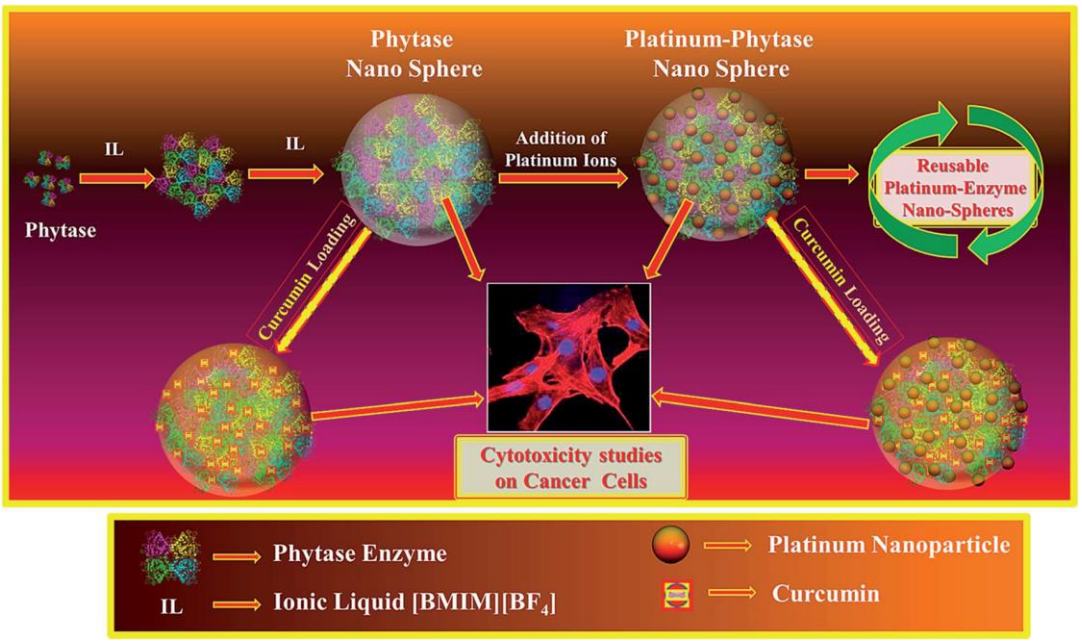


**Figure 1.8.** Schematic illustration for self-assembly of phytase enzyme (*Aspergillus niger phytase*) in $[C_4C_1Im][BF_4]$, leading to phytase nanospheres and platinum–phytase nanosphere. Curcumin was loaded on both samples and was entrapped in inner hydrophobic domains of protein template. Adapted from literature (55).

Although the number of publications regarding ILs has grown exponentially, there are still numerous unexplored applications for FILs family. Fluorocarbons or fluorinated amphiphiles have been widely studied for their application in oxygen therapeutics, pulmonary drug delivery systems, gel emulsions and micelle type containers for drug delivery devices (17,18). Recently, it was patented (56) the use of fluoropolymer-based emulsions for the intravenous delivery of fluorinated volatile anaesthetics. This type of emulsion enhanced the capability of delivering and releasing controlled amounts of fluorinated

volatile anaesthetic compounds inducing and maintaining anaesthesia. This work supports the improvement of gas solubility when fluorinated compounds are used. Other works have evaluated the use of FILs for gas separation processes. The separation performances of perfluorocarbons and carbon dioxide gases were examined and the results showed that 1-ethyl-3-methylpyridinium perfluorobutanesulfonate ($[C_1C_2py][C_4F_9SO_3]$) was the best candidate (57).

Kurczy *et al*. developed fluorinated gold nanoparticles (f-AuNPs) as agents for nanostructure imaging mass spectrometry (58). The fluorinated nanostructures used for laser desorption/ionization have generated low background interference yielding a minimal ultraviolet absorbance and fragmentation. Furthermore, this technique allowed the adsorption of metabolites from the surface of f-AuNPs resulting in high detection sensitivity. This multimodal imaging approach can be particularly useful for performing mass spectrometry-based metabolite imaging, where correlating metabolite concentrations with anatomical structures is key to data interpretation (58). Additionally, Johnson and co-workers have developed a technique for delivering interfering ribonucleic acid (siRNA) based on fluorocarbon chains compounds (59). They showed that fluorinated vectors could display strong self-assembly while providing resistance to nonspecific interactions in biological media in comparison with hydrocarbon chain vectors. This could lead to the development of new vectors with improved gene delivery efficiency and enhanced tissue specificity induced by any desired targeting moiety (59).

Concerning these recent results of the scientific community regarding ILs, the beneficial use of these compounds is clear. Then, FILs based on the imidazolium cation could be useful to drug delivery systems, for oxygen therapeutics (solubility and transport of respiratory gases), solubility enhancement of poorly soluble pharmaceutical compounds and biomolecules, among others. With this aim in mind, in **Chapter 2** the thermophysical and thermochemical characterization of two new FILs, 1-butyl-3-methylimidazolium perfluorobutanesulfonate ($[C_4C_1Im][C_4F_9SO_3]$) and 1-decyl-3-methylimidazolium perfluorobutanesulfonate ($[C_{10}C_1Im][C_4F_9SO_3]$), were investigated, namely melting and decomposition temperatures, density, dynamic viscosity, refractive index and ionic conductivity. Moreover, other parameters ionicity will be also evaluated. The aggregation behaviour of $[C_4C_1Im][C_4F_9SO_3]$ $[C_{10}C_1Im][C_4F_9SO_3]$ was studied through calculations of their critical micellar concentrations (CMC). The aggregation structures were characterized using transmission electron microscopy (TEM). In addition, the liquid-liquid equilibria (LLE) of the binary mixtures of FILs with water allowed the determination of the solubility of these FILs in aqueous solution. Additionally, lipophilicity/ hydrophobicity of several FILs was tested in **Chapter 3**. The influence of the fluorinated alkyl chain on the anion was studied using perfluorobutanesulfonate ($[C_4F_9SO_3]^-$) and perfluoroctanesulfonate ($[C_8F_{17}SO_3]^-$) anions. Moreover, the effect of cation was also analyzed using imidazolium and pyridinium cations. The size of the hydrogenated alkyl chain on imidazolium-based FILs was studied for the same $[C_nC_1Im][C_4F_9SO_3]$ family, with $n$ = 2, 4, 6 and 8. Finally, in **Chapter 4**, the hydrogen-

bonding capacity and polarizability of several FILs and conventional ILs (for neat and aqueous solutions) were studied in order to address the relevance of designing functionalized (so-called task-specific) ILs that have been synthesized with a particular application in mind, e.g. dissolution of therapeutic molecules.

## 1.3. References

**(1)** Kanaujia, P.; Poovizhi, P.; Ng W. K.; Tan, R. B. H. Amorphous Formulations for Dissolution and Bioavailability Enhancement of Poorly Soluble APIs. *Powder Technol.* **2015**, 285, 2–15.

**(2)** DiMasi, J. A.; Grabowski, H. G.; Hansen, R. W. Innovation in the Pharmaceutical Industry: New Estimates of R&D Costs. *J. Health. Econ.* **2016**, 47, 20–33.

**(3)** Huttunen, K. M.; Raunio, H.; Rautio, J. Prodrugs – From Serendipity to Rational Design. *J. Pharmacol. Rev.* **2011**, 63, 750–71.

**(4)** Gupta, A.; Eral, H. B.; Hatton, T. A.; Doyle, P. S. Nanoemulsions: Formation, Properties and Applications. *Soft Matter*. **2016**, 12, 2826–2841.

**(5)** Casal-Dujat, L.; Griffiths, P. C.; Rodríguez-Abreu, C.; Solans, C.; Rogers, S.; Pérez-García, L. Nanocarriers from Dicationic bis-Imidazolium Amphiphiles and their Interaction with Anionic Drugs. *J. Mater. Chem. B.* **2013**, 1, 4963-4971.

**(6)** Sanan, R.; Kaur, R.; Mahajan, R. K. Micellar Transitions in Catanionic Ionic liquid - Ibuprofen Aqueous Mixtures: Effects of Composition and Dilution. *RSC Adv.* **2014**, 4, 64877–64889.

**(7)** Vasconcelos, T.; Sarmento, B.; Costa, P. Solid Dispersions as Strategy to Improve Oral Bioavailability of Poor Water Soluble Drugs. *Drug Discov. Today*. **2007**, 12, 1068–1075.

**(8)** Marrucho, I. M.; Branco, L.C.; Rebelo, L. P. N. Ionic Liquids in Pharmaceutical Applications. *Annu. Rev. Chem. Biomol. Eng.* **2014**, 5, 527–46.

**(9)** Hough, W. L. et al. The Third Evolution of Ionic Liquids: Active Pharmaceutical Ingredients. *New. J. Chem.* **2007**, 31, 1429–1436.

**(10)** Moniruzzaman, M; Goto, M. Ionic liquids: Future Solvents and Reagents for Pharmaceuticals. *J. Chem. Eng. Japan*. **2011**, 44, 370–381.

**(11)** Araki, S.; Wakabayashi, R.; Moniruzzaman, M.; Kamiya, N.; Goto, M. Ionic Liquid-mediated Transcutaneous Protein Delivery with Solid-in-Oil nanodispersions. *Med. Chem. Commun*. 2015, 6, 2124–2128.

**(12)** Luís, A. *et al*. Influence of Nanosegregation on the Surface Tension of Fluorinated Ionic Liquids. *Langmuir* **2016**, 32, 6130−6139.

**(13)** Moniruzzaman, M.; Kamiya, N.; Goto, M. Ionic Liquid based Microemulsion with Pharmaceutically Accepted Components: Formulation and Potential Applications. *J. Colloid. Interface Sci.* **2010**, 352, 136–142.

**(14)** Williams, H. D.; Sahbaz, Y.; Ford, L.; Nguyen, T.; Scammells, P. J.; Porter, C. Ionic Liquids Provide Unique Opportunities for Oral Drug Delivery: Structure Optimization and *In vivo* Evidence of Utility. *J. H. Chem. Commun.* **2014**, 50, 1688–1690.

**(15)** Pereiro, A. B et al. Fluorinated Ionic Liquids: Properties and Applications. ACS *Sustain. Chem. Eng*. **2013**; 1, 427–439.

**(16)** Vieira, N. S. M. et al. Fluorination Effects on the Thermodynamic, Thermophysical and Surface Properties of Ionic Liquids. *J. Chem. Thermodyn.* 2016, 97, 354–361.

**(17)** Krafft, M. P. Fluorocarbons and Fluorinated Amphiphiles in Drug Delivery and Biomedical Research. *Adv. Drug Deliv. Rev.* **2001**, 47, 209–228.

**(18)** Krafft, M. P.; Riess, J. G.; Perfluorocarbons: Life Sciences and Biomedical Uses. *J. Polym. Sci. Part B: Polym. Phys.* **2007**, 45, 1185–1198.

**(19)** Plechkova, N. V.; Seddon, K. R. Applications of Ionic Liquids in the Chemical Industry. *Chem. Soc. Rev.* **2008**, 37, 123–150.

**(20)** Sivapragasam, M.; Moniruzzaman, M.; Goto, M. Recent Advances in Exploiting Ionic Liquids for Biomolecules: Solubility, Stability and Applications. *Biotechnol. J.* **2016**, 1–14.

**(21)** Petkovic, M.; Seddon, K. R.; Rebelo, L. P. N.; Pereira, C. S. Ionic Liquids: a Pathway to Environmental Acceptability. *Chem. Soc. Rev.* **2011**, 40, 1383–1403.

**(22)** Troter, D. Z.;, Todorović, Z.B; Đokić-Stojanović, D. R.; Stamenković, O. S.; Veljković, V.B.; Application of Ionic Liquids and Deep Eutectic Solvents in Biodiesel Production: A review. *Renew. Sustain. Energy. Rev.* **2016**, 61, 473–500.

**(23)** Dobler, D.; Schmidts, T.; Klingenhöfer, I.; Runkel, F. Ionic Liquids as Ingredients in Topical Drug Delivery Systems. *Int. J. Pharm.* **2013**, 441, 620–7.

**(24)** Domingos, S.; André, V.; Quaresma, S.; Martins, I. C. B.; Minas Da Piedade, M. F.; Duarte, M. T. New Forms of Old Drugs: Improving Without Changing. *J. Pharm. Pharmacol.* **2015**, 67, 830–846.

**(25)** Riess, J. G. Highly Fluorinated Amphiphilic Molecules and Self-assemblies With Biomedical Potential. *Curr. Opin. Colloid Interface Sci.* **2009**, 14, 294–304.

**(26)** Ferreira, A. M. C.; Esteves, P., Boal-Palheiros, I.; Pereiro, A. B.; Rebelo, L. P. N.; Freire, M. G. Enhanced Tunability Afforded by Aqueous Biphasic Systems Formed by Fluorinated Ionic Liquids and Carbohydrates. *Green. Chem.* 2015;1070–1079.

**(27)** Jeschke, P. The Unique Role of Fluorine in the Design of Active Ingredients for Modern Crop Protection. *Chem. Bio. Chem.* **2004**, 5, 570–589.

**(28)** Heller W. T.; O'Neill, H. M.; Zhang, Q.; Baker, G. A. Characterization of the Influence of the Ionic Liquid 1-Butyl-3-methylimidazolium Chloride on the Structure and Thermal Stability of Green Fluorescent Protein. *J. Phys. Chem. B.* **2010**, 114, 13866–13871.

**(29)** Krafft, M. P. Highly Fluorinated Compounds Induce Phase Separation in, and Nanostructuration of Liquid Media. Possible Impact on, and Use in Chemical Reactivity Control. *J. Polym. Sci. Part A: Polym. Chem.* **2006**, 44, 4251–42518.

**(30)** Pereiro, A. B. et al. On the Formation of a Third, Nanostructured Domain in Ionic Liquids. *J. Phys. Chem. B.* **2013**, 117, 10826–1033.

**(31)** Pereiro A. B.; Araújo, J. M. M.; Teixeira, F. S.; Marrucho, I. M.; Piñeiro, M. M.; Rebelo, L. P. N. Aggregation Behavior and Total Miscibility of Fluorinated Ionic Liquids in Water. *Langmuir*. **2015**, 31, 1283–1295.

**(32)** Riess, J. G. Fluorous Micro- and Nanophases With a Biomedical Perspective. *Tetrahedron*. **2002**, 58; 4113–4131.

**(33)** Lipinski, C. A. Particle Size Reduction to the Nanometer Range: a Promising Approach to Improve Buccal Absorption of Poorly Water-soluble Drugs. *Am. Pharm. Rev.* **2002**, 5, 82–85.

**(34)** Fletcher, K. A.; Pansdey, S. Surfactant Aggregation within Room-Temperature Ionic Liquid 1-Ethyl-3-methylimidazolium Bis(trifluoromethylsulfonyl)imide. *Langmuir*. **2004**, 20, 33–36.

**(35)** Bhadani, A.; Misono, T.; Singh, S.; Sakai, K.; Sakai, H.; Abe M. Structural Diversity, Physicochemical Properties and Application of Imidazolium Surfactants: Recent Advances. *Adv. Colloid Interface Sci*. **2016**, 231, 36–58.

**(36)** Moniruzzaman, M.; Tahara, Y.; Tamura, M.; Kamiya, N.; Goto, M. Ionic Liquid-assisted Transdermal Delivery of Sparingly Soluble Drugs. *Chem. Commun.* **2010**, 46, 1452–1454.

**(37)** Moniruzzaman, M.; Tamura, M.; Tahara, Y.; Kamiya, N.; Goto, M. Ionic Liquid-in-Oil Microemulsion as a Potential Carrier of Sparingly Soluble Drug: Characterization and Cytotoxicity Evaluation. *Int. J. Pharm.* **2010**, 400, 243–250.

**(38**) Goindi, S.; Kaur, R.; Kaur, R. An Ionic Liquid-in-Water Microemulsion as a Potential Carrier for Topical Delivery of Poorly Water Soluble Drug: Development, *Ex-vivo* and *In-vivo* Evaluation. *Int. J. Pharm.* **2015**, 495, 913–923.

**(39)** Simon, L. S.; et al. Economic and Gastrointestinal Safety Comparisons of Etodolac, Nabumetone, and Oxaprozin from Insurance Claims Data from Patients with Arthritis. *Clin Ther*. **1998**, 20, 1218–1235.

**(40**) Wang, X.; Chen, H.; Luo, Z.; Fu, X. Preparation of Starch Nanoparticles in Water-in-Oil Microemulsion System and their Drug Delivery Properties. *Carbohydr. Polym.* **2016**, 138, 192–200.

**(41)** Mahkam, M.; Rafi, A. A.; Gheshlaghi, L. M. Preparation of Novel pH-sensitive Nanocomposites Based on Ionic liquid Modified Montmorillonite for Colon Specific Drug Delivery System. *Polym Polym Compos.* **2014**, 37, 182–187.

**(42)** Tang, W.; et al. Doxorubicin-loaded Ionic Liquid–Polydopamine Nanoparticles for Combined Chemotherapy and Microwave Thermal Therapy of Cancer. *RSC Adv.* **2016**, 6, 32434–32440.

**(43)** Abd, E. D.; Albishri H. M. Protein/Ionic Liquid/Glassy Carbon Sensors Following Analyte Focusing by Ionic Liquid Micelle Collapse for Simultaneous Determination of Water Soluble Vitamins in Plasma Matrices. *Talanta.* **2015**, 139, 150–158.

**(44)** Quirino, J. P.; Haddad, P. R. Micelle Stacking in Micellar Electrokinetic Chromatography. *Anal. Chem.* **2008**, 80, 6824–6829.

**(45)** Li, T.; Joshi, M. D.; Ronning, D. R.; Anderson, J.L. Ionic Liquids as Solvents for *in Situ* Dispersive Liquid-Liquid Microextraction of DNA. *J. Chromatogr. A* **2013**, 1272, 8–14.

**(46)** Tateishi-Karimata, H.; Sugimoto, N. Structure, Stability and Behaviour of Nucleic Acids in Ionic Liquids. *Nucleic Acids Res.* **2014,** 42, 8831–8844.

**(47)** Patel, R.; Kumari, M.; Khan, A. B. Recent Advances in the Applications of Ionic Liquids in Protein Stability and Activity: A Review. *Appl. Biochem. Biotechnol.* **2014**, 172, 3701–3720.

**(48)** Wang, J.; Cheng, D.; Chen, X.; Du, Z.; Fang, Z. Direct Extraction of Double-Stranded DNA Into Ionic Liquid 1-Butyl-3-methylimidazolium Hexafluorophosphate and Its Quantification. *Anal. Bioanal. Chem.* **2007**, 79, 620–625.

**(49)** Gonzalez, G. E. et al. Direct Extraction of Genomic DNA from Maize with Aqueous Ionic Liquid Buffer Systems for Applications in Genetically Modified Organisms Analysis. *Anal. Bioanal. Chem.* **2014**, 406, 7773–7784.

**(50)** Cardoso, L.; Micaelo, N. M. DNA Molecular Solvation in Neat Ionic Liquids. *Chem. Phys. Chem.* **2011**, 12, 275–277.

**(51)** Ressmann, A. K.; Bica, K. Leaching of Active Ingredients from Plants with Ionic Liquids. In *Ionic Liquids for Better Separation Processes*. Springer Berlin Heidelberg, **2016**. 135-165.

**(52)** Geng, F.; Zheng, L.; Yu, L.; Li, G.; Tung, C. Interaction of Bovine Serum Albumin and Long Chain Imidazolium Ionic Liquid Measured by Fluorescence Spectra and Surface Tension. *Process Biochem.* **2010**, 45, 306–311.

**(53)** Noritomi, H.; Minamisawa, K.; Kamiya, R.; Kato, S. J. Thermal Stability of Proteins in the Presence of Aprotic Ionic Liquids. *Biomed Sci Eng.* **2011**, 4, 94–99.

**(54)** Machado, M. F.; Saraiva, J. M. Thermal Stability and Activity Regain of Horseradish Peroxidase in Aqueous Mixtures of Imidazolium-Based Ionic Liquids. *Biotechnol Lett.* **2005**, 27, 1233–1239.

**(55)** Soni, S. K.; Sarkar, S.; Selvakannan, P. R.; Sarkar, D.; Bhargava, S. K. Intrinsic Therapeutic and Biocatalytic Roles of Ionic Liquid Mediated Self-assembled Platinum-phytase Nanospheres. *RSC Adv.* **2015**, 5, 62871–81.

**(56)** Fast, J. P.; Perkins, M. G.; Pearce, R. A.; Mecozzi, S. Fluoropolymer-based Emulsions for the Intravenous Delivery of Sevoflurane. *Anesthesiology*, **2008**, 109, 651-656.

**(57)** Pereiro, A. B. A.; Tomé, L. C. L.; Martinho, S.; Rebelo, L. P. N.; Marrucho, I. M. Gas Permeation Properties of Fluorinated Ionic Liquids. *Ind. Eng. Chem. Res*. **2013**, 52, 4994–5001.

**(58)** Kurczy, M. E.; et al. Comprehensive Bioimaging with Fluorinated Nanoparticles using Breathable Liquids. *Nat. Commun.* **2015**, 6, 5998.

**(59)** Johnson, M. E.; et al. Fluorocarbon Modified Low-Molecular-Weight Polyethylenimine for siRNA Delivery. *Bioconjug. Chem.* **2016**, 27, 1784–1788.

# 2. Characterization of Fluorinated Ionic Liquids: Thermophysical, Phase Equilibria and Aggregation Behaviour

## 2.1 Introduction

One of the most outstanding advantage of ionic liquids, and thus of fluorinated ionic liquids, is the possibility of tuning the final characteristics through infinite combinations between cations and anions. This manipulation allows to control several characteristics such as thermal and thermophysical properties, solubility, hydrophobicity and toxicity (1). As the interest in ionic liquids increase exponentially, the demand for a comprehensive investigation of their physicochemical properties is clear. In order to evaluate the advantages of fluorinated ionic liquids, thermodynamic, thermophysical and thermal characterization, liquid-liquid equilibria, as well as the self-aggregation behaviour in aqueous solution were obtained for imidazolium-based ionic liquids with the perfluorobutanesulfonate anion.

Determination of density and viscosity could headlight FILs transport properties (2). On the other hand, viscosity can estimate the FIL ease of movement through different solvents, also called fluidity (3). Additionally, ionic conductivity related with FIL concentration may predict the formation of aggregates (4). The relationship between conductivities and viscosity, known as ionicity, is also important to characterize pure FILs (5). For instance, perfluorinated compounds (PFC) proved to be useful in several biomedical applications such as artificial blood substitutes and *in vivo* gas carriers (6). Since fluorinated ionic liquids share some common characteristics with PFC (1), a comparison between these two compounds is done when possible.

The self-aggregation behaviour of some FILs in aqueous solutions induces the formation of self-assembled structures that can be used advantageously in the delivery of different therapeutic compounds (4). For example, drug molecules exhibiting poor solubility due to their high molecular weights and structure complexity that lead to low bioavailability (7). Accordingly, designing novel excipients with tuneable physicochemical properties and capable of forming micelles or microemulsions is promising. With this aim in mind, a solubility and self-aggregation behaviour analysis for imidazolium-based fluorinated ILs was conducted.

In conclusion, the data obtained in this chapter will allow the critical evaluation of FILs thermophysical properties, and solution behaviour, acknowledging their use as biomaterials such as gas carrier compounds, surfactant for microemulsions or nanostructured drug delivery components (8).

## 2.2 Materials

1-Butyl-3-methylimidazolium perfluorobutanesulfonate, ≥98% mass fraction purity; and 1-decyl-3-methylimidazolium perfluorobutanesulfonate, ≥98% mass fraction purity; were synthetized in our lab according to the ion exchange resin method (9). 1-Hexyl-3-methylimidazolium perfluorobutanesulfonate, >99% mass fraction purity; 1-octyl-3-methylimidazolium

perfluorobutanesulfonate, >99% mass fraction purity and 1-dodecyl-3-methylimidazolium perfluorobutanesulfonate, >98% mass fraction purity were acquired from IoLiTec. Structures and acronyms are listed in **Table 2.1**

**Table 2.1.** Designation and chemical structure of each ionic liquid used along this study.

| IL designation | Chemical structure |
|---|---|
| 1-Buthyl-3-methylimidazolium perfluorobutanesulfonate<br>**[$C_4C_1Im$][$C_4F_9SO_3$]** | 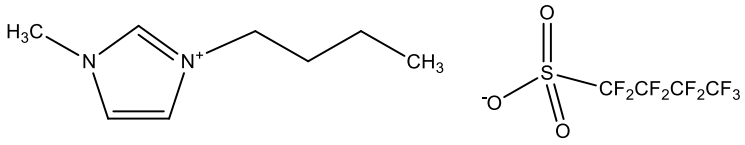 |
| 1-Hexyl-3-methylimidazolium perfluorobutanesulfonate<br>**[$C_6C_1Im$][$C_4F_9SO_3$]** | 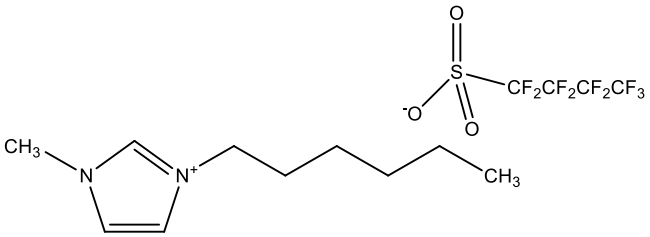 |
| 1-Octyl-3-methylimidazolium perfluorobutanesulfonate<br>**[$C_8C_1Im$][$C_4F_9SO_3$]** | 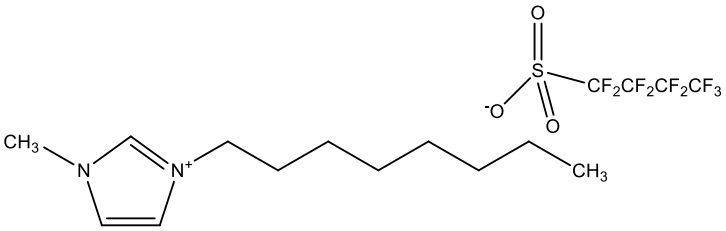 |
| 1-Decyl-3-methylimidazolium perfluorobutanesulfonate<br>**[$C_{10}C_1Im$][$C_4F_9SO_3$]** | 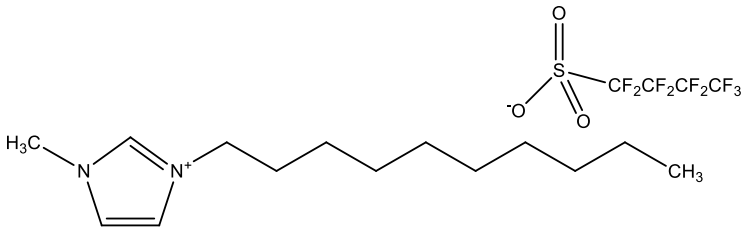 |
| 1-Dodecyl-3-methylimidazolium perfluorobutanesulfonate<br>**[$C_{12}C_1Im$][$C_4F_9SO_3$]** | 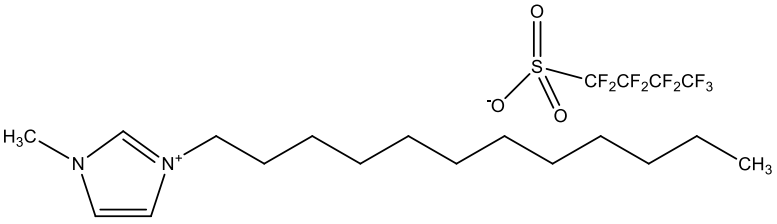 |

In order to confirm the purity of the compounds $^{1}H$ and $^{19}F$ NMR were performed. The compounds were first dried under a $3 \cdot 10^{-2}$ Torr vacuum with a continuous stirring at 323.15 K for at least 48h to reduce volatile impurities. The water content of FILs used in this work was determined using Karl Fisher

coulometric titration method (Metrohm 831 KF Coulometer) and it was less than 100 ppm. Milli-Q ultrapure water (Milli-Q Integral Water Purification System) was used when necessary throughout the work.

## 2.3 Experimental Procedures

## 2.3.1 Neat Fluorinated Ionic Liquids

## 2.3.1.1. Thermal Properties

The thermal stabilities of the FILs were determined using a thermogravimetric analysis (TGA), using the TA Instrument model Q50 represented in **Figure 2.1. a)**. Samples of FILs were loaded in an aluminium pan and heated with a nitrogen flow rate of 60 ml·min$^{-1}$ until complete thermal degradation using a scan rate of 1 K·min$^{-1}$. TA Universal Analysis (software version 4.4) was used to determinate the onset temperature ($T_{onset}$), starting temperature ($T_{start}$) and decomposition temperature ($T_{dec}$) which correspond to the temperatures at which the baseline slope changed during heating, the weight loss was less than 1%, and the weight loss was 50%, respectively. Duplicates were measured and the uncertainty of these temperatures is ± 3 K.

Melting points were determined using a Differential Scanning Calorimeter (DSC), TA Instrument model Q200 (see **Figure 2.1. b)**), calibrated with an Indium standard. In these experiments, samples of FILs were loaded in an aluminum pan and continuously purged with 50 ml·min$^{-1}$ of inert nitrogen gas. Next, the samples were cooled to 183.15 K, tempered during 30 min, and heated to 313.15 K. This process was repeated three times at different rates (10 K·min$^{-1}$, 5 K·min$^{-1}$ and 1 K·min$^{-1}$). The obtained values from the second and subsequent cycles were reproducible at the same rate. Duplicates were measured and the uncertainty of the melting temperature is ±2K

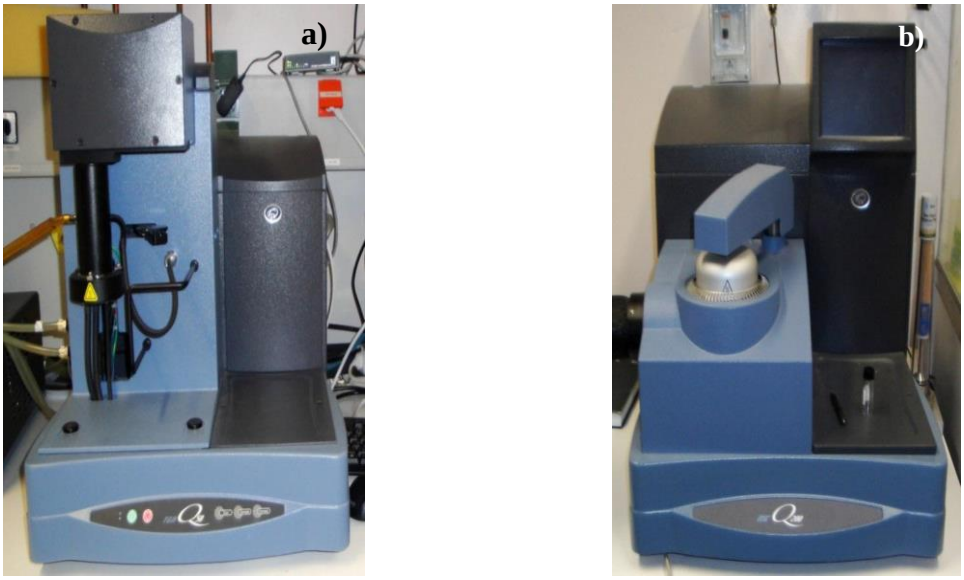


**Figure 2.1. a)** TA instrument Model TGA Q50 used for the measurements and **b)** TA Instrument Model DSC Q200 used for the measurements.

## 2.3.1.2. Viscosity and Density Measurements

Measurements of dynamic viscosity were carried out using an automated SVM 3000 Anton Paar rotational Stabinger viscometer (see **Figure 2.2. a)**) operating at atmospheric pressure in the temperature range 288.15 to 358.15 K. The equipment uses Peltier elements for fast and efficient thermostability with a temperature uncertainty of ± 0.02 K. Duplicates were measured and the reported data are average values with a maximum relative standard deviation of 1%. The uncertainty of the experimental values, taking into account the purity and handling of the samples is estimated to be 2%.

Density was measured with an Anton Paar vibrating tube densimeter, model DMA 5000 (**see Figure 2.2. b)**) operating at atmospheric pressure and in the temperature range 288.15 K to 358.15 K. The effect of viscosity was considered in all experiments using the internal calibration. The temperature was controlled by several Peltier units and the cell was embedded in a cavity inside a metallic block. This equipment allowed a temperature stability of 0.002 K. Duplicates were measured and the repeatability and expanded uncertainty of the density is better than $5 \cdot 10^{-5}$ and $\pm 3 \cdot 10^{-4}$ g·cm$^{-3}$, respectively.


**Figure 2.2. a)** Anton Paar SVM 300 used for viscosity measurements and **b)** Anton Paar DMA 5000 densimeter used for density measurements.

## 2.3.1.3. Refractive Index Measurements

An Anton Paar ABBEMAT 500 automatic refractometer with a resolution of $\pm 10^{-6}$ was used to measure the refractive index. The equipment was calibrated using Millipore quality water and tetrachloroethylene provided by the supplier. Duplicates were measured and the reported results have an uncertainty of $\pm 4 \cdot 10^{-5}$. The apparatus is represented in **Figure 2.3. a)**.

## 2.3.1.4. Ionic Conductivity Measurements

Ionic conductivity measurements were determined using a Radiometer Analytical CDM210 conductimeter in a jacketed glass cell with a magnetic stirrer as represented in **Figure 2.3. b)**.


**Figure 2.3. a)** Anton Paar ABBEMAT 500 automated refractometer and **b)** Radiometer Analytical CDM210 conductimeter.

A water bath was used to thermostatize the cell and the temperature was measured by a platinum resistance thermometer coupled to a Keithley 199 System DMM/Scanner with an uncertainty of ± 0.01 K. To ensure a secure seal and to prevent humidity, the sample was closed with dry nitrogen and screw caps. The calibration was performed at each temperature with 0.01 D KCl standard solutions supplied by Radiometer Analytical. The ionic conductivity values were validated as described previously (10). Duplicates were measured and the reported data are the average values with an uncertainty of ± 1%

## 2.3.2. Mixtures of Fluorinated Ionic Liquids and Water

## 2.3.2.1. Liquid-liquid Equilibria

In order to determine the temperature-composition phase diagrams, the turbidity of the binary system FIL + water was analyzed using a visual method at atmospheric pressure. Initial immiscible samples were prepared directly in Pyrex glass cells with incorporated magnetic stirrers using an analytical high-precision balance (uncertainty of ± 0.00002 g). Then, the cell was immersed in a thermostatic bath (a mixture of water and ethylene glycol was used as thermostatic fluid) and both mixture and thermostatic fluid were continuously stirred. The liquid-liquid phase transition was accomplished by taking the temperature when the turbidity of the system disappeared. The temperature was measured using a four-wire platinum resistance Pt100 thermometer coupled to a Keithley 199 System DMM/Scanner multimeter (uncertainty of 0.01 K). The overall uncertainty of the temperature transitions in this visual method was estimated to be ± 0.5 K and the uncertainty of the mixture composition was ± 0.0001 in mass fraction. **Figure 2.4.** depicts (a) cell with visible turbidity corresponding to immiscibility, a (b) cell with total miscibility and (c) the experimental setup for performing liquid-liquid equilibria measurements

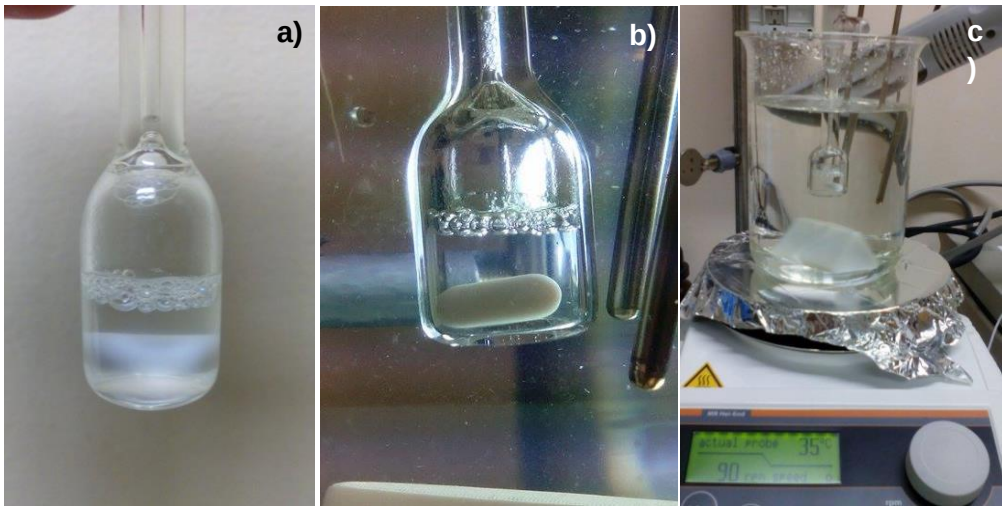


**Figure 2.4.** Cells used for liquid-liquid equilibrium measurements where a turbidity transition can be observed, from **a)** an immiscible sample to **b)** a miscible one, as well as the **c)** experimental setup.

## 2.3.2.2. Critical Micellar Concentration

To determine the critical micellar concentration (CMC), the Philips definition was used (11). According to Philips *et al*., the concentration at which there is a maximum change in gradient in the conductivity-concentration curve corresponds to a CMC. The ionic conductivities were measured at 298.15 K and performed with a Radiometer Analytical CDM210 conductimeter using a CDC749 electrode in a glass cell with a magnetic stirrer (see **Figure 2.3. b)**). The equipment was calibrated for each temperature by using a certified 0.01 D KCl standard solution provided by Radiometer Analytical. The cell was thermostatized with a water bath and the temperature was measured using a platinum resistance thermometer coupled to a Keithley 199 system DMM/scanner (uncertainty of ±0.01 K). Each aqueous solution was added to the cell and stirred for the experimental measurements. Conductivity was measured at least three times and the uncertainty of each sample was estimated to be 1%.

## 2.3.2.3. Transmission Electron Microscopy (TEM)

The samples analyzed with microscopy were placed on a 200 nesh copper grid with 3 mm diameter using a formvar film. A filter paper was used to remove the excess of aqueous solution. Solutions were dried and measured using a Philips CM20 model with LaB6 filament, at a working voltage of 200 kV. These measurements were carried out by an external service (University of Vigo).

# 2.4. Results and Discussion

## 2.4.1. Neat Fluorinated Ionic Liquids

## 2.4.1.1. Thermal Properties

Melting and decomposition temperatures are one of the most remarkable properties for ionic liquids which determine the liquid range, and, consequently, their range of applications (1). For this

purpose, $[C_4C_1Im][C_4F_9SO_3]$ and $[C_{10}C_1Im][C_4F_9SO_3]$ were analyzed and in **Table 2.2.** are reported the thermal properties (onset temperature, $T_{onset}$, start temperature, $T_{start}$, decomposition temperature, $T_{dec}$, and melting temperature, $T_m$) of the fluorinated ionic liquids studied in this work.

**Table 2.2.** Thermal properties of fluorinated ionic liquids: starting temperature, $T_{start}$, onset temperature, $T_{onset}$, decomposition temperature, $T_{dec}$, and melting temperature, $T_m$ at 1 K·min$^{-1}$.

| FIL | $T_m$ / K | $T_{start}$ / K | $T_{onset}$ / K | $T_{dec}$ / K |
|---|---|---|---|---|
| $[C_4C_1Im][C_4F_9SO_3]$ | 286 | 554 | 638 | 670 |
| $[C_{10}C_1Im][C_4F_9SO_3]$ | 307 | 545 | 627 | 655 |

Experimental data are plotted in **Figure 2.5.** where the melting temperatures specify the temperature at which the compound becomes liquid and the decomposition temperatures determine the upper operating temperature at which the fluid can be used (3). Also, the obtained results for the studied FILs were compared with the fluorinated ionic liquids $[C_2C_1Im][C_4F_9SO_3]$, $[C_6C_1Im][C_4F_9SO_3]$, $[C_8C_1Im][C_4F_9SO_3]$ and $[C_{12}C_1Im][C_4F_9SO_3]$ from previous works (1,3).

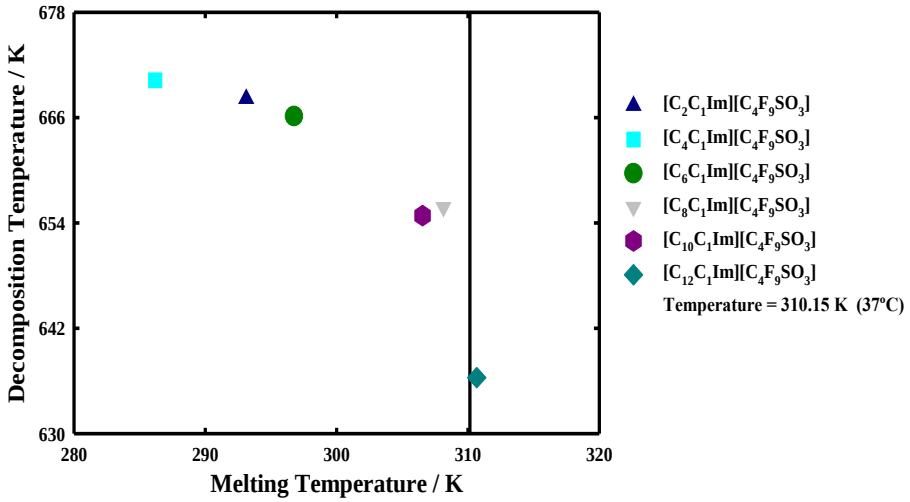


**Figure 2.5.** Decomposition temperatures versus melting temperatures for the fluorinated ionic liquids in this study, $[C_4C_1Im][C_4F_9SO_3]$ and $[C_{10}C_1Im][C_4F_9SO_3]$, and those found on literature for the same family (1,3).

In order to evaluate the use of these fluorinated ionic liquids for biomedical purposes the most relevant temperature is 310.15K, which is accepted to be the average body temperature in humans (1). With the available data, it is possible to analyse the effect of the increment of the hydrogenated alkyl side chain length on the imidazolium-based fluorinated ionic liquids with the perfluorobutanesulfonate anion, $[C_4F_9SO_3]^-$.

Taking into account the onset temperature values, $T_{onset}$, no substantial differences were found. These high thermal stabilities are characteristic of these compounds and an advantage for several applications in the electrochemical field, for example as battery electrolytes (12). Comparing the decomposition

temperatures ($T_{dec}$), corresponding to 50% of weight loss of the compound, it is possible to observe that the increment of the hydrogenated side chain decreases this temperature. When analyzed with other FILs it leads to the following trend: $[C_4C_1Im]^+ \approx [C_2C_1Im]^+ \approx [C_6C_1Im]^+ > [C_8C_1Im]^+ \approx [C_{10}C_1Im]^+ > [C_{12}C_1Im]^+$. The same trend is observed for the melting temperatures: $[C_4C_1Im]^+ \approx [C_2C_1Im]^+ \approx [C_6C_1Im]^+ > [C_{10}C_1Im]^+ \approx [C_8C_1Im]^+ > [C_{12}C_1Im]^+$. These trends are in agreement with the literature, where the increment of the hydrogenated alkyl chain length is related to an increase on the melting and decrease on the decomposition temperatures (1,3,5).

## 2.4.1.2. Thermophysical Characterization

The thermophysical properties measured in this work, namely density, dynamic viscosity, refractive index and ionic conductivity of the two fluorinated ionic liquids studied in this thesis are listed in **Table 2.3.** as function of temperature. The densities, fluidities (1 / dynamic viscosity) and ionic conductivities are represented in **Figure 2.6.**, **Figure 2.7.** and **Figure 2.8.**, respectively, together with data for $[C_2C_1Im][C_4F_9SO_3]$, $[C_6C_1Im][C_4F_9SO_3]$, $[C_8C_1Im][C_4F_9SO_3]$ and $[C_{12}C_1Im][C_4F_9SO_3]$ taken from the literature (1,3).

Density and fluidity are important parameters to be analyzed when one want to apply this novel compounds for biomedical applications, such as transport and delivery of respiratory gases (13), formulation of drug delivery systems (14),among others (1). The obtained density values were compared with $[C_2C_1Im][C_4F_9SO_3]$, $[C_6C_1Im][C_4F_9SO_3]$, $[C_8C_1Im][C_4F_9SO_3]$ and $[C_{12}C_1Im][C_4F_9SO_3]$ (1,3) in order to observe the effect of the hydrogenated alkyl chain length of the imidazolium cation.

In order to evaluate the density of fluorinated ionic liquids, the density of blood (1.05 $g \cdot cm^{-3}$) was taken into account (15). Additionally, since PFCs proved to be useful in a plethora of biomedical uses as surfactants for microemulsions and for drug delivery encapsulations, the density of these compounds (≈1.7 $g \cdot cm^{-3}$) is also considered as reference value (16). The best candidates will be the fluorinated ionic liquids with densities closer to the values mentioned above.

Analysing the results for $[C_4C_1Im][C_4F_9SO_3]$ and $[C_{10}C_1Im][C_4F_9SO_3]$ it can be concluded that in the range of temperatures studied the increase in the hydrogenated alkyl side chain length leads to a decrease of the densities: $[C_4C_1Im][C_4F_9SO_3] > [C_{10}C_1Im][C_4F_9SO_3]$. Comparing the results with blood density at approximately 310.15 K (average body temperature, 37ºC) the $[C_{10}C_1Im][C_4F_9SO_3]$ (≈1.29 $g \cdot cm^{-3}$) is closest to 1.05 $g \cdot cm^{-3}$. However, while increasing the hydrogenated chain length could be advantageous concerning the blood flow, it leads to an increase in lipophilicity (higher toxicity) as will be discussed in **Chapter 3**. Taking into account the density of PFCs (≈1.7 $g \cdot cm^{-3}$) (16), $[C_2C_1Im][C_4F_9SO_3]$ and $[C_4C_1Im][C_4F_9SO_3]$ presented the closest values ≈ 1.55 $g \cdot cm^{-3}$ and ≈ 1.44 $g \cdot cm^{-3}$ at 310.15 K, respectively. Consequently, these fluorinated ionic liquids could be promising biomaterials to replace

(either partially or totally) PFCs, in their distinct useful applications (e.g. drug delivery, contrast ultrasound imaging agent) (6).

Comparing the obtained results with those found in the literature for the same family of imidazolium-based ionic liquids (see **Figure 2.6**), it is verified that density decreases with the increase of temperature and with the increment of the hydrogenated alkyl side chain of the imidazolium cation. These results are in agreement with the literature (1,3,5)

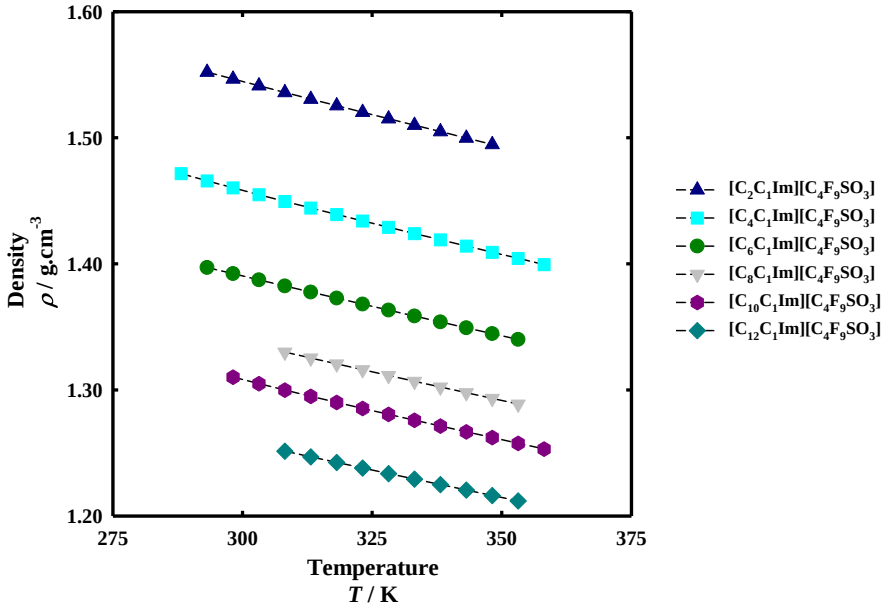


**Figure 2.6.** Density of the fluorinated ionic liquids measured in this work and comparison with $[C_2C_1Im][C_4F_9SO_3]$, $[C_6C_1Im][C_4F_9SO_3]$, $[C_8C_1Im][C_4F_9SO_3]$ and $[C_{12}C_1Im][C_4F_9SO_3]$ found on literature (1,3).

The average blood viscosity stands between 1.1 to 1.35 mPa·s, and so blood fluidity is in a range of 0.74-0.91 $mPa^{-1}s^{-1}$ (17). The PFCs viscosity varied from 0.6 to 5.4 mPa·s with a fluidity range of 0.19-1.67 $mPa^{-1}s^{-1}$ depending on the composition (18). In **Figure 2.7.,** it is possible to observe fluidity dependence on temperature for $[C_nC_1Im][C_4F_9SO_3]$ ($n$=2; 4; 6; 8; 10; 12) FILs. At 310.15 K, considered to be the average human body temperature, fluidities for all the FILs stand between 0.003-0.013 $mPa^{-1}s^{-1}$. However, with the increase in temperature the differences are more pronounced. Comparing the measurements for $[C_4C_1Im][C_4F_9SO_3]$ and $[C_{10}C_1Im][C_4F_9SO_3]$ it can be concluded that the increment of the hydrogenated alkyl chain length leads to a decrease in fluidity (3,5). Relating these results with those found on the literature for $[C_2C_1Im][C_4F_9SO_3]$, $[C_6C_1Im][C_4F_9SO_3]$, $[C_8C_1Im][C_4F_9SO_3]$ and $[C_{12}C_1Im][C_4F_9SO_3]$ the trend become more obvious (1,3).

Despite density and viscosity values (see **Table 2.3.**) being higher than actual blood physical properties and so creating an obstacle, addition of water may lead to a decrease on both properties (19). Rodríguez and Brennecke (19) studied the density and viscosity of aqueous solutions of imidazolium-based ILs with the anions ethylsulfate, trifluoroacetate and trifluoromethanesulfonate. Both properties were found to decrease with an increase in either temperature or in molar fraction of water.

**Table 2.3.** Density, $\rho$, dynamic viscosity, $\eta$, refractive index, $n_D$, and ionic conductivity, $k$, of fluorinated ionic liquids as function of temperature, $T$.

| $T$ / K | $\rho$ /g·cm$^{-3}$ | $\eta$ /mPa·s | $n_D$ | $k$ /mS·cm$^{-1}$ | $T$ / K | $\rho$ /g·cm$^{-3}$ | $\eta$ /mPa·s | $n_D$ | $k$ /mS·cm$^{-1}$ |
|---|---|---|---|---|---|---|---|---|---|
| | | [$C_4C_1Im$][$C_4F_9SO_3$] | | | | | [$C_{10}C_1Im$][$C_4F_9SO_3$] | | |
| 283.15 | | | 1.40782 | | 298.15 | 1.31015 | 597.1 | | 0.14 |
| 288.15 | 1.47155 | 615.4 | 1.40640 | 0.35 | 303.15 | 1.30496 | 423.2 | 1.41284 | 0.19 |
| 293.15 | 1.46582 | 469.5 | 1.40499 | 0.48 | 308.15 | 1.29992 | 307.2 | 1.41136 | 0.25 |
| 298.15 | 1.46027 | 307.3 | 1.40359 | 0.64 | 313.15 | 1.29499 | 223.6 | 1.40990 | 0.33 |
| 303.15 | 1.45486 | 225.4 | 1.40217 | 0.85 | 318.15 | 1.29015 | 172.3 | 1.40842 | 0.43 |
| 308.15 | 1.44954 | 168.9 | 1.40079 | 1.1 | 323.15 | 1.28538 | 132.6 | 1.40697 | 0.55 |
| 313.15 | 1.44432 | 126.7 | 1.39938 | 1.4 | 328.15 | 1.28067 | 103.7 | 1.40553 | |
| 318.15 | 1.43916 | 100.4 | 1.39799 | 1.7 | 333.15 | 1.27600 | 81.65 | 1.40408 | |
| 323.15 | 1.43406 | 79.37 | 1.39663 | 2.1 | 338.15 | 1.27137 | 66.27 | 1.40265 | |
| 328.15 | 1.42902 | 63.71 | 1.39526 | | 343.15 | 1.26679 | 54.04 | 1.40124 | |
| 333.15 | 1.42401 | 51.43 | 1.39393 | | 348.15 | 1.26223 | 44.54 | 1.39980 | |
| 338.15 | 1.41904 | 42.76 | 1.39257 | | 353.15 | 1.25769 | 37.10 | 1.39839 | |
| 343.15 | 1.41410 | 35.65 | 1.39121 | | 358.15 | 1.25318 | 31.31 | 1.39704 | |
| 348.15 | 1.40919 | 30.05 | 1.38991 | | | | | | |
| 353.15 | 1.40431 | 25.52 | 1.38854 | | | | | | |
| 358.15 | 1.39946 | 21.98 | 1.38718 | | | | | | |

The same behaviour was observed by Ge *et al.* (20) and by Carvalho *et al.* (21) with additional imidazolium-based ILs, and by Neves *et al.* (22) with phosphonium-based compounds. With this in mind, $[C_4C_1Im][C_4F_9SO_3]$ and $[C_{10}C_1Im][C_4F_9SO_3]$ can have manageable viscosity and density with the addition of water, making them suitable for biomedical application.

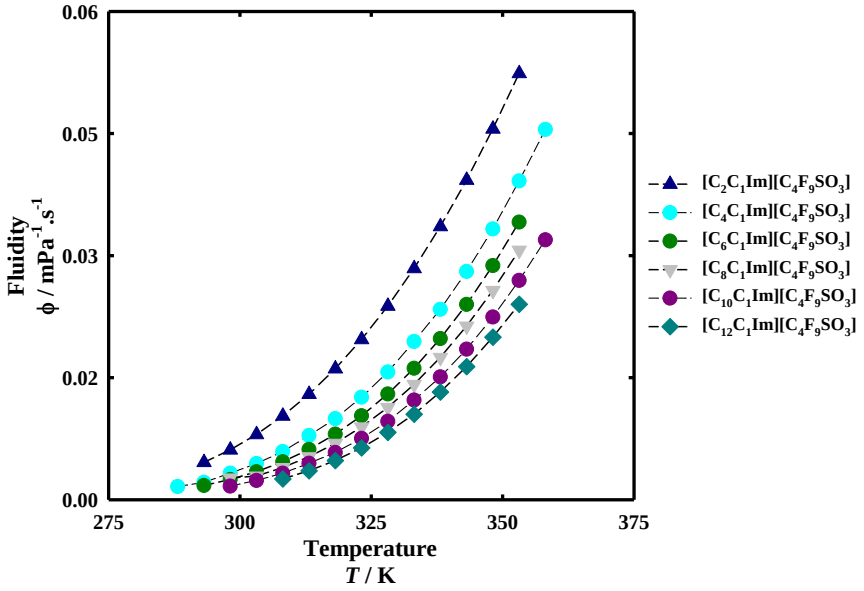


**Figure 2.7.** Fluidity of the fluorinated ionic liquids measured in this work and comparison with those found on literature (1,3).

The ionic conductivities for the fluorinated ionic liquids in study are represented in **Figure 2.8.**. This property not only helps to understand the ionic behaviour of these compounds but also can be useful for determination of other important parameters such as the Walden plot described in **Section 2.4.1.4**.

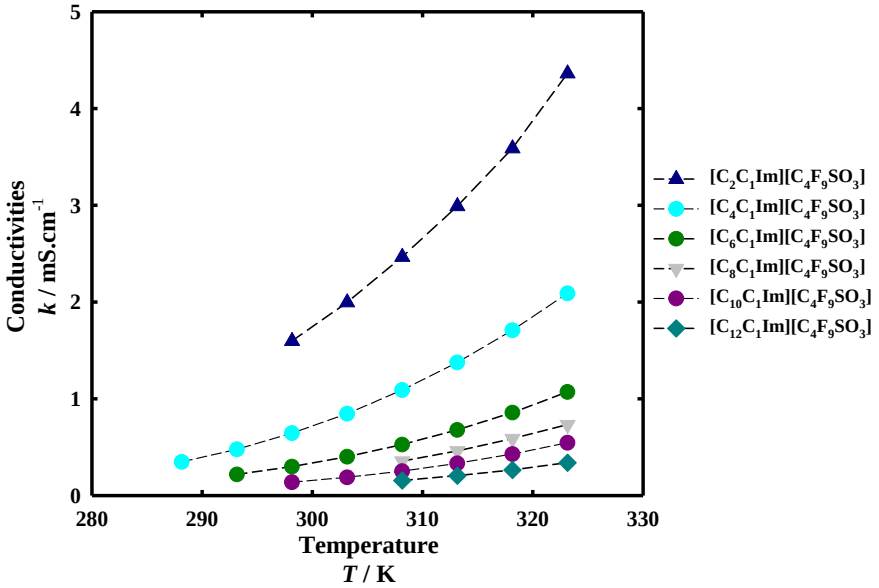


**Figure 2.8.** Ionic conductivities of the fluorinated ionic liquids measured in this work and comparison with those found on literature (1,3).

Analysing the results for $[C_4C_1Im][C_4F_9SO_3]$ and $[C_{10}C_1Im][C_4F_9SO_3]$, the $[C_4C_1Im][C_4F_9SO_3]$ presents a higher conductivity. Comparing the data for measured FILs with data found in the literature for

$[C_2C_1Im][C_4F_9SO_3]$, $[C_6C_1Im][C_4F_9SO_3]$, $[C_8C_1Im][C_4F_9SO_3]$ and $[C_{12}C_1Im][C_4F_9SO_3]$, it is possible to conclude that an increase in the hydrogenated alkyl chain length induces a decrease of ionic conductivity (1,3).

### 2.4.1.3. Walden-Plot

A Walden plot is a convenient and versatile method that provides a qualitative measure of the ionicity since it establishes a relationship between the molar conductivity and the viscosity or fluidity of a fluid (23).Thus, can give a useful information about transport properties, mobility and the possible formation of aggregates (3).

A straight line that passes through the origin is based on a 0.01 M KCl solution where the ions are known to be fully dissociated and to have equal mobility (24). Data from a wide range of electrolytes can then be placed on the Walden plot, including ionic liquids for which viscosity and conductivity measurements are available. For example, the Walden plot was implemented to evaluate the use of ILs as electrochemical devices, double layer capacitors and photo-electrochemical cells (25), as well as to evaluate the tendency to form associated species in permeation studies of pharmaceutically active ILs (26) For an ideal ionic conductor, conductivity can only be influenced by the viscosity of the medium (27):

$$\boldsymbol{\Lambda = \frac{C}{\eta}} \qquad \textbf{Equation 2.1.}$$

where $\boldsymbol{\Lambda}$, $\boldsymbol{\eta}$ and $\boldsymbol{C}$ are the molar conductivity expressed in $Scm^2mol^{-1}$, the viscosity expressed in poise and a constant, respectively. By adding an additional exponent $\alpha$ to the previous equation, yields the following "fractional" Walden rule (27) is obtained:

$$\boldsymbol{\Lambda \propto \frac{1^{\alpha}}{\eta}} \qquad \textbf{Equation 2.2.}$$

Then, the molar conductivity of an IL is calculated with density and conductivity values, using the following relation:

$$\boldsymbol{\Lambda = \frac{k}{\rho M_w}} \qquad \textbf{Equation 2.3.}$$

with $\Lambda$ the molar conductivity in $Scm^2mol^{-1}$, $k$ the conductivity in $Scm^{-1}$, $\rho$ the density in $g{\cdot}cm^{-3}$ and $M_w$ the molecular weight in $g{\cdot}mol^{-1}$(27). Moreover, **Equation 2.2.** can be rewritten as following:

$$\boldsymbol{log\,\Lambda = \alpha\, log\left(\frac{1}{\eta}\right) + log\, C} \qquad \textbf{Equation 2.4.}$$

In **Figure 2.10.**, it is possible to observe the Walden plot for the fluorinated ionic liquids studied herein, as well as those found on literature for the $[C_nC_1Im][C_4F_9SO_3]$ ($n$=2; 6; 8; 10; 12) (1,3), allowing the evaluation of the increment of the hydrogenated alkyl side-chain of the imidazolium cation.

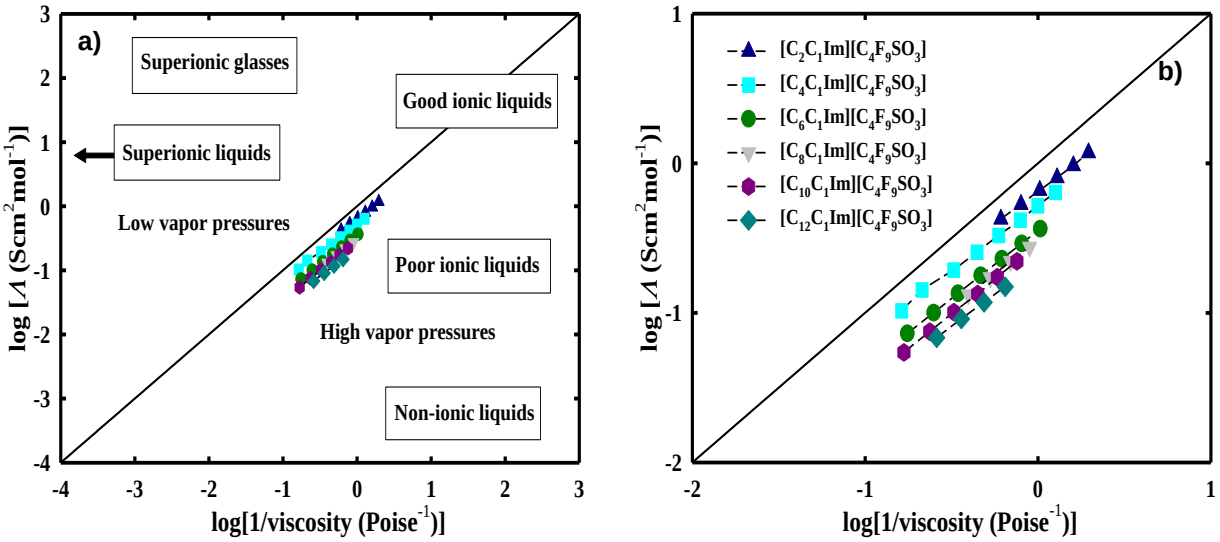


**Figure 2.9.** Walden plot for fluorinated ionic liquids studied in this work and for $[C_2C_1Im][C_4F_9SO_3]$, $[C_6C_1Im][C_4F_9SO_3]$, $[C_8C_1Im][C_4F_9SO_3]$ and $[C_{12}C_1Im][C_4F_9SO_3]$ from previous work (1,3), **a)** with Angell *et al.* (28) classification and **b)** an amplified version.

According to Angell *et al.* (28) classification, depending on the position occupied by the FIL close to or far from the ideal electrolyte represented by the black straight line, these compounds can be considered "good" or "poor" ionic fluids. The picture that emerges from this approach is of a highly associated liquid in which all motions are restricted by the interactions with the surrounding ions in which longer range motions can involve aggregates of ions, some of which do not contribute to conductivity intersecting close to an ideal line (28). Thus, it is expected that the increment of the hydrogenated alkyl chain length promotes a decrease in ionicity (1,3). Analysing **Figure 2.9.,** $[C_4C_1Im][C_4F_9SO_3]$ gives the best result in comparison with $[C_{10}C_1Im][C_4F_9SO_3]$, since the butyl chain presented a behaviour closest an ideal electrolyte.

## 2.4.2. Mixtures of Fluorinated Ionic Liquids and Water

The effect of the increment of the alkyl side chain of the 1-alkyl-3-methylimidazolium perfluorobutanesulfonate ($[C_nC_1Im][C_4F_9SO_3]$) family on the solubility in water and the aggregation behaviour in water is addressed in this section.

## 2.4.2.1. Liquid-liquid Equilibria

The liquid-liquid equilibrium (LLE) was studied in a large range of temperature for the following binary mixtures ($[C_4C_1Im][C_4F_9SO_3]$+water) and ($[C_{10}C_1Im][C_4F_9SO_3]$+water). The experimental data are presented in **Table 2.4.**.

The water/FIL phase diagrams are an advantageous graphical representation of phase equilibria in which it is possible to observe where the compound becomes miscible (29). The knowledge of the phase behaviour is crucial to understand the solubility behaviour of FILs in water and it is useful for the formulation of novel emulsions with tunable properties to partially of fully replace PFCs (29).

**Figure 2.10. a)** depicts the LLE behaviour of the ($[C_4C_1Im][C_4F_9SO_3]$+water) and ($[C_{10}C_1Im][C_4F_9SO_3]$+water) binary mixtures, and the comparison with $[C_6C_1Im][C_4F_9SO_3]$, $[C_8C_1Im][C_4F_9SO_3]$ and $[C_{12}C_1Im][C_4F_9SO_3]$ FILs from a previous study (30). The $[C_2C_1Im][C_4F_9SO_3]$ proved to be completely miscible in water due to their rich self-aggregation behaviour (4). Pereiro *et al.* recently showed that the stable self-assembled structures of this FIL could explain the complete water solubility (4). Finally, taking into account the experimental LLE determined in this work ($[C_4C_1Im][C_4F_9SO_3]$ and ($[C_{10}C_1Im][C_4F_9SO_3]$) and the LLE previously reported, $[C_6C_1Im][C_4F_9SO_3]$ $[C_8C_1Im][C_4F_9SO_3]$ and $[C_{12}C_1Im][C_4F_9SO_3]$ (29), an evaluation of hydrogenated alkyl side chain length in the LLE phase diagrams was performed.

The solubility of water in the FIL rich-phase (see **Figure 2.10. b)**) increases with the increment of the hydrogenated alkyl chain length, as expected for surfactant compounds (31). Thus, water solubility in FILs follows the trend $[C_{12}C_1Im][C_4F_9SO_3]$ ≈ $[C_{10}C_1Im][C_4F_9SO_3]$ ≈ $[C_8C_1Im][C_4F_9SO_3]$ > $[C_6C_1Im][C_4F_9SO_3]$ ≈ $[C_4C_1Im][C_4F_9SO_3]$ at proximally 350 K. However, a very distinct behaviour is observed in the water-rich phase as represented in a closer view in **Figure 2.10. c)**.

**Table 2.4.** Experimental liquid-liquid equilibria for the binary mixtures FIL + water. The superscripts water (1) and FIL (2) designate the water rich-phase and the FIL rich-phase, respectively.

| $T$ / K | $w^1_{FIL}$ | $w^1_{water}$ | $T$ / K | $w^2_{FIL}$ | $w^2_{water}$ |
|---|---|---|---|---|---|
| $[C_4C_1Im][C_4F_9SO_3]$ (1) + Water (2) | | | | | |
| 303.8 | 0.0193 | 0.9807 | 342.7 | 0.8534 | 0.1466 |
| 308.6 | 0.0194 | 0.9806 | 336.6 | 0.8587 | 0.1413 |
| 312.7 | 0.0195 | 0.9805 | 332.3 | 0.8672 | 0.1328 |
| 318.9 | 0.0201 | 0.9799 | 326.1 | 0.8745 | 0.1255 |
| 326.4 | 0.0217 | 0.9783 | 319.7 | 0.8834 | 0.1166 |
| 331.3 | 0.0228 | 0.9772 | 316.0 | 0.8888 | 0.1112 |
| 334.7 | 0.0240 | 0.9760 | 312.0 | 0.8941 | 0.1059 |
| 338.6 | 0.0252 | 0.9748 | 304.7 | 0.9003 | 0.0997 |
| 346.3 | 0.0262 | 0.9738 | 301.1 | 0.9058 | 0.0942 |
| 353.2 | 0.8310 | 0.1690 | 297.4 | 0.9112 | 0.0888 |
| 347.9 | 0.8424 | 0.1576 | | | |

| $T$ / K | $w^1_{FIL}$ | $w^1_{water}$ | $T$ / K | $w^2_{FIL}$ | $w^2_{water}$ |
|---|---|---|---|---|---|
| | | $[C_{10}C_1Im][C_4F_9SO_3]$ (1) + Water (2) | | | |
| 327.1 | 0.0149 | 0.9851 | 351.8 | 0.0553 | 0.9447 |
| 332.5 | 0.0151 | 0.9849 | 351.9 | 0.0508 | 0.9492 |
| 340.1 | 0.0182 | 0.9818 | 352.0 | 0.0684 | 0.9316 |
| 342.0 | 0.0188 | 0.9812 | 353.3 | 0.7879 | 0.2121 |
| 343.4 | 0.0192 | 0.9808 | 350.7 | 0.7976 | 0.2024 |
| 349.1 | 0.0205 | 0.9795 | 346.8 | 0.8083 | 0.1917 |
| 350.3 | 0.0220 | 0.9780 | 344.9 | 0.8229 | 0.1771 |
| 350.4 | 0.0320 | 0.9680 | 343.0 | 0.8286 | 0.1714 |
| 350.6 | 0.0294 | 0.9706 | 340.6 | 0.8358 | 0.1642 |
| 351.2 | 0.0386 | 0.9614 | 337.0 | 0.8424 | 0.1576 |
| 351.3 | 0.0475 | 0.9525 | 336.0 | 0.8488 | 0.1512 |
| 351.5 | 0.0430 | 0.9570 | | | |

The increment of the alkyl side chain length of the imidazolium cation decreases the solubility in water until a hexyl – octyl chain ($[C_6C_1Im][C_4F_9SO_3]$ – $[C_8C_1Im][C_4F_9SO_3]$). For instance, at ≈335 K the water-rich phase diagram follow the trend: $[C_4C_1Im][C_4F_9SO_3]$ > $[C_{12}C_1Im][C_4F_9SO_3]$ > $[C_{10}C_1Im][C_4F_9SO_3]$ > $[C_6C_1Im][C_4F_9SO_3]$ ≈ $[C_8C_1Im][C_4F_9SO_3]$ (see **Figure 2.10 d)**). The observed phase behaviour indicates a delicate balance between two competing effects: the entropic contributions that decrease the solubility of FILs in water and the FILs tendency to self-aggregate in aqueous media. This behaviour has been already observed in aqueous biphasic systems with surfactant ILs (31,32). The effect of the increase of hydrogenated alkyl side chain length of the imidazolium cation on the self-aggregation behaviour will be addressed in next section.

Additionally, a similar trend is observed for the surface tension of neat $[C_nC_1Im][C_4F_9SO_3]$ (n = 2, 4, 6, 8, 10, 12) FILs (33). It was expected that the increment of the hydrogenated alkyl side chain of the imidazolium cation would lead to a further decrease on surface tension. Instead, a "turn-over" on the trend was reported when $n$ = 8 (for $[C_8C_1Im][C_4F_9SO_3]$). The reason for such behaviour was attributed to a rearrangement of the internal structure of these FILs.

It is well established that FILs based on the perfluorobutanesulfonate anion, $[C_4F_9SO_3]^-$, are able to form three nanosegregated domains: polar, nonpolar aliphatic, and nonpolar fluorinated (34). A structure–property relationship between the chemical structure and the liquid nanostructure has been established (35). The segregation behaviour together with the surfactant behaviour of these compounds

could lead to the unexpected behaviour of the aqueous-rich phase of the LLE phase diagram reported in this work. A closer analysis regarding the reported trend is being conducted by our research group.

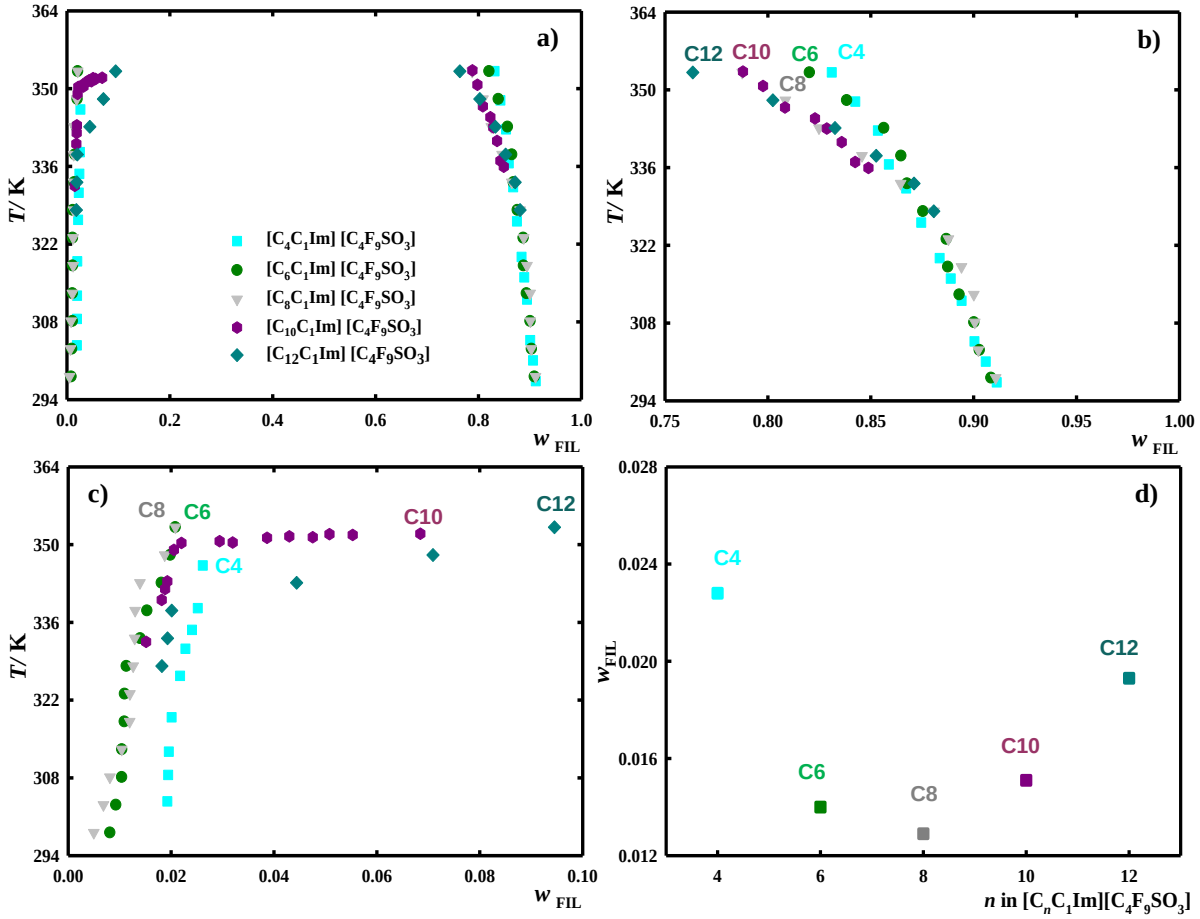


**Figure 2.10. a)** Full composition of the liquid-liquid phase diagram for binary mixtures (FILs (1) + water (2)) in terms of mass fraction; amplified liquid-liquid phase diagram at the **b)** water rich-phase and **c)** at ≈335 K and the **d)** FIL rich-phase.

## 2.4.2.2. Self-aggregation Behaviour

Fluorinated ionic liquids are amphiphilic molecules and are constituted by a polar head and a hydrophobic tail (34). In aqueous media, FILs can self-assembly in different of aggregate structures to hide their hydrophobic moieties and expose the hydrophilic ones. Some common forms of aggregates are tubules, vesicles, ribbons and helices (4). For instance, this ability of FILs to create organized nanostructures could be useful in the development of novel drug delivery systems where a drug with low solubility could be encapsulated in one of these structures and directed to the target (14). Additionally, their surfactant behaviour could be also useful to facilitate the formation and stabilization of microemulsions for enhanced biomolecule solubility (29,36).

Measurements of ionic conductivity are generally implemented in the study of ionic micellar solutions. The presence of micelles can decrease the mobility and as consequence a slope on conductivities could be noticed (11). Thus, ionic conductivity measurements for $[C_4C_1Im][C_4F_9SO_3]$ and

$[C_{10}C_1Im][C_4F_9SO_3]$ were performed at 298.15 K, 308.15 K and 318.15 K. **Figure 2.11.** illustrate these measurements at 298.15 K for $[C_{10}C_1Im][C_4F_9SO_3]$, where the experimental conductivities are depicted against FIL concentration. This change in behaviour is explained by Philips definition, where the critical micellar concentration (CMC) is the concentration corresponding to the maximum change in the gradient of the solution property, ionic conductivity, *versus* concentration curve (11). The CMC values can be determined using these plots.

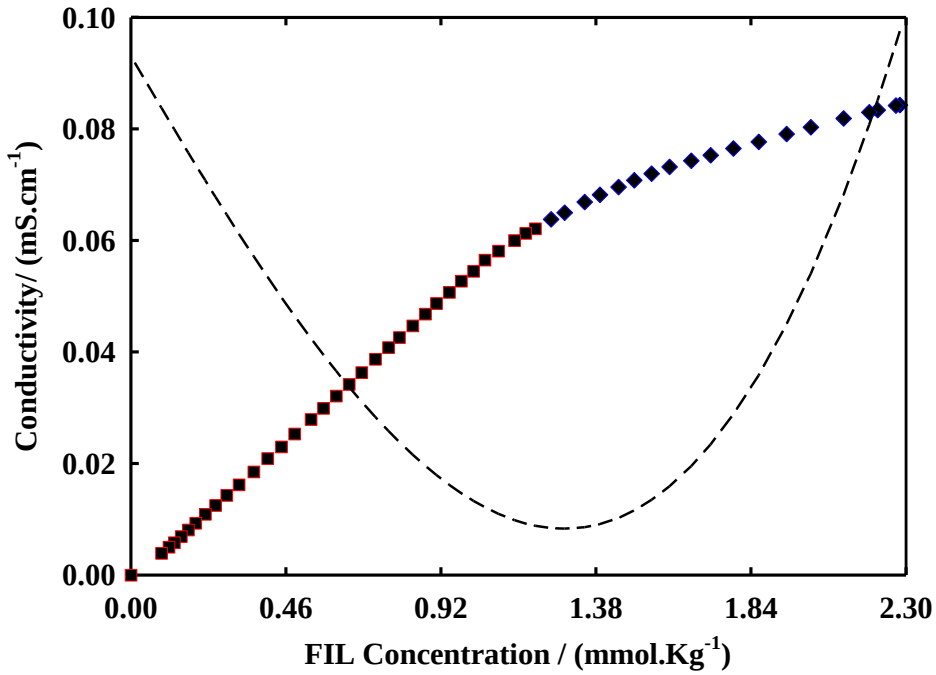


**Figure 2.11.** Concentration dependence of the ionic conductivity for $[C_{10}C_1Im][C_4F_9SO_3]$ in aqueous solution at 298.15 K at the CMC. The dashed line shows a maximum change in the gradient of ionic conductivity as a function of FIL concentration, obtained second derivative.

In this work, the ionic conductivity measurements were carried out at 298.15, 308.15 and 318.15 K and the CMC values calculated from these plots are reported in **Table 2.5** and compared with the CMC for FILs from same family measured at 298.15 K (4,30).

**Figure 2.12** illustrates the behaviour of the FILs studied in this work as well as of $[C_2C_1Im][C_4F_9SO_3]$, $[C_6C_1Im][C_4F_9SO_3]$, $[C_8C_1Im][C_4F_9SO_3]$ and $[C_{12}C_1Im][C_4F_9SO_3]$ (4,30). Taking into account these experimental results, it can be concluded that the increment of the hydrogenated alkyl side-chain of the imidazolium cation is directly related to lower CMC values, as expected (30).

The CMC is intimately related to the surfactant behaviour of a compound: a lower CMC leads to an increase of surfactant behaviour (1). The commercial perfluorocarbon surfactants such as sodium perfluorooctanoate and ammonium perfluorooctanoate have CMC values of ≈30 mmol·Kg (37–39) , approximately 30 times higher than some FILs, such as $[C_{10}C_1Im][C_4F_9SO_3]$. This advantageous characteristic could be useful for substituting (totally or partially) the PFCs in microemulsion formulations where the main purpose is their surfactant action (40).

**Table 2.5.** Values of critical micellar concentration, CMC, at different temperatures for FILs in this work and comparison with values found on literature * at 298.15 K (4,30).

| *T/K* | FILs | CMC (mmol/ Kg) |
|---|---|---|
| 298.15 | $[C_2C_1Im][C_4F_9SO_3]$ | 14.55* |
| | $[C_4C_1Im][C_4F_9SO_3]$ | 12.17 |
| | $[C_6C_1Im][C_4F_9SO_3]$ | 8.22* |
| | $[C_8C_1Im][C_4F_9SO_3]$ | 2.41* |
| | $[C_{10}C_1Im][C_4F_9SO_3]$ | 1.29 |
| | $[C_{12}C_1Im][C_4F_9SO_3]$ | 0.01* |
| 308.15 | $[C_4C_1Im][C_4F_9SO_3]$ | 11.36 |
| | $[C_{10}C_1Im][C_4F_9SO_3]$ | 1.21 |
| 318.15 | $[C_4C_1Im][C_4F_9SO_3]$ | 11.31 |
| | $[C_{10}C_1Im][C_4F_9SO_3]$ | 1.14 |

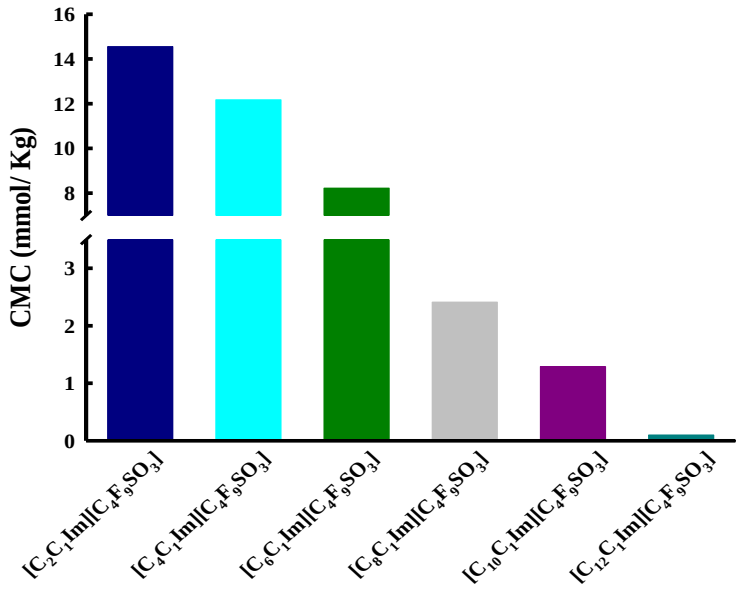


**Figure 2.12.** Comparison of the CMCs values of the fluorinated ionic liquids studied in this work at 298.15 K and those found in the literature (4,30) for the same temperature.

The degree of ionization of the aggregates, $\alpha_{CMC}$, is also a parameter to be evaluated. It is related with the fraction of charges of surfactant ions in the micelle neutralized by micelle-bound counterions. The ions of these surfactants are completely dissociated in aqueous solutions. However, they are partly associated with counterions when forming their aggregates (4). The degree of ionization of the aggregates can be calculated from the ratio of the slopes of the linear fragments above and below the CMC concentration (4). These values are presented in **Table 2.6.** for the studied $[C_nC_1Im][C_4F_9SO_3]$ ($n$ = 2, 4, 6, 8, 10, 12) FILs. A lower value of $\alpha_{CMC}$ indicates a better packed micelle (4). Furthermore, the degree of ionization of the aggregates is more pronouced at lower temperatures. On the other hand,

the degree of counterion binding or counterions condensed on the micellar interface, $\beta_{CMC}$, can be determined though the relationship (4):

$$\boldsymbol{\beta_{CMC} = 1 - \alpha_{CMC}} \qquad \textbf{Equation 2.5.}$$

This parameter, $\beta_{CMC}$, is related to the size of the aggregate, the charge density at the aggregate surface, and the hydrophobic nature of the counterions (4). FILs with long chains can form bulkier aggregate structures, comparatively to smaller FILs ([$C_2C_1Im$][$C_4F_9SO_3$]) (30). Then, the number of ions per aggregate and the volume per surfactant ion in the case of [$C_{10}C_1Im$][$C_4F_9SO_3$] are higher. Moreover, the polar headgroups of these surfactants are packed more closely and they are neutralized by a larger fraction of their counterions (30). For the [$C_nC_1Im$][$C_4F_9SO_3$] the $\alpha_{CMC}$ decreases and $\beta_{CMC}$ increases with the increase of the hydrogenated alkyl chain up to a decyl ($n$=10). However, [$C_{12}C_1Im$][$C_4F_9SO_3$] does not follow this trend. In order to understand these results, a comprehensive study needs to be done to evaluate the $\alpha_{CMC}$ and $\beta_{CMC}$ values for the imidazolium-based FILs up to a dodecyl.

**Table 2.6.** Degree of ionization of the aggregates, $\alpha_{CMC}$, degree of counterion binding or fraction of counterions condensed on the micellar interface, $\beta_{CMC}$, and standard free energy of the aggregation process, $\Delta G^0_{agg}$, measured for FILs in this work at 298.15 K and compared with those found on literature* for the same family (4,30).

| FILs | $\alpha_{CMC}$ | $\beta_{CMC}$ | $\Delta G^0_{agg}$ |
|---|---|---|---|
| [$C_2C_1Im$][$C_4F_9SO_3$]* | 0.79 | 0.21 | -24.7 |
| [$C_4C_1Im$][$C_4F_9SO_3$] | 0.89 | 0.11 | -23.2 |
| [$C_6C_1Im$][$C_4F_9SO_3$]* | 0.63 | 0.37 | -29.9 |
| [$C_8C_1Im$][$C_4F_9SO_3$]* | 0.38 | 0.62 | -40.3 |
| [$C_{10}C_1Im$][$C_4F_9SO_3$] | 0.35 | 0.65 | -43.8 |
| [$C_{12}C_1Im$][$C_4F_9SO_3$]* | 0.73 | 0.27 | -41.7 |

The standard free energy of the aggregation process ($\Delta G^0_{agg}$, mmol·Kg$^{-1}$) was also calculated taking into account the pseudophase model of micellization (43):

$$\boldsymbol{\Delta G^0_{agg} = RT(1 + \beta_{CMC})\, ln\, x_{CMC}} \qquad \textbf{Equation 2.6.}$$

where the $R$ and $T$ are the universal gas constant and absolute temperature, respectively. The $\boldsymbol{x_{CMC}}$ is the critical micellar concentration expressed in mole fraction. **Table 2.6.** lists standard free energies of the aggregation process for the FILs in this study and includes values for other FILs taken from the literature (4,30). The standard Gibbs free energy of aggregation, $\Delta G^0_{agg}$, quantifies the free energy difference per mole between FIL monomers in aqueous solutions and in the aggregates formed (30). Negative values for this parameter indicate spontaneous aggregation of these surfactants. Considering the $\Delta G^0_{agg}$ values here reported, the aggregation process is spontaneous as indicated from the negative

values. Additionally, an increase on the hydrogenated alkyl side chain lentgh leads to an increase of the aggregation process as the $\Delta G^0_{agg}$ values become more negative (30).

In order to better understand the self-aggregation behaviour of these FILs based on the perfluorobutanesulfonate anion, TEM images were obtained for the first time for $[C_6C_1Im][C_4F_9SO_3]$, $[C_8C_1Im][C_4F_9SO_3]$ and $[C_{12}C_1Im][C_4F_9SO_3]$ (see **Figure 2.13**). The self-assembly of $[C_2C_1Im][C_4F_9SO_3]$ (**Figure 2.13 a)**) was previously published (4) and used for comparison. To ensure the micelle formation, the concentrations used in the aqueous solutions were 2-4 times higher than the CMC values previously calculated.

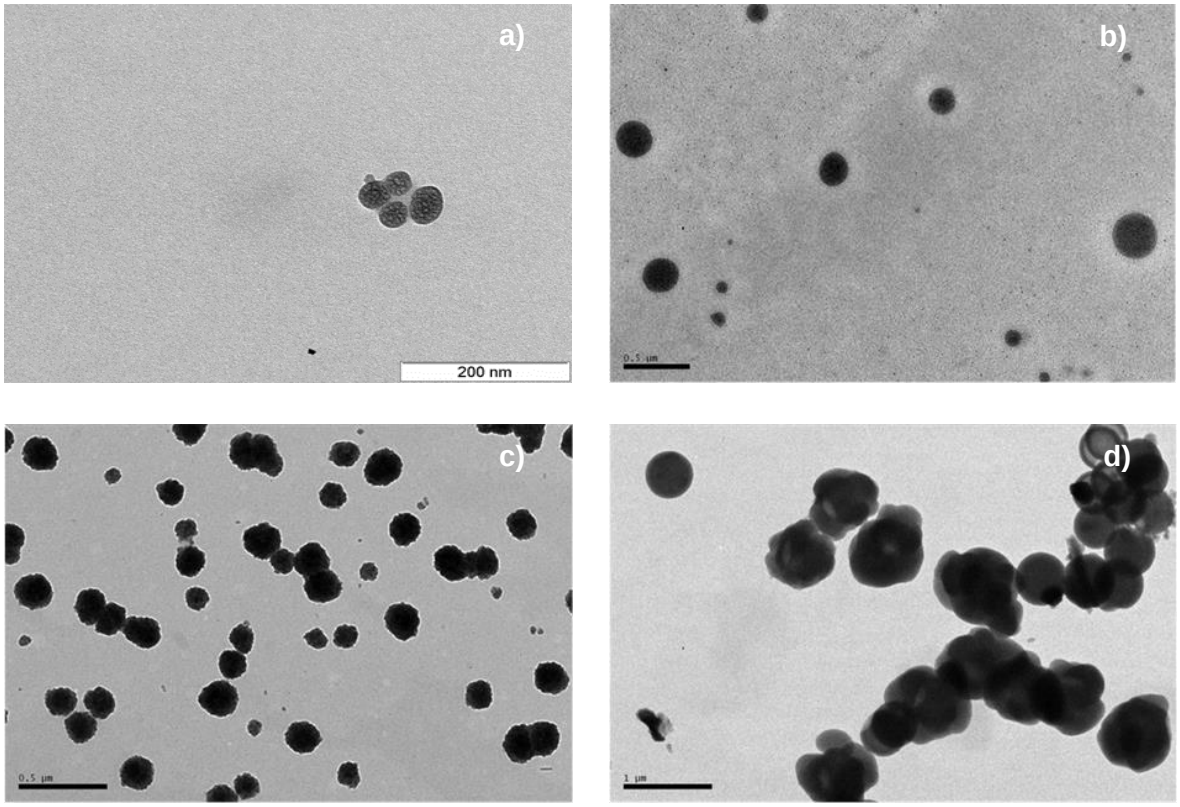


**Figure 2.13**. TEM images of **a)** $[C_2C_1Im][C_4F_9SO_3]$ at a concentration 2.5 times higher than CMC (4), **b)** $[C_6C_1Im]$ $[C_4F_9SO_3]$ at a concentration 2 times higher than CMC, **c)** $[C_8C_1Im]$ $[C_4F_9SO_3]$ at a concentration 4 times higher than CMC and **d)** $[C_{12}C_1Im]$ $[C_4F_9SO_3]$ at a concentration 4 times higher than CMC. The scales of images are 200 nm, 0.5 µm, 0.5 µm and 1 µm, respectively.

Analyzing the results, it is possible to see that aggregates size increases with the increment of the hydrogenated alkyl chain length. The $[C_2C_1Im][C_4F_9SO_3]$ and $[C_6C_1Im]$ $[C_4F_9SO_3]$ yield a more spherical micelle shape whereas $[C_8C_1Im][C_4F_9SO_3]$ and $[C_{12}C_1Im]$ $[C_4F_9SO_3]$ seem to form micelles growing from spherical to globular.

## 2.5. Conclusions

The main objective of this chapter was to characterize the $[C_4C_1Im][C_4F_9SO_3]$ and $[C_{10}C_1Im]$ $[C_4F_9SO_3]$ FILs in order to expand the knowledge on the perfluorobutanesulfonate-based FILs, and to

assess their most remarkable features in the selection of the most suitable FIL for biomedical applications. Thermal and thermophysical properties, as well as their behaviour on aqueous solutions were studied. The results were compared with other members of the $[C_nC_1Im][C_4F_9SO_3]$ family to understand how the increment of the hydrogenated side-chain of the imidazolium cation (n=2, 4, 6, 8, 10, and 12) could influence the behaviour of these FILs.

Taking into account the thermal properties, both $[C_4C_1Im][C_4F_9SO_3]$ and $[C_{10}C_1Im]$ $[C_4F_9SO_3]$ showed a good thermal stability and higher decomposition temperatures. Then, they can be liquid in a large range of temperatures and yet not decompose. Moreover, the melting temperatures increased with the increment of the hydrogenated alkyl side-chain length and the opposite behaviour was observed for the decomposition temperatures, as expected. The $[C_4C_1Im][C_4F_9SO_3]$ showed to be a better option in comparison with $[C_{10}C_1Im][C_4F_9SO_3]$ when analysing the thermophysical and thermochemical properties here reported. In the range of temperatures studied, the increase in the hydrogenated alkyl side-chain length lead to a decrease on densities and fluidity, being the $[C_4C_1Im][C_4F_9SO_3]$ with a density ($\approx$1.44 $g{\cdot}cm^{-3}$) and fluidity (0.01-0.05 $mPa^{-1}{\cdot}s^{-1}$) closer to PFCs 1.7 $g{\cdot}cm^{-3}$ and 0.19-1.67 $mPa^{-1}{\cdot}s^{-1}$, respectively. Moreover, conductivities proven to be better for fluorinated ionic liquids with short hydrogenated alkyl side chain lengths showing higher ionicity.

The aggregation behaviour was here evaluated by measurements of CMC and characterized by electron microscopy. The FILs with long hydrogenated chains have smaller CMC and form more stable and organized micelles. These self-assemblies could influence the solubility of FILs in aqueous solution since they have distinct rearrangements depending on the hydrogenated chain length. These findings corroborate the results from LLE in which the FILs solubility in the water phase appears to be closely linked to the hydrogenated chain length: up to $[C_6C_1Im]^+$ / $[C_8C_1Im]^+$ the solubility increases and then a further increase on the alkyl chain leads to a increment on the solubility.

## 2.6. References

**(1)** Pereiro A. B. et al. Fluorinated Ionic Liquids: Properties and Applications. *ACS Sustain. Chem. Eng.* **2013**, 1, 427–439.

**(2)** Tariq, M.; Forte, P. A. S.; Gomes, M. F. C.; Lopes, J. N. C; Rebelo, L. P. N. Densities and Refractive Indices of Imidazolium- and Phosphonium-based Ionic Liquids: Effect of Temperature, Alkyl Chain Length, and Anion. *J. Chem. Thermodyn.* **2009**, 41, 790–798.

**(3)** Vieira, N. S. M. et al. A Thermophysical and Structural Characterization of Ionic Liquids with Alkyl and Perfluoroalkyl Side Chains. *RSC Adv.* **2015**, 5, 65337–65350.

**(4)** Pereiro, A. B.; Araújo, J. M. M.; Teixeira, F. S.; Marrucho, I. M.; Piñeiro, M. M; Rebelo, L. P. N. Aggregation Behavior and Total Miscibility of Fluorinated Ionic Liquids in Water. *Langmuir*. **2015**, 31, 1283–1295.

**(5)** Vieira, N. S. M. et al. Fluorination Effects on the Thermodynamic, Thermophysical and Surface Properties of Ionic Liquids *J. Chem. Thermodyn.* **2016**, 97, 354–361.

**(6)** Krafft, M. P.; Riess, J. G. Perfluorocarbons: Life Sciences and Biomedical Uses. *J. PJ Polym. Sci. Part B: Polym. Phys.* **2007**, 45, 1185–1198.

**(7)** Jin, W. et al. Self-assembly Induced Solubilization of Drug-like Molecules in Nanostructured Ionic Liquids. *Chem. Commun*. **2015**; 51, 13170–13173.

**(8)** Marrucho, I. M.; Branco, L. C.; Rebelo, L. P. N. Ionic Liquids in Pharmaceutical Applications. *Annu. Rev. Chem. Biomol. Eng.* **2014**, 5, 527–546.

**(9)** Fukumoto, K.; Yoshizawa, M.; Ohno, H. Room Temperature Ionic Liquids from 20 Natural Amino Acids. *J. Amer. Chem. Soc.* **2005**, 127, 2398–2399.

**(10)** Łuczak, J; Paszkiewicz, M.; Krukowska, A.; Malankowska, A.; Zaleska-Medynska, A. Ionic liquids for Nano- and Microstructures Preparation. Part 1: Properties and Multifunctional Role. *Adv. Colloid Interface Sci*. 2016, 230, 13–28.

**(11)** Phillips, J. N. The Energetics of Micelle Formation. *Trans. Faraday Soc.* **1955**, 51 ,561-569.

**(12)** Plechkova, N. V.; Seddon, K. R. Applications of Ionic Liquids in the Chemical Industry. *Chem. Soc. Rev.* **2008**, 37, 123–150.

**(13)** Riess, J. G.; Krafft, M. P. Fluorinated Materials for *In vivo* Oxygen Transport (Blood Substitutes), Diagnosis and Drug Delivery. *Biomaterials*. **1998**, 19, 1529–1539.

**(14)** Krafft, M. P. Fluorocarbons and Fluorinated Amphiphiles in Drug Delivery and Biomedical Research. *Adv. Drug Deliv. Rev.* **2001**, 47, 209–228.

**(15)** Owens, C. D.; Rybicki, F. J.; Wake, N.; Schanzer, A.; Gerhard-herman, M. D.; Conte, M. S. Early Remodelling of Lower Extremity Vein Grafts: Inflammation Influences Biomechanical Adaption. *J. Vasc. Surg.* **2008**, 47, 1235–1242.

**(16)** Dias, A. M. A. et al. Densities and Vapor Pressures of Highly Fluorinated Compounds. *J. Chem. Eng. Data.* **2005**, 50, 1328–1333.

**(17)** Melorose, J.; Perroy, R.; Careas, S.; Endothelium : molecular aspects of metabolic disorders. *CRC Press*. **2015**.

**(18)** Freire, M. G.; Ferreira, A. G. M.; Fonseca, I. M. A.; Marrucho, I. M.; Coutinho, J. A. P. Surface Tension of Liquid Fluorocompounds. *J. Chem. Eng. Data.* **2008**, 53, 538–542.

**(19)** Rodríguez, H.; Brennecke, J. Temperature and Composition Dependence of the Density and Viscosity of Binary Mixtures of Water + Ionic Liquid. *J. Chem. Eng.* **2006**, 2145–2155.

**(20)** Ge, M.; Ren, X.; Song, Y. Densities and Viscosities of 1-Propyl-2,3-dimethylimidazolium Tetrafluoroborate + H2O at T = (298.15 to 343.15) K. 1400 *J. Chem. Eng. Data* **2009**, 54, 1400–1402.

**(21)** Carvalho, P. J.; Regueira, T.; Santos, L. M.; Fernandez, J; Coutinho J. A. P. Effect of Water on the Viscosities and Densities of 1-Butyl-3-methylimidazolium Dicyanamide and 1-Butyl-3-methylimidazolium Tricyanomethane at Atmospheric Pressure. *J. Chem. Eng. Data.* **2010**, 55, 645–652.

**(22)** Neves, C. M. S. S.; Carvalho, P. J.; Freire, M. G.; Coutinho, J. A. P. Thermophysical Properties of Pure and Water-saturated Tetradecyltrihexylphosphonium-based Ionic Liquids. *J. Chem. Thermodyn.* **2011**, 43, 948–957.

**(23)** Walden P. *Organic Solutions - and Ionisation Mean III. Chapter: Internal Friction and It Connection with Conductivity*. Plenum Press, **1906**.

**(24)** MacFarlane, D. R.; Forsyth, M.; Izgorodina, E. I; Abbott, A. P.; Annat, G.; Fraser, K. On the Concept of Ionicity in Ionic Liquids. *Phys. Chem. Chem. Phys.* **2009**, 11, 4962–4967.

**(25)** Ueno, K.; Tokuda, H; Watanabe, M. Ionicity in Ionic Liquids: Correlation with Ionic Structure and Physicochemical Properties. *Phys. Chem. Chem. Phys.*, **2010**, 12, 1649–1658.

**(26)** Florindo, C. et al. Evaluation of Solubility and Partition Properties of Ampicillin-based Ionic Liquids. *Int. J. Pharm.* **2013**, 456, 553–559.

**(27)** Papaiconomou, N et al. The Effect of Position and Length of Alkyl Substituents in Pyridinium based Ionic Liquids on Temperature Dependent Transport Properties *Electrochim. Acta.* **2012**, 70, 124–130.

**(28)** Xu, W.; Cooper, E. I.; Angell, C. A. Ionic Liquids: Ion Mobilities, Glass Temperatures, and Fragilities. *J. Phys. Chem. B.* **2003**, 107, 6170–6178.

**(29)** Martinho, S.; Araújo, J. M. M.; Rebelo, L. P. N.; Pereiro, A. B.; Marrucho, I. M. (Liquid + liquid) Equilibria of Perfluorocarbons with Fluorinated Ionic Liquids. *J. Chem. Thermodyn.* **2013**, 64, 71–79.

**(30)** Teixeira, F. S. et al. Phase Equilibria and Surfactant Behavior of Fluorinated Ionic Liquids with Water. *J. Chem. Thermodyn.* **2015**, 82, 99–107.

**(31)** Najdanovic-Visak, V.; Lopes, J. N. C.; Visak, Z. P.; Trindade, J.; Rebelo, L. P. N. Salting-out in Aqueous Solutions of Ionic Liquids and $K_3PO_4$: Aqueous Biphasic Systems and Salt Precipitation. *Int. J. Mol. Sci.* **2007**, 8, 736–748.

**(32)** Freire, M. G.; Neves, C. M. S. S.; Lopes, J. N. C.; Marrucho, I. M.; Coutinho, J. A. P.; Rebelo, L. P. N. Impact of Self-Aggregation on the Formation of Ionic-Liquid-Based Aqueous Biphasic Systems. *J. Phys. Chem. B.* **2012**, 116, 7660-7668.

**(33)** Luís, A. et al. Influence of Nanosegregation on the Surface Tension of Fluorinated Ionic Liquids. *Langmuir*. **2016**, 32, 6130−6139.

**(34)** Pereiro A. B. et al. On the Formation of a Third, Nanostructured Domain in Ionic Liquids. *J. Phys. Chem. B.* **2013**, 117, 10826–10833.

**(35)** Shen, Y. et al. Protic Ionic Liquids with Fluorous Anions: Physicochemical Properties and Self-assembly Nanostructure. *Phys. Chem. Chem. Phys.* **2012**, 14, 7981-7992.

**(36)** Sivapragasam, M.; Moniruzzaman, M.; Goto, M. Recent Advances in Exploiting Ionic Liquids for Biomolecules: Solubility, Stability and Applications. *Biotechnol. J.* **2016**, 1–14.

**(37)** González-Pérez, A.; Ruso, J. M.; Prieto, G.; Sarmiento. F. Apparent Molar Quantities of Sodium Octanoate in Aqueous Solutions. *J. M. Colloid Polym. Sci.* **2004**, 282, 1133–1139.

**(38)** López-Fontán, J. L.; Sarmiento, F.; Schulz, P. The Aggregation of Sodium Perfluorooctanoate in Water. *Colloid Polym. Sci.* **2005**, 283, 862–871.

**(39)** Szajdzinska-Pietek, E.; Wolszczak, M. Time-Resolved Fluorescence Quenching Study of Aqueous Solutions of Perfluorinated Surfactants with the Use of Protiated Luminophore and Quencher. *Langmuir*. **2000**, 16, 1675-1680.

**(40)** Krafft, M. P.; Chittofrati, A.; Riess, J. G. Synthesis of Ordered Mesoporous Materials using Surfactant Liquid Crystals or Micellar Solutions. *Colloid and Interface Sci.* **2003**, 8, 145-155.

# 3.Partition Properties of Fluorinated Ionic Liquids

## 3.1 Introduction

Understanding the permeability of ionic liquids in both aqueous (hydrophilic) and biological media (lipophilic) is essential to assess biopharmaceutical properties, toxicity, bioavailability, activity, or ecological effects (1). An emerging research field of interest is the use of ionic liquids in pharmaceutical applications. The potential of ILs as pharmaceutical solvents to dissolve poorly soluble Active Pharmaceutical Ingredients (API) has been reported (2). Additionally, their use as drug delivery vehicles has been investigated (3-5). Moreover, some works have taken a further step in developing ILs that are themselves the API (6-8). For example, a potential drug candidate has to cross several barriers until reach his target. These barriers can be summarized as absorption, distribution, metabolism and excretion (ADME). An early prediction of such parameters can serve as an indication of the most suitable ILs to be developed for pharmaceutical applications (9).

One of the core properties required to estimate absorption, distribution and transport in biological systems is lipophilicity, also designated as lipophilicity/hydrophobicity balance. Lipophilicity is referred to the ability of a compound to dissolve in fats, oils, lipids and general non-polar solvents (9). The determination of the 1-octanol/water partition coefficient ($K_{ow}$) is the most common method to assess the lipophilicity/hydrophobicity balance of a compound (10). By definition, $K_{ow}$ represents the difference in solubility of a given compound between 1-octanol and water at given temperature (11). If a compound is dissolved in a 1-octanol/water biphasic system, equilibrium is reached after a certain period of time for both phases at a certain temperature. Thus, during the prevalence of equilibrium distribution of the compound under study between the 1-octanol rich phase and the water rich phase, activity will be same in both the phases (11).

Additionally, 1-octanol is an amphiphilic solvent which possesses a relative permittivity almost comparable to the phospholipids found in biological membranes (7). The $K_{ow}$ value is calculated according to **Equation 3.1.** and it represents the ratio of the compound concentrations in both water rich-phase ($C_i^W$) and 1-octanol rich-phase ($C_i^O$) when equilibrium is reached (12). If the compound is in the 1-octanol phase, it means that has a lipophilic behaviour (Log $K_{ow}$ > 0). However, if the compound is mainly on the water phase, it can be classified as hydrophilic (Log $K_{ow}$ < 0),(7). see **Figure 3.1.**

$$\boldsymbol{K_{ow} = \frac{C_i^O}{C_i^W}} \qquad \textbf{Equation 3.1}$$

For ionisable species such as ionic liquids, three forms of distribution in both aqueous and organic solvent phases can be found: intact ion pair, loose ion pair or ion separation by the solvent (13). The intact ion par form is the most accurate to evaluate $K_{ow}$ values, yet extreme dilute solutions are needed to ensure that the coefficients should not change with small concentration variation (11,12).

Different experimental approaches have been developed to measure the partition coefficients. Indirect measurements, such as estimations by high-performance liquid chromatography (HPLC) and the generator column method, are based on the compound chemical affinity for each column phase (14). For example, in the HPLC method the affinity for each phase is measured by comparing the retentions times of the test compound with retentions times of several reference chemicals and it is the correlation established between the reference chemicals that is used to calculate the $K_{ow}$ values. However, this technique is only recommended for test compounds with $K_{ow}$ values greater than one (14). In the generator column method, water presaturated with 1-octanol is slowly passed through a column packed with a solid support and coated with octanol containing small amounts of the test chemical. However, the test chemical can interact with the column packing and induce errors on the measurements (15). Direct measurements, such as the *Shake Flask* and *Slow Stirring* methods, are the most recommended (14). In the *Shake Flask*, octanol and water are mutually saturated and the test compound is placed directly in the same container tube which is then centrifuged to separate the phases. Then, the concentrations of the test chemical are measured in each phase individually. However, even after centrifugation microdroplets of 1-octanol may remain in the water phase resulting in erroneous $K_{ow}$ values (12,16).

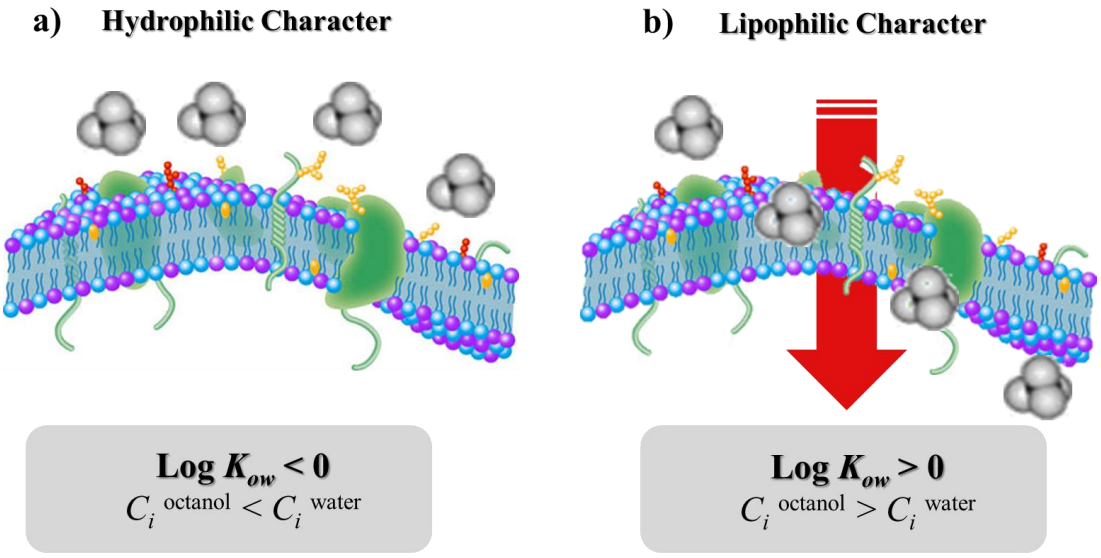


**Figure 3.1.** Representation of the **a)** hydrophilic and **b)** lipophilic characters of ILs according to Log $K_{ow}$ values.

The method used in this study was the *Slow Stirring* because it produces accurate results in a wide range of values without the need of complex equipment (17). In this approach, a small amount of the compound is mixed in either water or 1-octanol pre-saturated and slowly stirred in a vial. Hence, the stagnant diffusion layer between the phases is minimized and also the smooth agitation can prevent emulsification (14). After the concentrations in each phase have stabilized, the $K_{ow}$ value is determined. Moreover, this method as the advantage of evaluating the diffusion of the compounds over time by using samples replicates (18).

## 3.2 Materials

1-Ethyl-3-methylpyridinium perfluorobutanesulfonate, >99% mass fraction purity, 1-ethyl-3-methylimidazolium perfluorobutanesulfonate, >97% mass fraction purity, 1-hexyl-3-methylimidazolium perfluorobutanesulfonate, >99% mass fraction purity, 1-octyl-3-methylimidazolium perfluorobutanesulfonate,], > 98% mass fraction purity, 1-ethyl-3-methylimidazolium perfluorooctanesulfonate, >98% mass fraction purity were acquired from IoLiTec. 1-Butyl-3-methylimidazolium perfluorooctanesulfonate was synthetized in our lab by a ion exchange resin method (19). Structures and acronyms are listed in **Table 3.1.**.

**Table 3.1.** Designation and chemical structure of each fluorinated ionic liquid used in this study.

| FIL Designation | Chemical Structure |
|---|---|
| 1-Ethyl-3-methypyridinium perfluorobutanesulfonate **[$C_2C_1$py] [$C_4F_9SO_3$]** | 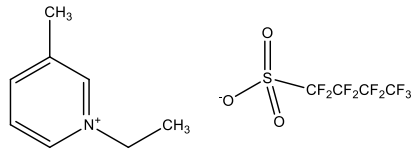 |
| 1-Ethyl-3-methylimidazolium perfluorobutanesulfonate **[$C_2C_1$Im][$C_4F_9SO_3$]** | 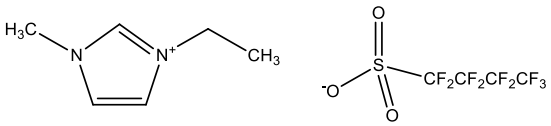 |
| 1-Butyl-3-methylimidazolium perfluorobutanesulfonate **[$C_4C_1$Im][$C_4F_9SO_3$]** | 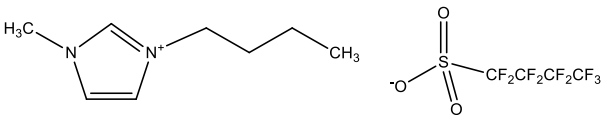 |
| 1-Hexyl-3-methylimidazolium perfluorobutanesulfonate **[$C_6C_1$Im][$C_4F_9SO_3$]** | 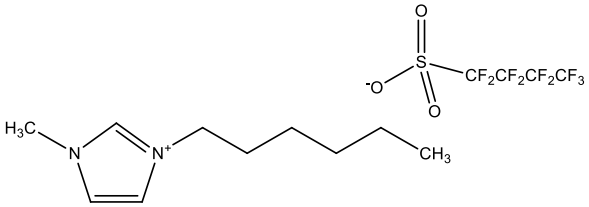 |
| 1-Octyl-3-methylimidazolium perfluorobutanesulfonate **[$C_8C_1$Im][$C_4F_9SO_3$]** | 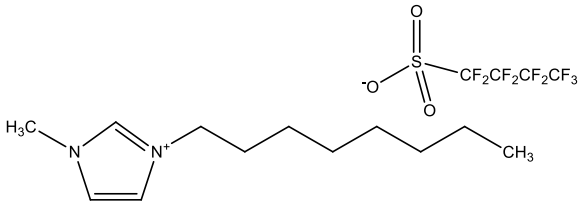 |
| 1-Ethyl-3-methylimidazolium perfluoroctanesulfonate **[$C_2C_1$Im][$C_8F_{17}SO_3$]** | 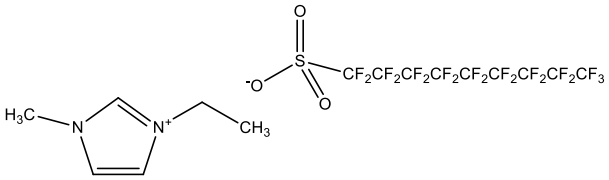 |

The purity of the ionic liquids was analyzed by $^{1}H$, $^{13}C$ and $^{19}F$ NMR. In order to reduce volatile impurities, all fluorinated ionic liquids were dried under a $3 \cdot 10^{-2}$ Torr vacuum and vigorous stirring at

323.15K for at least 48 hours prior to their use. The water content of FILs used in this work was determined using Karl Ficher coulometric titration method (Metrohm 831 KF Coulometer) and it was less than 100 ppm. 1-Octanol ACS reagent, ≥ 99% purity, from Sigma-Aldrich and Milli-Q ultrapure water (Milli-Q Integral Water Purification System) were used in all experiments throughout the work.

## 3.3 Experimental Procedure

In order to mutualy saturate the water and 1-octanol phases, an equal quantity of both substances were vigorously mixed in a separation funnel and left to stand for at least 72 hours. Due to the immiscibility of these components, two distinguishable phases were observed corresponding to water saturated with 1-octanol (top) and 1-octanol saturated with water (bottom). To evaluate if both phases were completely saturated / separated, the density of water and 1-octanol phases were measured with an Anton Paar vibrating tube densimeter, model DMA 5000. The values were obtained at atmospheric pressure and 298.15 K. The effect of viscosity was considered in all experimental measurements using the internal calibration. The temperature was controlled by several Peltier units and the cell was embedded in a cavity inside a metallic block. This equipment allowed a temperature stability of 0.002 K. Duplicates were measured and the repeatability and expanded uncertainty of the density is better than $5 \cdot 10^{-5}$ and $\pm\ 3 \cdot 10^{-4}$ g·cm$^{-3}$, respectively.

### 3.3.1. *Slow stirring* Method

Three stock solutions containing 1-octanol saturated with water and a known quantity of each FIL were prepared in order to evaluate the diffusion of the compounds over time. The concentrations varied from $1.14 \cdot 10^{-4}$ mol/L to $1.76 \cdot 10^{-3}$ mol/L. Then, a glass vial, containing a magnetic stiring bar and an open top screw-cap sealed with a silicone septum, was filled with 5 mL of water saturated in 1-octanol and the same quantity of stock solution. To prevent the contamination of each phase during sampling, a sealed syringe was inserted in the system as shown in **Figure 3.2. a)**. The vials were placed in an ethylene glycol bath with a controlled temperature of 298.15 K (± 2 K) and stirred slowly to prevent emulsification as represented in **Figure 3.2. b)**.

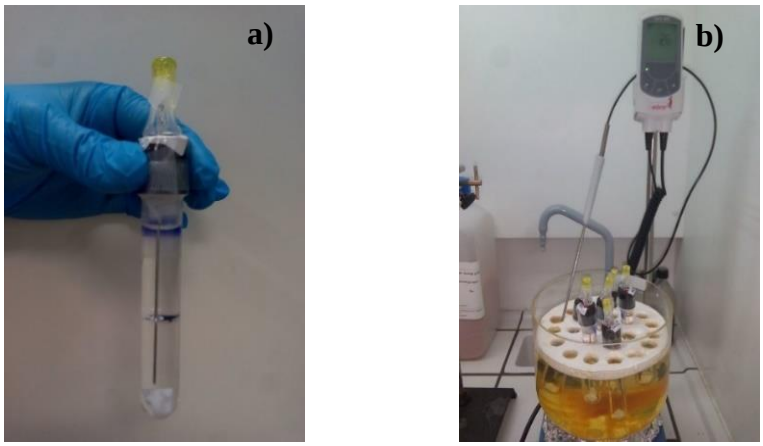


**Figure 3.2.** Representation of the **a)** sample vial preparation and **b)** apparatus for the *Slow Stirring* method used in this work.

Samples were collected between 7 and 57 days. The sampling process was carried out until the concentrations in both phases were stabilized and $K_{ow}$ values no longer changed with time. After samples from both phases were carefully collected, the octanol-rich phase was centrifuged for 1 hour at 3720 rpm and 277.15 K in an VWR® Mega Star 600 R Centrifuge (see **Figure 3.3. a)**). This process eliminated possible micellization of FILs in the octanol phase (18).

All the FIL concentrations were measured using a VWR® spectrophotometer, model UV-6300PC illustrated in **Figure 3.3. b)** This technique detects the maximum absorbance, Abs, of the aromatic rings on the cation at approximately 212 nm for imidazolium cation and 266 nm for pyridinium cation with an uncertainty of 1%. The samples were diluted prior to measurements to ensure that the measured absorbance was less than 1.2.

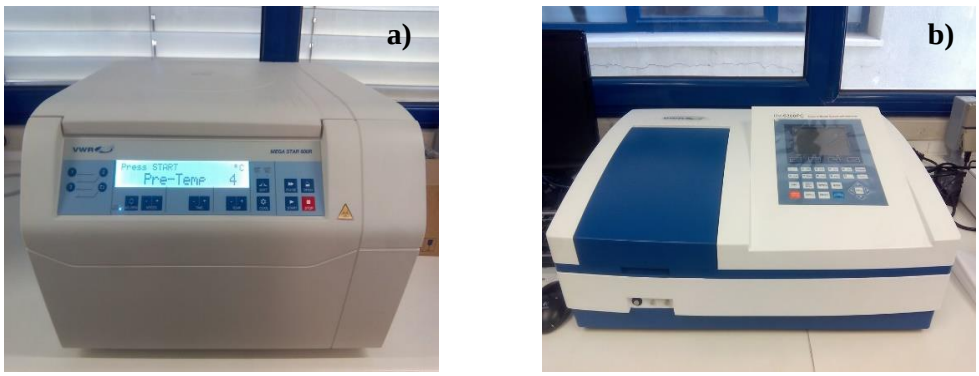


**Figure 3.3. a)** VWR® Mega Star 600 R Centrifuge and **b)** VWR® spectrophotometer, model UV-6300PC.

## 3.4 Results and Discussion

In this section, the effect in the $K_{ow}$ values of two different cations, imidazolium and pyridinium, as well as the increment of hydrogenated alkyl side chain length of the imidazolium cation and the increment of the fluorinated alkyl side chain length of the anion were investigated. In **Table 3.2.** FIL concentrations in water and octanol phases are showen as well as the respective $K_{ow}$ values calculated by **Equation 3.1.**.

**Table 3.2.** $K_{ow}$ values and FIL initial concentration on 1-octanol-rich phase.

| FIL | Initial FIL concentration in 1-octanol-rich phase (mol/L) | $K_{ow}$ |
|---|---|---|
| $[C_2C_1py]$ $[C_4F_9SO_3]$ | $1.86\cdot10^{-4} – 5.30\cdot10^{-4}$ | 0.04 ± 0.007 |
| $[C_2C_1Im][C_4F_9SO_3]$ | $2.71\cdot10^{-4} – 1.76\cdot10^{-3}$ | 0.24 ± 0.01 |
| $[C_4C_1Im][C_4F_9SO_3]$ | $1.14\cdot10^{-4} – 4.56\cdot10^{-4}$ | 0.43 ± 0.04 |
| $[C_6C_1Im][C_4F_9SO_3]$ | $1.70\cdot10^{-4} – 2.83\cdot10^{-4}$ | 0.76 ± 0.06 |
| $[C_8C_1Im][C_4F_9SO_3]$ | $1.62\cdot10^{-4} – 4.62\cdot10^{-4}$ | 1.39 ± 0.05 |
| $[C_2C_1Im][C_8F_{17}SO_3]$ | $1.23\cdot10^{-4} – 4.25\cdot10^{-4}$ | 3.78 ± 0.06 |

In **Figure 3.3.** it is possible to observe the trends of the $K_{ow}$ values with the studied range of FILs concentrations. In all cases no substantial differences were found. Then it can be concluded that for the range of concentrations herein studied, $K_{ow}$ is concentration independent and can be determined.

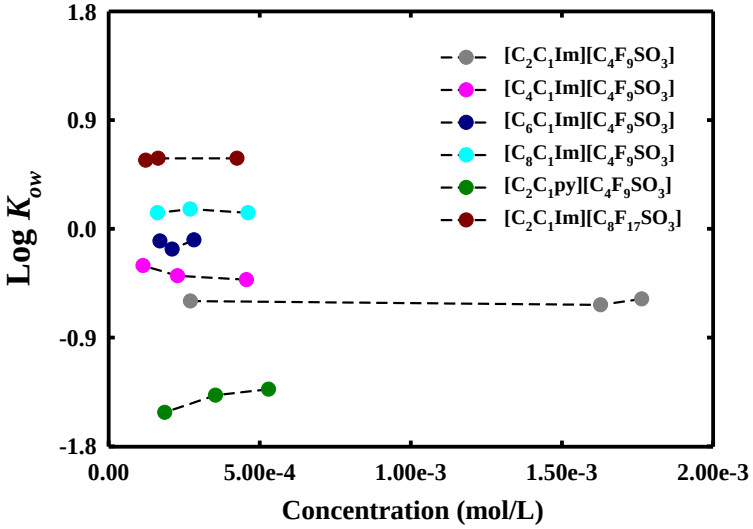


**Figure 3.3.** Variation of $K_{ow}$ with concentration for the studied FILs.

The influence of the alkyl side chain length of the imidazolium cation on the $K_{ow}$ value is also an important parameter to take in to consideration. Thus, the [$C_nC_1Im$] [$C_4F_9SO_3$] family ($n$=2, 4, 6 and 8) was studied. Taking the analysis of the results into consideration (see **Figure 3.4.**), it is possible to verify that the increment of the alkyl side chain provides an increase on $K_{ow}$ values. By definition, if the $K_{ow}$ is ≥ 1 (Log Kow > 0) it is expected that all the test compound remain in the octanol-phase (see **Equation 3.1**) demonstrating a lipophilic behaviour (12). Thus, a trend regarding lipophilicity of the test compounds could be made, since alkyl chains higher than an octyl ($n$=8) could be considered lipophilic.

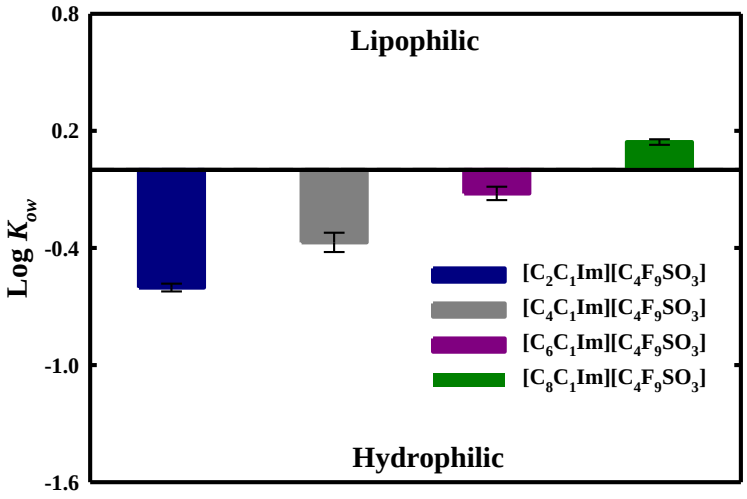


**Figure 3.4.** Influence of the imidazolium hydrogenated side-chain length on $K_{ow}$ values.

A change from [$C_2C_1Im$][$C_4F_9SO_3$] to [$C_8C_1Im$][$C_4F_9SO_3$] leads to an increase of lipophilicity with a $K_{ow}$ approximately 6 times higher. This behaviour is explained since alkyl chain length of the cationic

ring creates strong van der Waals interactions between the alkyl group of the FIL and the hydrophobic part of 1-octanol (11,18). These results are consistent with the findings of other authors for conventional ILs with fluorinated anions such as bis(trifluoromethylsulfonyl)imide, $[NTf_2]^-$, (20) hexafluorophosphate, $[PF_6]^-$, and tetrafluoroborate, $[BF_4]^-$ (21) as well as for ionic liquids in general (12, 14). Moreover, Ropel *et al*. reported that solubility of imidazolium based ionic liquids in alcohols increases with alkyl chain length (18).

The distribution and position of the fluorine atoms, as well as the amount of fluorination, are known to affect the lipophilic behaviour (22). Therefore, the effect of changing a perfluorobutanesulfonate, $[C_4F_9SO_3]^-$, for a perfluoroctanesulfonate anion, $[C_8F_{17}SO_3]^-$, was analysed. The increase of the fluorinated chain length of the anion promotes an extreme decrease of the hydrophilicity. The $K_{ow}$ value for the $[C_8F_{17}SO_3]$-based FIL is approximately 16 times higher than the $[C_4F_9SO_3]$-based FIL, as shown in **Figure 3.5.**.

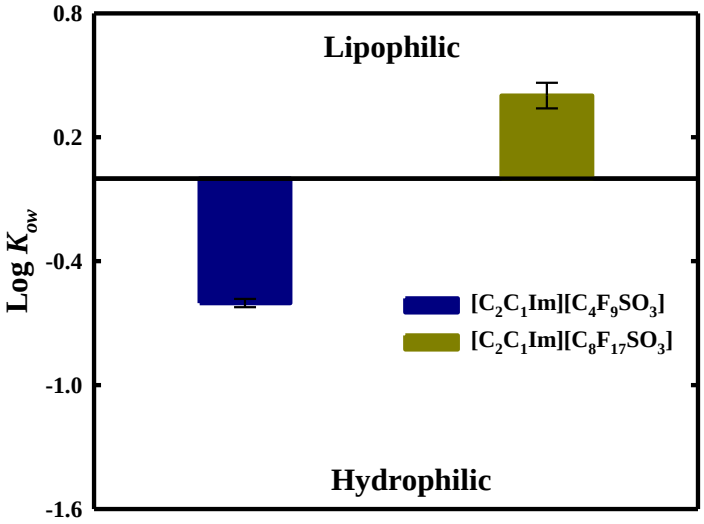


**Figure 3.5.** Influence of the fluorinated chain length on $K_{ow}$ values.

These trends are consistent with the literature and follow an empirical rule which dictates that a fluorine content representing ca. 60% of the total molecular weight can influence the hydrophilicity behaviour of the compound (23). In this case, the $[C_2C_1Im][C_4F_9SO_3]$ exhibited 41.6 %*w*t and $[C_2C_1Im][C_8F_{17}SO_3]$ 52.9 %*wt*. Purser *et al*. reported that aromatic fluorination, per/polyfluorination and fluorination adjacent to atoms with π-bonds (as present on the imidazolium cation) exponentially increases lipophilicity (24). This behaviour is due to the excellent overlap between the fluorine 2s or 2p orbitals with the corresponding orbitals on carbon, making the C–F bond highly non-polarizable, thereby contributing to increased lipophilicity (24). In addition, the $K_{ow}$ of 1-butyl-3-methyilimidazolium trifluoromethylsulfonate $[C_4C_1Im][CF_3SO_3]$ was not measured in this work but can be found in the literature with a value of 0.20 (20). Thus, comparing our measurements for $[C_4C_1Im][C_4F_9SO_3]$, with a $K_{ow}$ of 0.43, the same trend can be seen. The over methylation and fluorination of the cation enhances FIL solubility in lipophilic constituents which will allow their entry in cells (10,22).

The last study was carried out in order to understand how the cationic ring present in FILs can influence the hydrophilicity. Considering $[C_4F_9SO_3]$-based FILs, the imidazolium ($[C_2C_1Im]^+$) and pyridinium ($[C_2C_1py]^+$) cations were compared. Both ionic liquids present a highly hydrophilic behaviour (see **Figure 3.6.**). In the literature, the same trend for imidazolium and pyridinium-based ILs was observed (20,21). Montalbán et *al*. mesured the $K_{ow}$ for $[C_4C_1py][BF_6]$ and $[C_4C_1Im][BF_6]$ (21) and Lee *et al*. for $[C_6C_1py][NTf_2]$ and $[C_6C_1Im][NTf_2]$(20). Both authors demonstrated that the $K_{ow}$ of imidazolium-based ILs are slightly higher when compared to pyridinium.

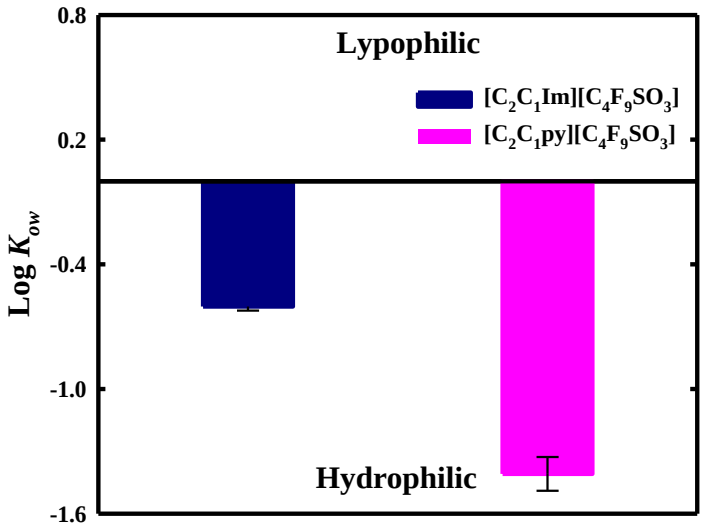


**Figure 3.6.** Evaluation of $K_{ow}$ values for imidazolium and pyridinium $[C_4F_9SO_3]$-based FILs.

## 3.5 Conclusion

Compounds with low $K_{ow}$ can prevent bioaccumulation on human cells and ensure a suitable circulation of the compounds in the blood stream (10). Thus, $[C_2C_1Im][C_4F_9SO_3]$ and $[C_2C_1py][C_4F_9SO_3]$ with $K_{ow} \leq 0.3$ are the most suitable FILs for the development of a drug coating device. For instance, using those FILs drugs are delivered into the tissues but the compounds are kept in the blood stream. On the other hand, if an API is conjugated with a FIL a high $K_{ow}$ ($[C_2C_1Im][C_8F_{17}SO_3]$ or $[C_8C_1Im][C_4F_9SO_3]$) is required. In this way, the FIL enhance the permittivity of the drug though cellular membranes (6).

For the $[C_nC_1Im][C_4F_9SO_3]$ family, a further increase of the alkyl chain length (up to an octyl, $n$=8), FILs concentrations in octanol are higher suggesting a lipophilic behaviour. Concerning the anionic fluorinated chain, when comparing $[C_4F_9SO_3]^-$ and $[C_8F_{17}SO_3]^-$ anions the $K_{ow}$ values were approximately 15 times higher. Thus, by increasing fluorination on the FIL anion lipophilicity is enhanced. Finally, both short alkyl chain length FILs based on imidazolium and pyridinium with a perfluorobutanesulfonate anion presented a highly hydrophilic behaviour.

## 3.6 References

**(1)** Lipinski, C. A.; Lombardo, F.; Dominy, B. W.; Feeney, P. J. Experimental and Computational Approaches to Estimate Solubility and Permeability in Drug Discovery and Development Settings. *Adv. Drug. Deliv. Rev.* **2012**, 64, 4-17.

**(2)** Mizuuch, H.; Jaitely, S.; Murdan, S.; Florence, A.T. Room Temperature Ionic Liquids and Their Mixtures: Potential Pharmaceutical Solvents. *Pharm. Sci.*, **2008**, 33, 326–331.

**(3)** Moniruzzaman, M.; Kamiya, N.; Goto, M. Ionic Liquid Based Microemulsion With Pharmaceutically Accepted Components: Formulation and Potential Applications *J. Colloid Interface Sci.*, **2010**, 352, 136–142.

**(4)** Moniruzzaman, M.; Tamura, M.; Tahara, Y; Kamiya, N.; Goto, M. Ionic Liquid-in-Oil Microemulsion as a Potential Carrier of Sparingly Soluble Drug: Characterization and Cytotoxicity Evaluation. *Int. J. Pharm.*, **2010**, 400, 243–250.

**(5)** Jaitely, V.; Karatas, A.; Florence, A. T. Water-immiscible Room Temperature Ionic Liquids (RTILs) as Drug Reservoirs for Controlled Release. *Int. J. Pharm.*, **2008**, 354, 168–173.

**(6)** Araújo J. M. M.; Florindo, C.; Pereiro, A. B.; Vieira, N. M. S.; Matias, A. A.; Duarte, C. M. M.; Rebelo, L. N. R.; Marrucho, I. M. Cholinium-based Ionic Liquids with Pharmaceutically Active Anions *RSC Adv.*, **2014**, 4, 28126–28132.

**(7)** Florindo, C. et al. Evaluation of Solubility and Partition Properties of Ampicillin-based Ionic Liquids. *Int. J. Pharm.* 2013, 456, 553–559.

**(8)** Ferraz, R.; Branco, L. C. B.; Marrucho, I. M. Development of Novel Ionic Liquids Based on Ampicillin. *Med. Chem. Commun.*, **2012**, 3, 494-497.

**(9)** Boethling, R. S.; Mackay, D.; Lyman, W. J. Handbook of property estimation methods for chemicals: environmental and health sciences; **2000**, *CRC press*.

**(10)** Finizio, A.; Vighi, M.; Sandroni, D. Determination of n-Octanol/Water PartitionCoefficient ($K_{ow}$) of Pesticide: Critical Review and Comparison of Methods. *Chemosphere*. **1997**; 34; 131–161.

**(11)** Jain, P.; Kumar, A. Concentration-Dependent Apparent Partition Coefficients of Ionic Liquids Possessing Ethyl- and Bi-sulphate Anions. *Phys. Chem. Chem.* **2016**, 18, 1105–13.

**(12)** Lee, S. H.; Lee. S. B. Octanol/Water Partition Coefficients of Ionic Liquids. *J. Chem. Technol. Biotechnol.* **2009**, 84, 202–207.

**(13)** Köddrmann, T.; Reith, D.; Arnold, A. Why the Partition Coefficient of Ionic Liquids Is Concentration-Dependent. *J. Phys. Chem. B.* **2013**, 117, 10711−10718.

**(14)** Kah, M.; Brown, C. D. LogD: Lipophilicity for Ionisable Compounds. *Chemosphere*. **2008**, 72, 1401–1408.

**(15)** Poole, S. K.; Poole, C. F. Separation Methods for Estimating Octanol–Water Partition Coefficient. *J. Chromatogr. B.* **2003**, 797, 3–19.

**(16)** Ingram, T.; Richter, U.; Mehling, T.; Smirnova. I. Modelling of pH Dependent n-Octanol/Water Partition Coefficients of Ionizable Pharmaceuticals. *Fluid Phase Equilib.* **2011**, 305, 197–203.

**(17)** Bruijn, J.; Busser, F.; Seinen, W.; Hermens, J. Determination of Octanol/Water Partition

Coefficients for Hydrophobic Organic Chemicals with the "Slow-stirring" Method. *Environ. Toxicol. Chem.* **1989**, 8, 499–512.

**(18)** Ropel, L.; Belvèze, L. S.; Aki, S. N. V. K.; Stadtherr, M. A.; Brennecke, J. F. Octanol–Water Partition Coefficients of Imidazolium-based Ionic Liquids. *Green Chem.* **2005**, 7, 83–90.

**(19)** Fukumoto, K.; Yoshizawa, M.; Ohno, H. Room Temperature Ionic Liquids from 20 Natural Amino Acids. *J. Amer. Chem. Soc.* **2005**, 127, 2398–9.

**(20)** Lee, B. S.; Lin, S. T. A priori Pediction of the Octanol-Water Partition Coefficient ($K_{ow}$) of Ionic Liquids. *Fluid. Phase. Equilib.* **2014**, 363, 233–8.

**(21)** Montalbán, M. G.; Collado-González M.; Trigo, R.; Díaz, F. G. B.; Víllora, G. Experimental Measurements of Octanol-Water Partition Coefficients of Ionic Liquids. *J. Adv. Chem. Eng.* **2015**, 5.

**(22)** Jeschke, P. The Unique Role of Fluorine in the Design of Active Ingredients for Modern Crop Protection. *Chem. Bio. Chem.* **2004**, 5, 570–89.

**(23)** Ojogun, V.; Knutson, B. L.; Vyas, S.; Lehmler, H. J. Fluorophilicity of Alkyl and Polyfluoroalkyl Nicotinic Acid Ester Prodrugs. *J. Fluor. Chem.* **2010**, 131, 784–790.

**(24)** Purser, S.; Moore, P. R.; Swallow, S.; Gouverneur, V. Fluorine in Medicinal Chemistry. *Chem. Soc. Rev.* **2008**, 37, 320–330.

# 4.Kamlet-Taft Solvatochromic Parameters of Fluorinated Ionic Liquids

## 4.1 Introduction

Recently, ionic liquids are becoming of particular interest as new and highly efficient solvents or co-solvents for biomolecule-based applications due to their unique characteristics and biocompatibility (1). Using ILs can dramatically enhance solubility and stability of proteins (2), DNA (3) and enzymes (4). The key characteristics of a solvent are those that determine how it will interact with potential solutes. Polarity scales have been used to describe the affinity of solutes for molecular solvents as well as ionic liquids (5).

One of the most used polarity scales was devised by Kamlet and Taft in 1975 (6). The Kamlet-Taft method is based on the comparison of the effects on the UV-vis spectra of sets of dyes. Three polarity parameters have been proposed: the dipolarity/polarizability effects ($\pi^*$); the hydrogen bond acidity ($\alpha$), that is, hydrogen bond donation (HBD) ability; and the hydrogen bond basicity ($\beta$), that is, hydrogen bond acceptance (HBA) or electron pair donation ability to form a coordination bond (6). It should be highlighted that the hydrogen bond acceptor strength of an IL is dominated by the anion while the hydrogen bond donor ability is essentially controlled by the cation (7). However, cation-anion interactions could influence the IL's ability for hydrogen bonding (7). In addition, the Kamlet-Taft descriptors proved to be temperature dependent (8,9).

The hydrogen bond acceptor capacity, $\beta$, can be measured by comparison of $\lambda_{max}$ values for a homomorphic pair of solvatochromic dyes such as 4-nitroaniline/N,N-diethyl-4-nitroaniline. In **Figure 4.1** are illustrated the 4-nitroaniline (**Figure 4.1a)**) and the N,N-diethyl-4-nitroaniline (**Figure 4.1b)**). In red is represented the chemical bond that is the origin of the solvatochromic transition (10).

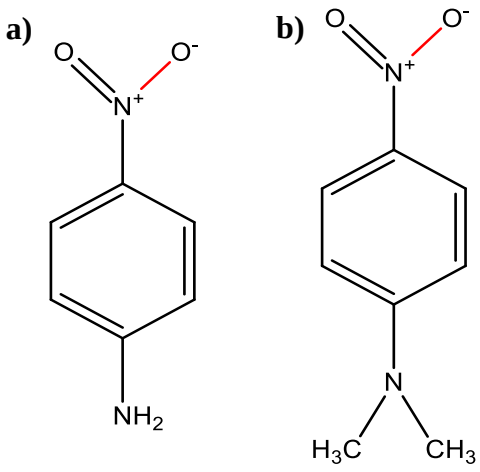


**Figure 4.1.** Chemical structures of **a)** 4-nitroaniline and **b)** N,N-diethyl-4-nitroaniline. The red line at the nitro oxygen represent the solvatochromic transition.

Measurements of the intramolecular charge-transfer $\pi \rightarrow \pi^*$ by the 4-nitroaniline and N,N-diethyl-4-nitroaniline $\lambda_{max}$ can deduce the element of wavelength change due to hydrogen bonding (10). In

**Equation 4.1.**, the relationship between the maximum absorption wavelength for the solvatochromic dyes ($\bar{\nu}$) in kilo Kysers ($cm^{-1}$), and the maximum absorption wavelength for the test compound ($\lambda_{max}$) in nanometers (nm) is represented (8).

$$\bar{\nu} = \frac{10^7}{\lambda_{max}} \qquad \textbf{Equation 4.1.}$$

The hydrogen bond acceptor ability ($\beta$) can be calculated by **Equation 4.2.** (8).

$$\beta = \frac{1.035\bar{\nu}_{N-N-diethyl-4-nitroaniline} + 2.64 - \bar{\nu}_{4-nitroaniline}}{2.80} \qquad \textbf{Equation 4.2.}$$

The method used to determine the hydrogen bond donation capacity ($\alpha$) is similar. The solvatochromic dyes used in this calculation are Reichardt's dye (2,6-Diphenyl-4-(2,4,6-triphenyl-1-pyridinio)phenolate) and 4-nitroaniline. In this case they act as a non-HBD solute. In **Figure 4.2.** is illustrated the chemical structure of Reichardt's dye as well as the chemical bond that is the origin of the solvatochromic transition (10).

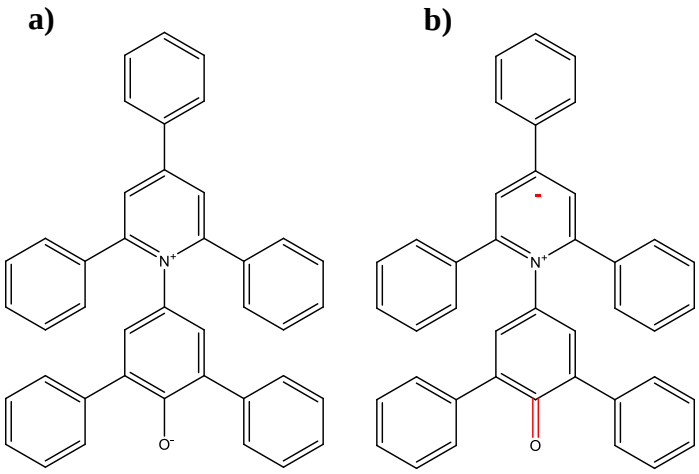


**Figure 4.2. a)** Chemical structure of Reichardt's dye and **b)** the solvatochromic transition in red.

Reichardt's dye exhibits a larger solvatochromic range. The intramolecular charge transfer $\pi \rightarrow \pi^*$ is observed around 500 nm, from $\lambda_{max}$ = 453 nm in water (polar solvent) to $\lambda_{max}$ = 925 nm in hexane (nonpolar solvent) (10). The $E_T^{30}$ is a polarity scale based only on Reichardt's dye and proposed by Dimroth *et al.* to calculate the $\alpha$ parameter of the Kamlet-Taft method as shown in **Equation 4.3.** and **Equation 4.4.** (8,10).

$$E_T^{30} = \frac{28592}{\lambda_{max}} \qquad \textbf{Equation 4.3.}$$

$$\alpha = 0.0649E_T^{30} - 2.03 - 0.72\pi^* \qquad \textbf{Equation 4.4.}$$

The dipolarity/polarizability evaluation is accomplished by the $\pi^*$-scale. The $\pi^*$ parameter is only dependent on one dye, N-N-diethyl-4-nitroaniline, and it is calculated by **Equation 4.5.** (8).

$$\boldsymbol{\pi^* = 0.314(27.52 - \bar{\nu}_{N,N-diethyl-4-nitroaniline})} \qquad \textbf{Equation 4.5.}$$

In this chapter, the hydrogen bond acidity ($\alpha$), hydrogen bond basicity ($\beta$) and dipolarity/polarizability ($\pi^*$) were first calculated to characterize pure fluorinated ionic liquids. Furthermore, the effect of water on the Kamlet-Taft parameters of FILs was evaluated to address the relevance of designing functionalized (so-called task-specific) ILs that have been synthesized with a particular application in mind.

## 4.2 Materials

1-Ethyl-3-methylimidazolium trifluoromethanesulfonate, ≥ 99% mass fraction purity; 1-butyl-3-methylimidazolium trifluoromethanesulfonate, ≥ 99% mass faction purity; 1-ethyl-3-methylpyridinium perfluorobutanesulfonate, >99% mass fraction purity; 1-ethyl-3-methylimidazolium perfluorobutanesulfonate >97% mass fraction purity; 1-hexyl-3-methylimidazolium perfluorobutanesulfonate, > 99% mass faction purity; 1-octyl-3-methylimidazolium perfluorobutanesulfonate, > 98% mass fraction purity; choline perfluorobutanesulfonate, 97% mass fraction purity; tetrabutylammonium perfluorobutanesulfonate, 98% mass fraction purity; tetrabutylammonium perfluorooctanesulfonate > 98% mass fraction purity; 1-ethyl-3-methylimidazolium acetate, > 95 % mass faction purity; 1-ethyl-3-methylpyridinium bromide, 99 % mass faction purity; 1-ethyl-3-methylimidazolium chloride, ≥ 98 %; were acquired from IoLiTec. Choline chloride, ≥ 98% mass fraction purity was acquired from Sigma-Aldrich. The purity of all ionic liquids was verified by $^{1}H$, $^{13}C$ and $^{19}F$ NMR. Prior to any use, all samples were dried under a $3 \cdot 10^{-2}$ Torr vacuum and vigorous stirring for at least 48 hours to avoid volatile impurities. Choline and acetate-based ILs were kept at 313.15 K and the remaining ILs at 323.15 K.

The water content was determined using Karl Ficher coulometric titration method (Metrohm 831 KF Coulometer) to be less than 100 ppm. The structures and acronyms of the ionic liquids are listed in **Table 4.1.**

**Table 4.1.** Designation and chemical structure of each ionic liquid used along this study.

| IL designation | Chemical structure |
|---|---|
| 1-Ethyl-3-methylimidazolium trifluoromethanesulfonate **[$C_2C_1Im$][$CF_3SO_3$]** | 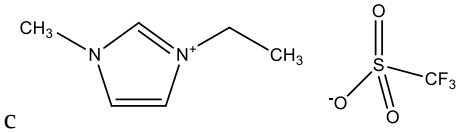 |

| IL designation | Chemical structure |
|---|---|
| 1-Butyl-3-methylimidazolium trifluoromethanesulfonate **[$C_4C_1Im$][$CF_3SO_3$]** | 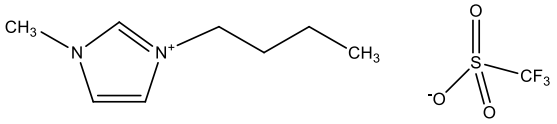 |
| 1-Ethyl-3-methylpyridinium perfluorobutanesulfonate **[$C_2C_1py$][$C_4F_9SO_3$]** | 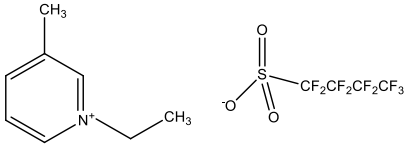 |
| 1-Ethyl-3-methylimidazolium perfluorobutanesulfonate **[$C_2C_1Im$][$C_4F_9SO_3$]** | 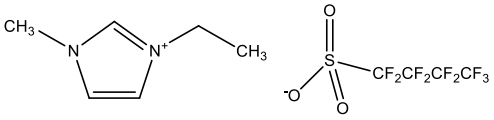 |
| 1-Hexyl-3-methylimidazolium perfluorobutanesulfonate **[$C_6C_1Im$][$C_4F_9SO_3$]** | 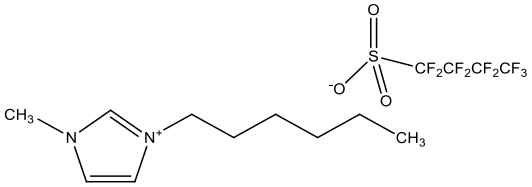 |
| 1-Octyl-3-methylimidazolium perfluorobutanesulfonate **[$C_8C_1Im$][$C_4F_9SO_3$]** | 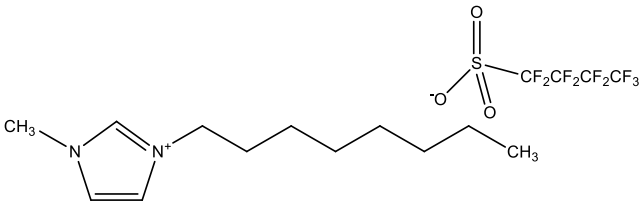 |
| Choline perfluorobutanesulfonate **[$N_{1112OH}$][$C_4F_9SO_3$]** | 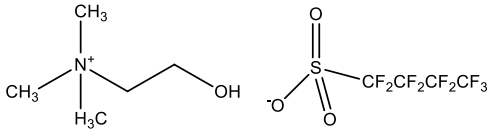 |
| Choline chloride **[$N_{1112OH}$] Cl** | 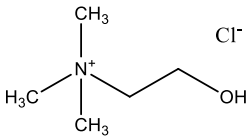 |
| Tetrabutylammonium perfluorobutanesulfonate **[$N_{4444}$][$C_4F_9SO_3$]** | 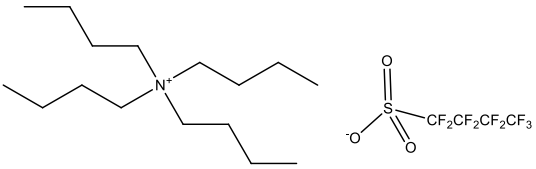 |
| Tetrabutylammonium perfluoroctanesulfonate **[$N_{4444}$][$C_8F_{17}SO_3$]** | 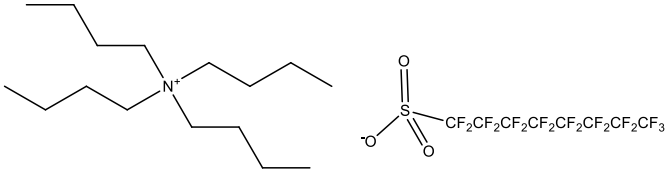 |
| 1-Ethyl-3-methylimidazolium acetate **[$C_2C_1Im$][$C_1CO_2$]** | 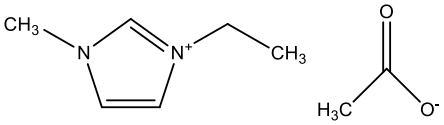 |

| IL designation | Chemical structure |
|---|---|
| 1-Ethyl-3-methylpyridinium bromide **[$C_2C_1$py] Br** | 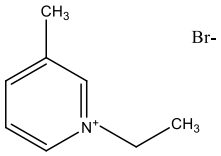 |
| 1-Ethyl-3-methylimidazolium chloride **[$C_2C_1$Im] Cl** | 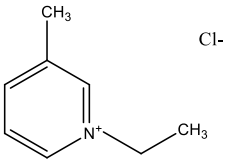 |

In order to characterize the polarity by the Kamlet-Taft method three dyes were used 4-Nitroanliline, ≥99% purity acquired from Fluka; N-N-diethyl-4-nitroaniline, ≥97% acquired from Fluorochem Ltd.; and 2,6-Diphenyl-4-(2,4,6-triphenyl-1-pyridinio)phenolate also known as Reichardt's dye, with 90% purity acquired from Sigma-Aldrich. Dichloromethane, ≥ 99.9% purity acquired from Sigma-Aldrich, was used to dilute the dyes and Milli-Q ultrapure water (Milli-Q Integral Water Purification System) to dilute the samples.

## 4.3 Experimental Procedure

### 4.3.1 Dye Solutions and Samples Preparation

The stock solutions of 4-nitroanliline, N-N-diethyl-4-nitroaniline and Reichardt's dyes were prepared using ±10 mg of dye in a glass vial and mixed with 10 mL of dichloromethane (DCM). An additional 1:10 dilution with DCM was made in the case of Reichardt's dye to ensure an absorbance less than 1.2. All the stock solutions were kept at 4ºC after their preparation to avoid DCM evaporation.

Roughly 0.34 mL of 4-nitroanliline and N-N-diethyl-4-nitroaniline and 1.3 mL of Reichardt's dye were added to a glass vial with an open top screw-cap sealed with a silicone septum. To remove the DCM from the dye solutions, samples were submitted to a $3 \cdot 10^{-2}$ Torr vacuum at room-temperature for at least 30 minutes. In order to prevent leakages in such extreme vacuum conditions, a 0.8 x 30 mm regular needle was slightly skewered in to the silicone septum. The drying process is represented in **Figure 4.3 a)**. Thus, 0.4 mg of sample (neat IL or mixture of IL+water) is added to the vial and vigorously stirred in a vortex until all blended. The final product is shown in **Figure 4.3 b)**.

To evaluate the water effect, 1.6 mL of ionic liquid aqueous solution was prepared in a clear glass vial using Milli-Q water. The different IL concentrations were prepared by weighting the ionic liquid and the Milli-Q water at fixed weight fractions. The range of concentrations varied from 75 *wt*% to 30 *wt*% for solid room-temperature ILs, and 90 *wt*% to 30 *wt*% for liquid room-temperature ILs.

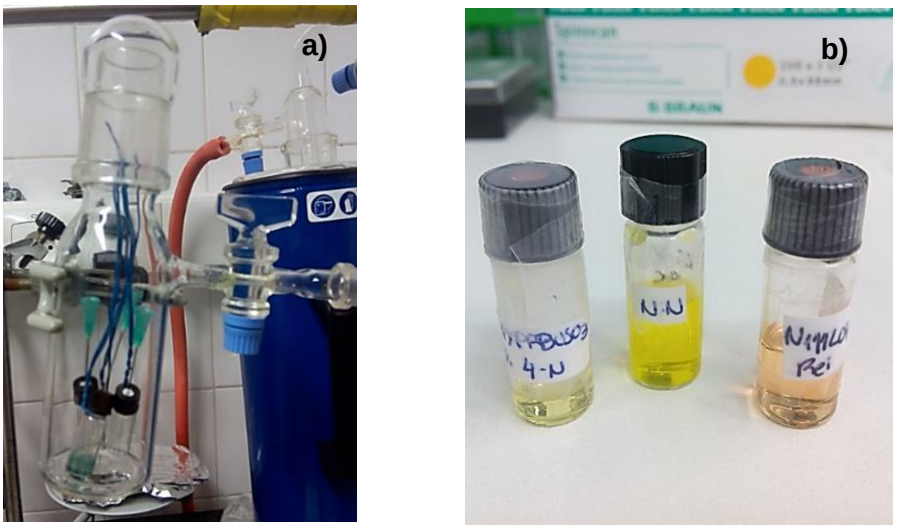


**Figure 4.3. a)** Picture of the drying process for the dye solutions and **b)** mixtures of ionic liquids and dyes.

## 4.3.2 UV-Vis Measurements

Kamlet-Taft solvatochromic parameters were obtained using an UV-Vis VWR® spectrophotometer, model UV-6300PC (see **Figure 4.4**). Each sample was loaded into a dry cuvette and measured in a scan range of 250 to 800 nm at 100.00 nm/min. In order to obtain a high spectra resolution a 0.1 nm step was chosen. The spectrum for each sample was recorded two times and the wavelengths at which the absorbance was maximum were determined. The spectra at 50ºC were obtained using a 1-Cell Water-Jack F.UV6300PC attached to a circulating bath. All spectra were analyzed using the UV-Vis Analyst Software.

**Figure 4.4.** Spectrophotometer VWR®, model UV-6300PC.

## 4.4 Results and Discussion

## 4.4.1 Kamlet-Taft Parameters of Neat Fluorinated Ionic Liquids

Imidazolium, pyridinium and tetrabutylammonium-based ionic liquids are studied for syntheses, extraction and purification of proteins (11), drug molecules (12) and other organic

compounds (13). Thus, the determination of the Kamlet-Taft descriptors for those FILs is of upmost importance.

To obtain the Kamlet-Taft descriptors for $[N_{4444}][C_4F_9SO_3]$ FIL, UV measurements were conducted at 323.15 K (14). Since Kamlet-Taft method is temperature dependent (8,15), measurements at 323.15 K were carried out on others FILs in order to compare the influence of the cation and fluorinated chain length. All the results are represented in **Table 4.2**.

**Table 4.2.** Kamlet-Taft parameters, hydrogen-bond donor ($\alpha$), hydrogen-bond acceptor ($\beta$), and dipolarity/polarizability ($\pi^*$), determined for the neat FILs studied in this work at 298.15 K and *323.15 K. Water (8) and perfluorohexane (16) parameters were obtained from literature.

| FILs | $\alpha$ | RSD (%) | $\beta$ | RSD (%) | $\pi^*$ | RSD (%) |
|---|---|---|---|---|---|---|
| **$[C_2C_1Im][CF_3SO_3]$** | 0.62 | 3.59 | 0.48 | 1.25 | 1.02 | 0.09 |
| **$[C_4C_1Im][CF_3SO_3]$** | 0.62 | 3.87 | 0.48 | 0.80 | 1.02 | 0.09 |
| **$[C_2C_1py][C_4F_9SO_3]$** | 0.62 | 1.01 | 0.50 | 0.48 | 0.94 | 0.10 |
| | 0.60* | 0.45 | 0.49* | 0.04 | 0.93* | 0.08 |
| **$[N_{4444}][C_4F_9SO_3]$** | 0.24* | 6.29 | 0.67* | 0.05 | 0.88* | 0.04 |
| **$[N_{4444}][C_8F_{17}SO_3]$** | 0.42 | 0.29 | 1.09 | 0.43 | 0.88 | 0.37 |
| | 0.37* | 0.95 | 1.10* | 0.28 | 0.85* | 0.26 |
| **$[C_2C_1Im][C_4F_9SO_3]$** | 0.76 | 0.13 | 0.48 | 1.24 | 0.89 | 0.05 |
| | 0.72* | 0.51 | 0.47* | 0.00 | 0.88* | 0.05 |
| **$[C_6C_1Im][C_4F_9SO_3]$** | 0.74 | 0.02 | 0.53 | 0.26 | 0.88 | 0.08 |
| | 0.71* | 0.76 | 0.52* | 0.01 | 0.87* | 0.02 |
| **$[C_8C_1Im][C_4F_9SO_3]$** | 0.73 | 0.13 | 0.55 | 0.03 | 0.86 | 0.06 |
| | 0.69* | 0.45 | 0.54* | 0.12 | 0.85* | 0.07 |
| **Water** (8) | 1.02–1.17 | | 0.14–0.18 | | 1.09 | |
| **Perfluorohexane** (16) | - | | - | | -0.40 | |

## 4.4.1.1 Influence of the Imidazolium, Pyridinium and Tetrabutylammonium Cations

In **Figure 4.5** the $\alpha$, $\beta$ and $\pi^*$ parameters are evaluated for the $[C_2C_1Im][C_4F_9SO_3]$, $[C_2C_1py][C_4F_9SO_3]$ and $[N_{4444}][C_4F_9SO_3]$. The $\alpha$ values for imidazolium-based ionic liquids are generally higher compared to other cations in study (16). The behavior of $[C_2C_1Im][C_4F_9SO_3]$ can be explained mainly due to the acidic hydrogen attached to the carbon between the two nitrogen atoms in

the imidazolium ring and the highly acidic methylene groups (7) promoting hydrogen bond donation. The pyridinium cation also have methylene groups in the constitutive ring, endorsing a highly acidic behavior and making the $\alpha$ values very similar to the imidazolium-based ILs (15).

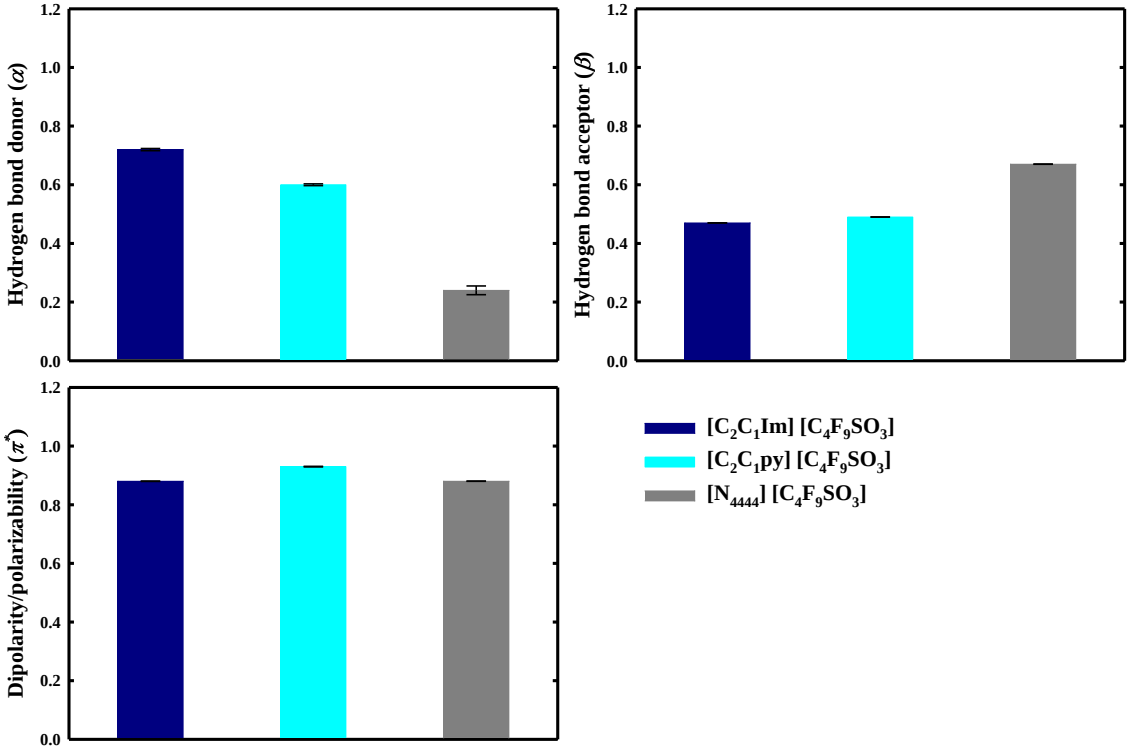


**Figure 4.5.** Kamlet-Taft parameters, hydrogen-bond donor ($\alpha$), hydrogen-bond acceptor ($\beta$), and dipolarity/polarizability ($\pi$*), measured at 323.15 K for the imidazolium, pyridinium and tetrabutylammonium-based FILs.

On the other hand, tetrabutylammonium-based ILs are considered poor H-bonding donors due to the lack of acidic hydrogens in the cation structure. The stabilization of the dipolarity present on the $[N_{4444}]^+$ cation is mainly related to coulombic interactions (17).

The $\beta$ parameter mainly depends on the anion (7). Then, FILs with the same anion should have similar HBA abilities, which was true for $[C_2C_1Im][C_4F_9SO_3]$ and $[C_2C_1py][C_4F_9SO_3]$. The cation can also play a secondary role in which cation–anion interactions can influence the ability of an anion to interact with the dye (18). Thus, $[N_{4444}][C_4F_9SO_3]$ demonstrated a high $\beta$ showing a main dependency on the anion. These findings are in agreement with the literature (16,17). Taking into account the polarizability of $[C_2C_1Im][C_4F_9SO_3]$, $[C_2C_1py][C_4F_9SO_3]$ and $[N_{4444}][C_4F_9SO_3]$, all have similar $\pi$* values, closest to the water (1.09) being considered highly hydrophilic compared to perfluorohexane (-0.40), an extremely lipophilic solvent.

## 4.4.1.2 Influence of the Hydrogenated Alkyl Chain Length of the Cation

The tendencies of Kamlet-Taft parameters taking into account the hydrogenated alkyl chain length of the cation in $[C_nC_1Im][C_4F_9SO_3]$ ($n$ = 2; 6; 8) and $[C_nC_1Im][CF_3SO_3]$ ($n$ = 2; 4) families are

represented in **Figure 4.6** and listed in **Table 4.2**. The results indicate that the hydrogen-bond donation slightly decreases with the increment of the alkyl chain length in the $[C_nC_1Im][C_4F_9SO_3]$ family which are in agreement with the literature (7,19). This behavior can be attributed to the partial positive charge distribution and accessibility in the imidazolium cation head group. Longer chains could produce a steric shield leading to a more difficult access of the solvatochromic dye to establish hydrogen bonds with the IL cation (7).

Lee *et al*. correlated the hydrophobicity and the $\beta$ parameter of ILs (15). According to the authors, a high HBA corresponds to a more hydrophobic behavior. In **Chapter 3** it was shown for the set of FILs here represented ($[C_nC_1Im][C_4F_9SO_3]$, $n$=2, 6, 8) that an increasing hydrogenated chain length leads to an increase on hydrophobicity. Thus, the trend of the $\beta$ values here reported are expected and in agreement with the literature (15,20). On the other hand, in the $[C_nC_1Im][CF_3SO_3]$ family no differences were noticed for both $\alpha$, $\beta$ and $\pi^*$ descriptors. These results suggest that a small fluorinated chain could not influence the IL capability of hydrogen bonding and polarizability with the increase of the alkyl chain on the cation (from ethyl to butyl).

Moreover, the $[C_nC_1Im][CF_3SO_3]$ family presents a polarizability most closer to water ($\pi^*$= 1.02–1.17) than $[C_nC_1Im][C_4F_9SO_3]$, yet both are considered highly hydrophilic.

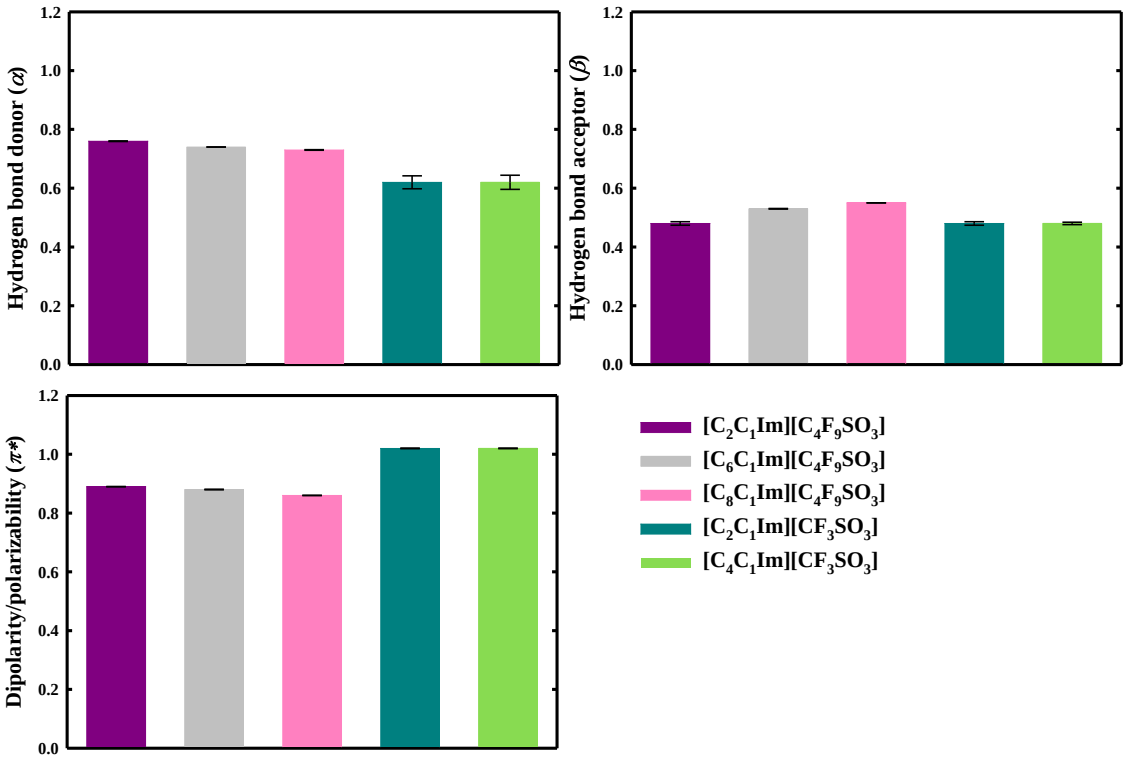


**Figure 4.6.** Kamlet-Taft parameters, hydrogen-bond donor ($\alpha$), hydrogen-bond acceptor ($\beta$), and dipolarity/polarizability ($\pi^*$), measured at 298.15 K for the $[C_nC_1Im]$ $[C_4F_9SO_3]$ family with $n$= 2, 6 and 8 and $[C_nC_1Im]$ $[CF_9SO_3]$ with $n$= 2 and 4.

## 4.4.1.3. Influence of the Fluorinated Chain Length of the Anion

It has been reported that the anionic fluorinated chain length has an influence on the Kamlet-Taft descriptors (18). A fluorinated anionic group is capable of additional interactions with polar components making them suitable for enhanced solubility of hydrophobic bioactive compounds (21). For instance, Cardoso and Micaelo (22) examined the molecular solvation of double-strand DNA (dsDNA) and single-stranded DNA (ssDNA) in neat ILs based on $[BF_4]^-$ and $[PF_6]^-$ anions. The authors found that ssDNA bases are preferentially solvated by the anions via hydrogen bonding with the fluorine atoms. Herein, the dependence of the Kamlet-Taft descriptors on the anion fluorinated chain length in imidazolium ($[CF_3SO_3]^-$ and $[C_4F_9SO_3]^-$) and tetrabutylammonium-based ($[C_4F_9SO_3]^-$ and $[C_8F_{17}SO_3]^-$) FILs is evaluated (see **Figure 4.7**). The results are listed in **Table 4.2**.

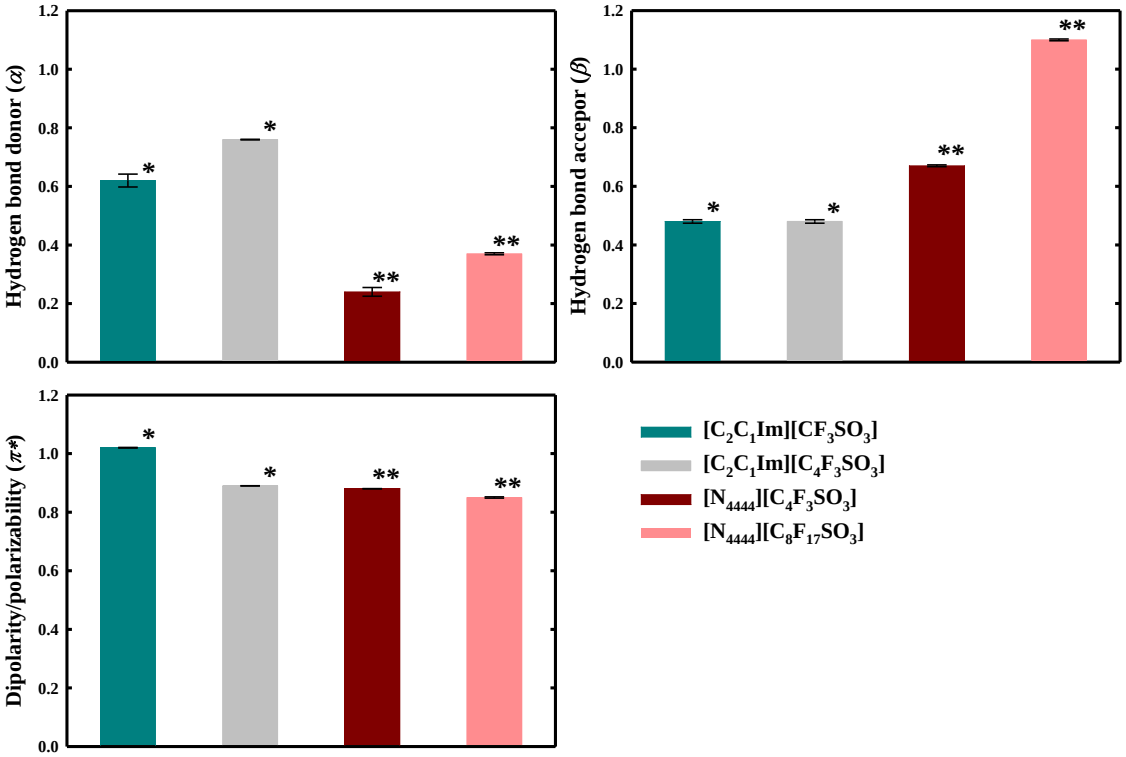


**Figure 4.7.** Kamlet-Taft parameters, hydrogen-bond donor ($\alpha$), hydrogen-bond acceptor ($\beta$), and dipolarity/polarizability ($\pi^*$), measured at * 298.15 K for imidazolium-based ILs and at ** 323.15 K for tetrabutylammonium-based ILs.

Increasing the fluorinated chain length leads to an increase of $\alpha$ values for both families being the imidazolium-based ILs the ones with a more pronounced ability to donate hydrogen bonds. As mentioned above for ammonium-based ILs, the stabilization of the dipolar ground state is mainly originated from coulombic interactions (17). Consequently, $[N_{4444}]^+$ is a poor H-bonding donor due to the lack of acidic hydrogens compared to the imidazolium based rings (see **Table 4.1**).

In tetrabutylammonium-based ILs, the increase of fluorinated chain length produces an increase on HBA. These results are not surprising because $\beta$ values for this family mainly depend on the anion (17).

The acidity/basicity is proportional to the charge density of the compound and to the relative size-to-charge ratio (7). The $[C_8F_{17}SO_3]^-$ anion is larger than the $[C_4F_9SO_3]^-$ anion, which allows a higher dispersion of the negative charges, promoting hydrogen bonding with $H^+$ available on the media. For imidazolium-based FILs, it can be concluded that HBA does not change by increasing the fluorination of the anion. In fact, the $-CF_2$ added to the anion core only increases the acidity maintaining the FILs basicity.

Imidazolium-based ILs with $[NTf_2]^-$ and $[PF_6]^-$ anions proved to be useful to enhance the solubility of biomolecules for several processes (1). Thus, a comparison of the $\alpha$ and $\beta$ values obtained for the imidazolium-based ILs with $[CF_3SO_3]^-$ and $[C_4F_9SO_3]^-$ anions is made in **Figure 4.8**.

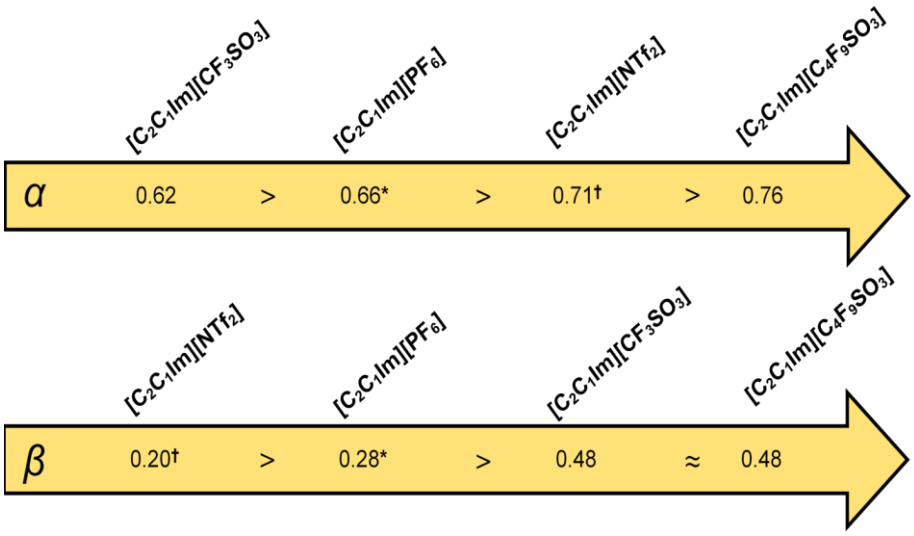


**Figure 4.8.** Kamlet-Taft descriptors $\alpha$ and $\beta$ for 1-ethyl-3-methylimidazolium based ILs with fluorinated anions. The $\alpha$ and $\beta$ for $[CF_3SO_3]^-$ and $[C_4F_9SO_3]^-$ were obtained in this work. The values for $^*[PF_6]^-$ (16) and $^\dagger[NTf_2]^-$ (20) were obtained from the literature.

In **Figure 4.8.** an acidity ($\alpha$) and basicity ($\beta$) scale is represented. Analyzing the ILs overall it is possible to observe the possibility to manage the final characteristics of the compounds though the diverse combination of the anions. The $[C_2C_1Im][C_4F_9SO_3]$ proved to be the most acidic and basic in which hydrogen bonding is more favorable. This result could be useful when addressing the design of functionalized ILs with a particular application in mind.

For instance, the hydrogen bonding capacity of nucleobases is responsible for correct DNA base-pairing and structure stabilization (22). Araújo *et al*. (5) investigated the solvation of nucleobases and concluded that the ionic liquid must be a good hydrogen bond acceptor and moderate bond donor to dissolve the nucleobases. In addition, a high-HBA ionic liquid can strongly coordinate the HBD groups of cellulose and trigger solute-solvent interactions that are required for cellulose dissolution (8). In some cases, a strong hydrogen bonding ability is also related to enzyme denaturation, which lowers the enzymatic

activity (1). On the other hand, in hydrophobic ILs media (lowest $\alpha$ and $\beta$) enzymes can retain their activity and their stability is enhanced in comparison with traditional solvents (1).

## 4.4.2 Kamlet-Taft Solvatochromic Parameters of Aqueous Solutions of Fluorinated Ionic Liquids

Ionic liquids usually have high viscosities and high polarities due to their charged structures and relatively strong anion-cation interactions (2). However, adding water into hydrophilic ionic liquids a decrease in their viscosity is noticed (23). Nevertheless, IL + water mixtures can still exhibit satisfactory extraction efficiency for polar bioactive compounds (24).

The hydrogen-bond basicity ($\beta$) it is one of the most important parameters reflecting the hydrogen bond accepting ability of the IL anion (7). Most of the relevant properties of ILs regarding the solute-solvent interaction are significantly determined by the nature of the anion rather than the cation (18). In fact, the $\beta$ parameter is widely used to explain (and correlates with) diverse properties, such as solvation ability and phase equilibrium behavior of ILs (25, 26).

A good example of the application of solvatochromic polarity scales for ionic liquids are the studies focused on the cellulose solubility in 1,3-dialkylimidazolium-based ILs. The measurement of Kamlet-Taft parameters showed that ILs characterized by a high $\beta$ parameter, indicating an increase in the hydrogen bonding accepting capability of the anion, displayed increased cellulose solubility (5). The IL 1-ethyl-3-methylimidazolium acetate ($[C_2C_1Im][C_1CO_2]$ represented in **Table 4.1**), characterized by a high $\beta$ parameter, has been increasingly recognized as a promising solvent and can be regarded as an enzyme-friendly co-solvent for biocatalysis as well as a good solvent for biomacromolecules such as cellulose and suberin, DNA, proteins, small solutes such as carbohydrates, and nucleic acid bases and has significant ability for sour gas sequestration (27). Recently, Doherty *et al.* (8) demonstrated that the $\beta$ parameter provides a measure for the efficiency of ILs to serve as solvent in lignocellulosic biomass pretreatment. The extraction power for lignin and yields of fermentable sugar were reported to increase among with the $\beta$ value. Moreover, these authors reported that the addition of water into ILs has the greatest impact on the $\beta$ parameter (8) mainly due to the relatively poor hydrogen bond basicity of water ($\beta$ = 0.14–0.18) (2).

Among ionic liquids, $\beta$ displays the greatest variation compared to $\alpha$ and $\pi^*$ values when water is added to the system (8). In this section the Kamlet-Taft descriptors were measured for water mixtures with fluorinated ionic liquids and conventional ionic liquids (see **Table 4.3**). In this way, it could be assessed how IL+ water system can influence the hydrogen bond capacity and polarizability. The main aim of this study is to design an IL that do not loses the $\beta$ property in aqueous solutions, addressing the design of functionalized (so-called task-specific) ILs that have been synthesized with a particular application in mind.

**Table 4.3.** Kamlet-Taft parameters hydrogen-bond donor, $\alpha$, hydrogen-bond acceptor, $\beta$, and dipolarity/polarizability, $\pi^*$, determined for the aqueous solutions with FILs and conventional ILs at 298.15 K.

| Water (*wt* %) | $\alpha$ | RSD (%) | $\beta$ | RSD (%) | $\pi^*$ | RSD (%) | Water (*wt* %) | $\alpha$ | RSD (%) | $\beta$ | RSD (%) | $\pi^*$ | RSD (%) |
|---|---|---|---|---|---|---|---|---|---|---|---|---|---|
| | **$[C_2C_1Im][CF_3SO_3]$** | | | | | | | **$[C_4C_1Im][CF_3SO_3]$** | | | | | |
| Neat | 0.62 | 3.59 | 0.48 | 1.25 | 1.02 | 0.09 | Neat | 0.62 | 3.87 | 0.48 | 0.80 | 1.02 | 0.09 |
| 12 | 0.74 | 1.79 | 0.45 | 6.74 | 1.10 | 1.68 | 10 | 0.72 | 0.19 | 0.45 | 0.77 | 1.08 | 0.18 |
| 31 | 0.84 | 0.63 | 0.39 | 3.55 | 1.19 | 0.35 | 30 | 0.78 | 0.47 | 0.40 | 0.59 | 1.17 | 0.01 |
| 50 | 0.85 | 0.29 | 0.35 | 2.11 | 1.25 | 0.08 | 50 | 0.77 | 0.06 | 0.36 | 0.31 | 1.22 | 0.01 |
| 69 | 0.80 | 0.66 | 0.29 | 0.59 | 1.32 | 0.08 | 70 | 0.75 | 0.03 | 0.26 | 4.95 | 1.31 | 0.26 |
| | **$[C_2C_1py][C_4F_9SO_3]$** | | | | | | | **$[C_2C_1Im][C_4F_9SO_3]$** | | | | | |
| Neat | 0.62 | 1.01 | 0.50 | 0.48 | 0.94 | 0.10 | Neat | 0.76 | 0.13 | 0.48 | 1.24 | 0.89 | 0.05 |
| 14 | 0.86 | 1.09 | 0.49 | 1.59 | 1.07 | 0.20 | 9 | 0.99 | 0.13 | 0.49 | 1.48 | 1.01 | 0.11 |
| 31 | 0.92 | 0.43 | 0.49 | 0.49 | 1.09 | 0.50 | 30 | 1.00 | 1.14 | 0.48 | 4.53 | 1.06 | 0.21 |
| 50 | 0.96 | 0.31 | 0.50 | 0.37 | 1.08 | 0.20 | 50 | 1.03 | 0.43 | 0.49 | 1.33 | 1.05 | 0.53 |
| 67 | 1.07 | 3.87 | 0.50 | 1.15 | 1.08 | 0.10 | 70 | 0.98 | 0.32 | 0.53 | 0.53 | 1.06 | 0.00 |
| | **$[N_{1112OH}][C_4F_9SO_3]$** | | | | | | | **$[C_2C_1Im]$ $C_1CO_2$** | | | | | |
| 10 | 1.14 | 0.21 | 0.42 | 0.50 | 1.05 | 0.32 | 11 | 0.49 | 0.44 | 0.91 | 0.15 | 1.11 | 0.00 |
| 30 | 1.14 | 1.02 | 0.46 | 8.53 | 1.06 | 0.42 | 22 | 0.58 | 0.76 | 0.67 | 0.65 | 1.22 | 0.17 |
| 50 | 1.14 | 0.13 | 0.46 | 1.83 | 1.05 | 0.53 | 44 | 0.53 | 0.14 | 0.49 | 1.47 | 1.31 | 0.08 |
| 69 | 1.13 | 0.37 | 0.48 | 2.09 | 1.04 | 0.21 | 70 | 0.82 | 0.09 | 0.37 | 4.25 | 1.34 | 0.08 |
| | **$[N_{1112OH}]$ Cl** | | | | | | | **$[C_2C_1Im]$ Cl** | | | | | |
| 24 | 0.95 | 0.51 | 0.48 | 0.23 | 1.21 | 0.61 | 25 | 0.52 | 0.01 | 0.55 | 1.69 | 1.27 | 0.16 |
| 32 | 0.94 | 0.04 | 0.40 | 0.30 | 1.24 | 0.00 | 30 | 0.51 | 0.01 | 0.47 | 1.25 | 1.31 | 0.07 |
| 36 | 0.96 | 0.79 | 0.38 | 2.95 | 1.25 | 0.08 | 35 | 0.66 | 0.96 | 0.50 | 1.24 | 1.31 | 0.31 |
| 51 | 0.97 | 0.04 | 0.30 | 0.40 | 1.29 | 0.00 | 52 | 0.69 | 0.09 | 0.37 | 1.65 | 1.35 | 0.06 |
| 71 | 0.94 | 0.26 | 0.22 | 0.71 | 1.32 | 0.26 | 72 | 0.80 | 0.25 | 0.20 | 2.01 | 1.40 | 0.24 |
| | **$[C_2C_1py]$ Br** | | | | | | | | | | | | |
| 24 | 0.54 | 0.92 | 0.48 | 0.71 | 1.35 | 0.30 | | | | | | | |
| 32 | 0.57 | 0.45 | 0.42 | 0.47 | 1.37 | 0.12 | | | | | | | |
| 35 | 0.62 | 0.84 | 0.45 | 0.92 | 1.39 | 0.00 | | | | | | | |
| 52 | 0.70 | 1.20 | 0.36 | 1.98 | 1.42 | 0.07 | | | | | | | |
| 71 | 0.91 | 1.84 | 0.28 | 2.53 | 1.39 | 0.00 | | | | | | | |

### 4.4.2.1 Influence of the Imidazolium, Pyridinium and Cholinium Cation

In **Figure 4.9** it is possible to observe the trends for $[C_2C_1Im][C_4F_9SO_3]$, $[C_2C_1py][C_4F_9SO_3]$ and $[N_{1112OH}][C_4F_9SO_3]$ regarding their $\alpha$, $\beta$ and $\pi*$ descriptors. $[N_{1112OH}][C_4F_9SO_3]$ with a melting temperature of of 436 K (14), is solid at room-temperature, thus measuredfor this neat FIL were not accomplish.

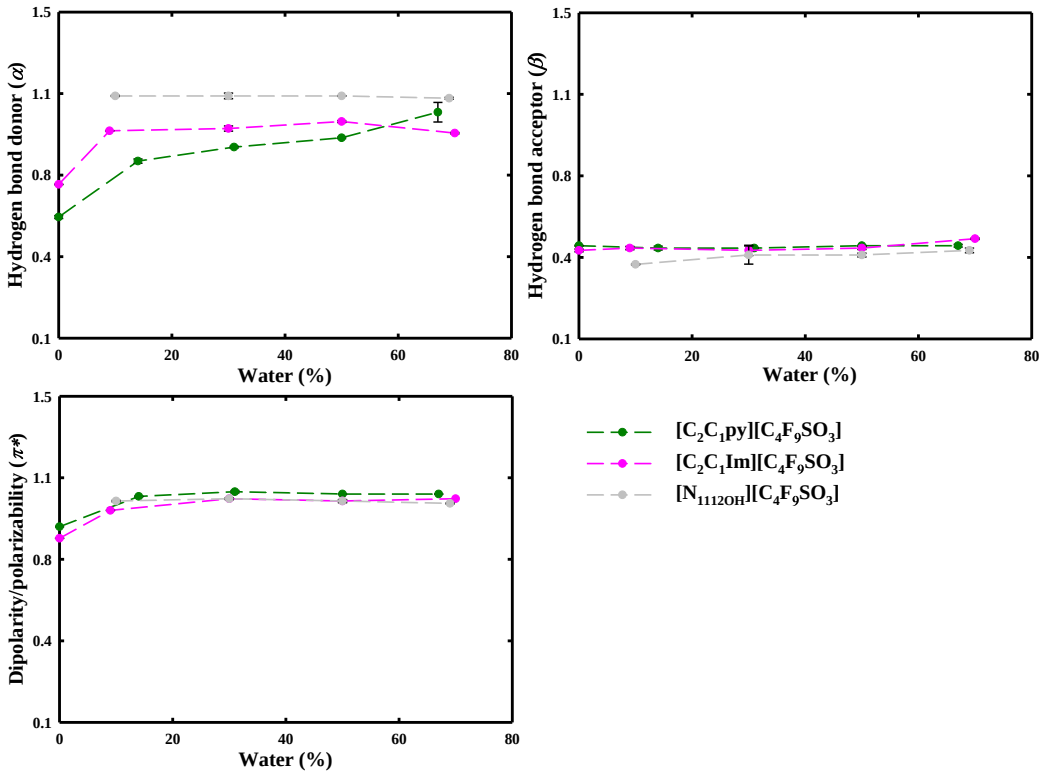


**Figure 4.9.** Kamlet-Taft parameters, hydrogen-bond donor ($\alpha$), hydrogen-bond acceptor ($\beta$), and dipolarity/polarizability ($\pi$*), measured at room-temperature for pyridinium, imidazolium and choline-based FILs at different aqueous concentrations at 298.15 K.

The choline-based ILs have the higher $\alpha$ values compared to imidazolium and pyridinium. That result is not surprising since choline itself has a permanent dipole moment promoted by the non-symmetrical structure and, in particular due to its terminal OH group, increasing the acidity (28). Then, $[N_{1112OH}][C_4F_9SO_3]$ has an increased ability to donate hydrogen bonds flowed by the imidazolium and pyridinium-based FILs. For all FILs represented in **Figure 4.9**, the $\alpha$ and $\pi$* values increase only at low dilutions and remain stable when increasing the water content. Thus, the addition of water into neat FILs enhances their HBD and polarizability.

As discussed above, the $\beta$ parameter is mainly determined by the origin of the anion (18) and so no significant differences are found on HBA for the $[C_4F_9SO_3]^-$ based FILs. In fact, no clear impact is observed in the $\beta$ tendency in opposition to conventional ILs, where the addition of water has the greatest impact on the HBA ability (26). This behavior will be discussed in **section 4.4.2.3** of this chapter.

### 4.4.2.2 Influence of the Hydrogenated Alkyl Chain Length on the Imidazolium Cation

In order to evaluate the effect of the hydrogenated alkyl chain length of the imidazolium ring, the Kamlet-Taft descriptors for $[C_2C_1Im][CF_3SO_3]$ and $[C_4C_1Im][CF_3SO_3]$ were measured and are represented in **Table 4.3**. The trends for both FILs are identical as can be seen in **Figure 4.10**.

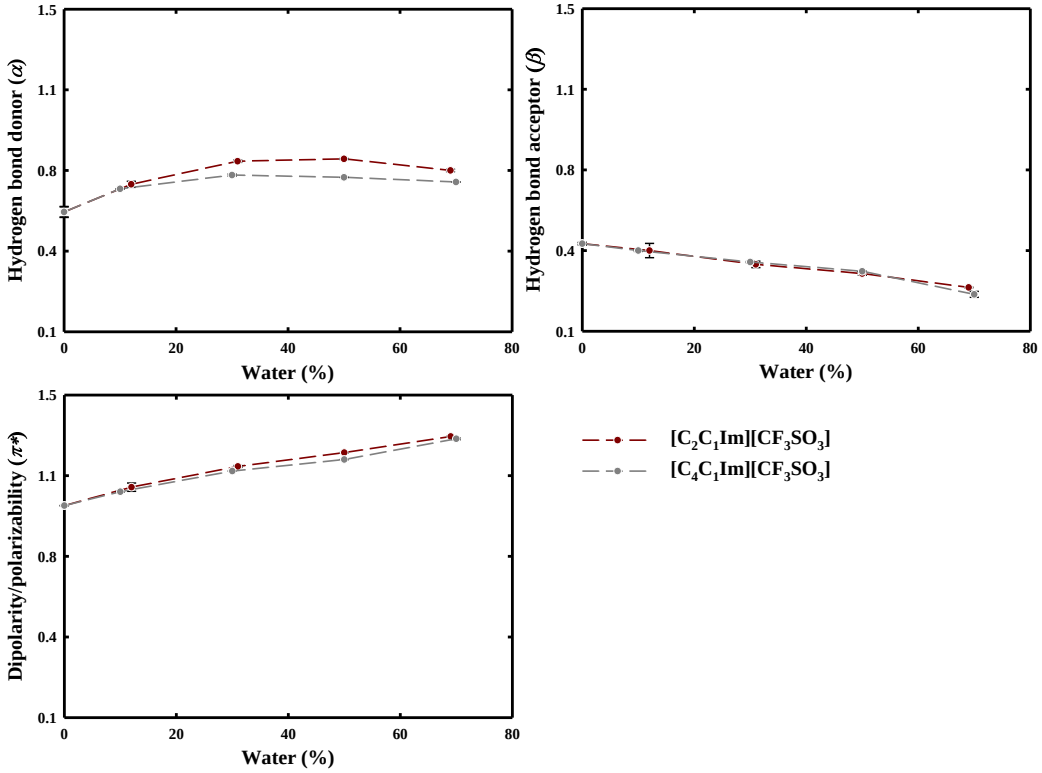


**Figure 4.10.** Kamlet-Taft parameters, hydrogen-bond donor ($\alpha$), hydrogen-bond acceptor ($\beta$), and dipolarity/polarizability ($\pi^*$), measured at room temperature with the increase of hydrogenated chain on imidazolium cation at different aqueous concentrations at 298.15 K.

With the addition of water, the $\alpha$ values increased until proximally 20 *wt*% of water and then remain relatively stable. On the other hand, the $\pi^*$ values are drastically increased in both cases indicating a greater hydrophilicity (20). The $\beta$ parameter for both $[C_2C_1Im][CF_3SO_3]$ and $[C_4C_1Im][CF_3SO_3]$ decreased with the addition of water into the bulk. For instance, Cláudio *et al*. reported that an introduction of fluorinated groups from $[CH_3SO_3]^-$ to $[CF_3SO_3]^-$ leads to a decrease in IL's hydrogen bond basicity for neat compounds (18). The low polarizability of the fluorinated groups and their electron withdrawing effect weaken the hydrogen bonding ability with the HBD of the solvatochromic probe (18). This trend can be related to the poor HBD (2) of the water and the small value for $[CF_3SO_3]^-$ based ILs anion.

Nevertheless, comparing these results with those obtained for $[C_4F_9SO_3]^-$ (see **Table 4.3**) it is noticed that increasing the fluorinated chain revoke the $\beta$ variation. This behavior will be discussed in the next section.

### 4.4.2.3 Influence of the Fluorinated Chain Length on the Anion

The influence of the anion will be discussed for the imidazolium, pyridinium and cholinium-based ionic liquids. The presence of a fluorinated anion, and its chain length, versus conventional anions (acetate ($[C_1CO_2]^-$), chloride ($Cl^-$) and bromide ($Br^-$)) will be evaluated regarding the $\alpha$, $\beta$ and $\pi^*$ parameters. Focusing on the $[C_2C_1Im]^+$ cation with conventional anions, the ILs become more acidic (increasing $\alpha$) and the $\beta$ decreases with the addition of water (see **Figure 4.11**), as expected from previous studies (29).

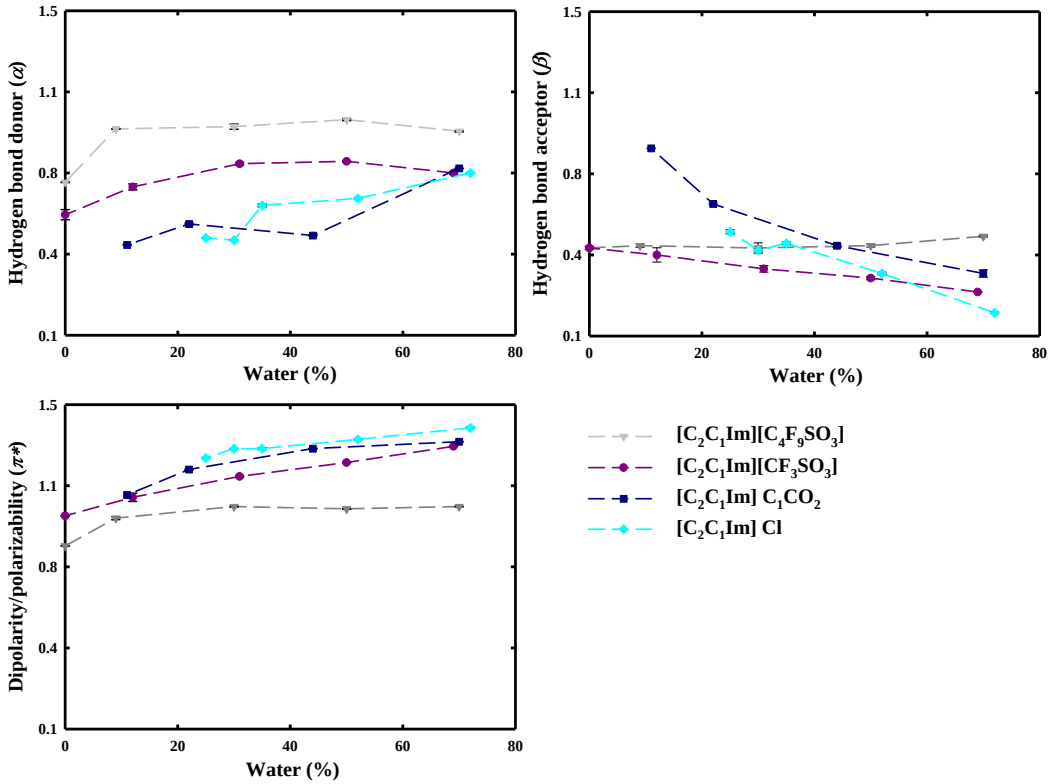


**Figure 4.11.** Kamlet-Taft parameters, hydrogen-bond donor ($\alpha$), hydrogen-bond acceptor ($\beta$), and dipolarity/polarizability ($\pi^*$), measured at room for imidazolium-based ionic liquids with conventional ($C_1CO_2^-$ and $Cl^-$) and fluorinated anions ($[C_4F_9SO_3]^-$ and $[CF_3SO_3]^-$) at different aqueous concentrations at 298.15 K.

However, the fluorinated anions (especially $[C_4F_9SO_3]^-$) preserve their basicity along with the increased water content. These results could be explained by the favorable high electronegativity of the fluorine atom ($F^-$) and by the strong hydrogen bond between C–F ⋯ H–O (2.4 kcal.mol$^{-1}$), half of the average O ⋯ H strength present on water molecules (21). Thus, the hydrogen bonding of fluorinated anions can be considered stable. Concerning the $\pi^*$ values, all ionic liquids presented an excellent polarizability, higher than water (1.09) (8). In addition, $[C_2C_1Im][C_4F_9SO_3]$ retains the same $\pi^*$ value with the addition of water.

As discussed above, high $\beta$ values are advantageous for several procedures involving biomacromolecules (27). Ionic liquids based on the acetate anion ($[C_1CO_2]^-$) proved to be useful for lignocellulose pretreatment (8,30) and for nucleobases solvation (5,27) due to their strong HBA ability

(see **Table 4.3**). Concerning the ILs basicity ($\beta$), the $[C_2C_1Im][C_1CO_2]$ has highest $\beta$ values up to nearly 50 *wt*% water content. Then, the $[C_2C_1Im][C_4F_9SO_3]$ demonstrated to be more advantageous with a higher $\beta$. Concerning the water content up to 50 *wt*% the following basicity scale according to the anions could be established: $[C_1CO_2]$ > Cl ≈ $[C_4F_9SO_3]$ > $[CF_3SO_3]$. However, between 50 *wt*% and 80 *wt*% the basicity trend changes to: $[C_4F_9SO_3]$ > $[C_1CO_2]$ > $[CF_3SO_3]$ > $Cl^-$. This result shown the amazing ability of ILs to "tune" characteristics according to a particular application in mind.

**Figure 4.12** illustrate the influence of a fluorinated ($[C_4F_9SO_3]^-$) versus conventional ($Br^-$) anion for pyridinium-based ILs in terms of $\alpha$, $\beta$ and $\pi^*$ descriptors. The bromide anion combined with the pyridinium cation has being studied for several biochemical processes such as extraction and separation of bioactive compounds from plants (31). Thus, understanding the hydrogen bonding of this ILs will be beneficial to enhance extraction and separation yields.

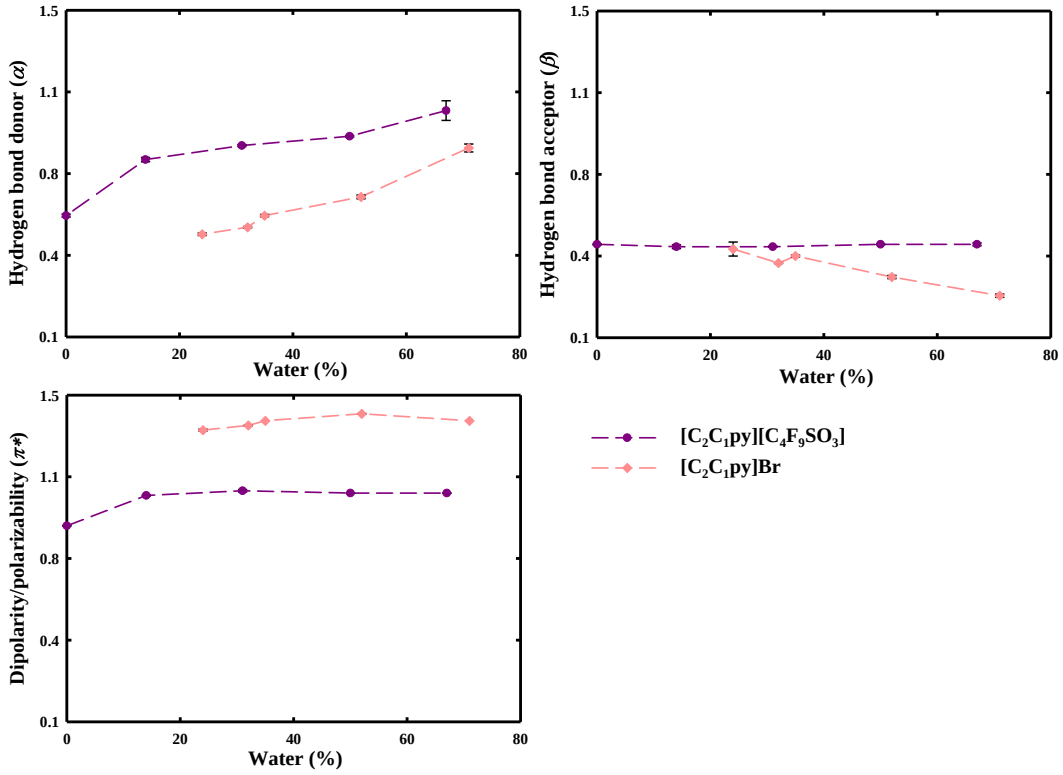


**Figure 4.12.** Kamlet-Taft parameters, hydrogen-bond donor ($\alpha$), hydrogen-bond acceptor ($\beta$), and dipolarity/polarizability ($\pi^*$), measured at room for pyridinium-based ionic liquids with a conventional ($Br^-$) and a fluorinated anion ($[C_4F_9SO_3]^-$) at different aqueous concentrations at 298.15 K.

One advantageous characteristic of $Br^-$ anions is their highly hydrophilicity which could increase ILs solubility (32). Thus, the $\pi^*$ values for $[C_2C_1py]$ $Br^-$ are remarkably higher. Comparing both HBA and HBD results, it is clear that the fluorination of the anion promotes a higher hydrogen bonding ability (see **Figure 4.12**). Concerning the $\alpha$ values, at all water concentrations the $[C_2C1py][C_4F_9SO_3]$ is considered the most acidic (increased $\alpha$). Regardless the $\beta$ descriptor, the $[C_2C_1py]$ $Br^-$ at ≈ 25 *wt*% has a basicity similar to $[C_2C_1py][C_4F_9SO_3]$ but it drastically declines with the further addition of water.

This behavior could be explained by the water's strong HBD which solvate a $Br^-$ anion at increased water concentrations (22). The same behavior is reported for choline-based ILs.

For $[N_{1112OH}][C_4F_9SO_3]$ an higher acidity and basicity is reported compared to $[N_{1112OH}]$ $Cl^-$ (see **Figure 4.13**).

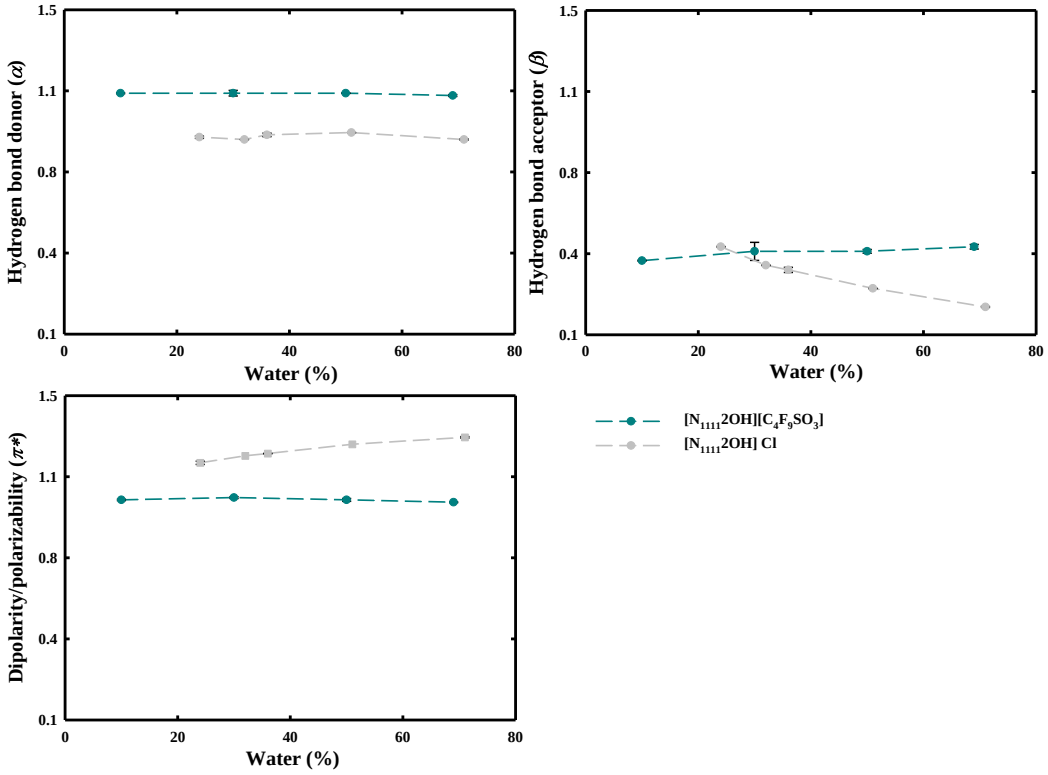


**Figure 4.13.** Kamlet-Taft parameters, hydrogen-bond donor ($\alpha$), hydrogen-bond acceptor ($\beta$), and dipolarity/polarizability ($\pi^*$), measured at room for choline-based ionic liquids with a conventional ($Cl^-$) and a fluorinated anion ($[C_4F_9SO_3]^-$) at different aqueous concentrations at 298.15 K.

The $\alpha$ is higher for the choline containing the fluorinated anion. Regardless the $\beta$ parameter, until ≈ 20 *wt*% the $[N_{1112OH}]$ $Cl^-$ presented a higher basicity. Then, with increasing water concentrations their $\beta$ values decrease linearly. Additionally, Jingyi Hu *et al*. observed the same $\beta$ behavior for chloride imidazolium-based ILs (33). On the other hand, $[N_{1112OH}][C_4F_9SO_3]$ maintained their basicity regardless adding water into the bulk. The polarizability represented by the $\pi^*$ parameter is higher for $Cl^-$ choline-based ILs. Like $Br^-$ pyridinium-based IL (see **Figure 4.12**), those containing the chloride anion have higher solubility due to $Cl^-$ solvation by water.

## 4.5 Conclusion

To date, it is proven that ionic liquids can provide a new and powerful platform for proteins, enzymes and DNA enhanced solubility, activity and stability (1). In this chapter, the hydrogen bonding and polarizability were evaluated for neat and aqueous solutions of FILs.

From the analysis of the Kamlet-Taft descriptors for neat FILs, several conclusions could be made: i) imidazolium and pyridinium-based FILs have similar hydrogen bonding ability at 323.15 K; ii) tetrabutylammonium-based FILs achieved the higher basicity and the lowest acidity at 323.15 K; iii) the hydrogenated alkyl chain on the imidazolium cation has a small influence on hydrogen bonding for [$C_nC_1$Im $CF_3SO_3$] ($n$= 2; 4) and [$C_nC_1$Im $C_4F_9SO_3$] ($n$= 2; 6; 8) at 298.15 K; iv) a further increase on the fluorinated chain on the anion produces higher HBD while preserving the HBA for imidazolium-based FILs; v) for tetrabutylammonium-based FILs fluorination of the anion results in an increase of both $\alpha$ and $\beta$ parameters (higher acidity and basicity). Finally, all the FILs presented a higher hydrophilic behaviour with $\pi^*$ values close to pure water.

The water effect on Kamlet-Taft parameters was evaluated by assessing the $\alpha$, $\beta$ and $\pi^*$ at different concentrations at room-temperature. The main purpose of this study was to find an IL that do not loses its basicity ($\beta$) in aqueous solutions, an important property regarding the solute-solvent interaction. A series of imidazolium, pyridinium and choline-based ILs with fluorinated anions ([$CF_3SO_3$] and [$C_4F_9SO_3$]) were tested and compared with conventional ILs such as [$C_2C_1$Im] $C_1CO_2$, [$C_2C_1$Im] Cl, [$C_2C_1$py] Br and [$N_{1112OH}$] Cl. The analysis of the results suggested that the increasing fluorination on the anion ([$CF_3SO_3$]$^-$ versus [$C_4F_9SO_3$]$^-$) promotes ILs acidity and a further stabilization of their basicity. In fact, ILs with the perfluorobutanesulfonate anion do not lose their basicity with increased water concentrations. Herein, the hydrogenated alkyl chain length affects mainly the HBD ability and does not change the HBA trend for the [$C_nC_1$Im][$CF_3SO_3$] ($n$=2; 4) family. Finally, the increased water content promoted the polarizability of all ILs, increasing their hydrophilicity.

These overall results further stress that the IL cation and anion, to a large extent, can be used to tune the hydrogen bonding and dipolarity/polarizability of ILs, depending on the desired application.

## 4.6 References

**(1)** Sivapragasam, M.; Moniruzzaman, M.; Goto, M. Recent Advances in Exploiting Ionic Liquids for Biomolecules: Solubility, Stability and Applications. *Biotechnol. J.* **2016**, 11, 1–14.

**(2)** Jin, W.; et al. Enhanced Solubilization and Extraction of Hydrophobic Bioactive Compounds Using Water/Ionic Liquid Mixtures. *Green Chem.* **2016**, 18, 3549–3557.

**(3)** Zhao, H. DNA Stability in Ionic Liquids and Deep Eutectic Solvents *J. Chem. Technol. Biotechnol.* **2015**, 90, 19–25.

**(4)** Patel, R.; Kumari, M.; Khan, A. B.; Recent Advances in the Applications of Ionic Liquids in Protein Stability and Activity: A Review. *Appl. Biochem. Biotechnol.* **2014**, 172, 3701–3720.

**(5)** Araújo, J. M. M.; Ferreira, R., Marrucho, I.M.; Rebelo, L. P. N. Solvation of Nucleobases in 1,3-Dialkylimidazolium Acetate Ionic Liquids: NMR Spectroscopy Insights into the Dissolution Mechanism. *J. Phys. Chem. B.* **2011**, 115, 10739–10749.

**(6)** Kamlet, M. J.; Taft, R. W. Solvatochromic Comparison Method. I. The B-Scale of Solvent Hydrogen-Bond Acceptor (HBA) Basicities. *J. Amer. Chem. Soc.* **1975**, 99, 377–383.

**(7**) Kurnia, K. A.; Lima, F.; Claudio, A. F.; Coutinho, J. A. P.; Freire, M. G. Hydrogen-bond Acidity of Ionic Liquids: an Extended Scale. *Phys. Chem. Chem. Phys.* **2015**, 17, 18980–18990.

**(8)** Doherty, T. V.; Mora-Pale, M.; Foley, S. E.; Linhardt, R. J.; Dordick, J. S. Ionic Liquid Solvent Properties as Predictors of Lignocellulose Pretreatment Efficacy. *Green Chem.* **2010**, 12, 1967.

**(9)** Lee, J. M.; Prausnitz, J. M. Polarity and Hydrogen-Bond-Donor Strength for Some Ionic Liquids: Effect of Alkyl Chain Length on the Pyrrolidinium Cation. *Chem. Phys. Lett.* **2010**, 492, 55–59.

**(10)** Crowhurst, L. Acidity in Ionic Liquids, *University of London: Imperial College London*. **2005**, 20-108.

**(11)** Ventura, S. P. M.; Sousa, S. G.; Freire, M. G.; Serafim, L. S.; Lima, A. S.; Coutinho, J. A. P. Design of Ionic Liquids for Lipase Purification. *J. Chromatogr. B.* **2011**, 879, 2679–2687.

**(12)** Restolho, J.; Barroso, M.; Dias, M.; Afonso, C. A. M.; Saramago, B. Capture of Opiates by Ionic Liquids. *J. Solution Chem.* **2015**, 44, 440–453.

**(13)** Yu, Y.; Miao, J.; Jiang, Z.; Sun, H.; Zhang, L. Cellulose Esters Synthesized Using a Tetrabutylammonium Acetate and Dimethylsulfoxide Solvent System. *Appl. Phys. A.* **2016**, 122, 656.

**(14**) Pereiro, A. B.; et al. Fluorinated Ionic Liquids: Properties and Applications. *ACS Sustain. Chem. Eng*. **2013**, 1, 427–439.

**(15)** Lee, J. M.; Ruckes, S.; Prausnitz, J. M. Solvent Polarities and Kamlet-Taft Parameters for Ionic Liquids Containing a Pyridinium Cation. *J. Phys. Chem B.* **2008**, 112, 1473–1476.

**(16)** Jessop, P. G.; Jessop, D.; Fu, D.; Phan, L. Solvatochromic Parameters for Solvents of Interest in Green Chemistry. *Green Chem.* **2012**, 14, 1245.

**(17)** Zhang, S.; Chen, Z.; Qi, X.; Deng, Y. Distinct Influence of the Anion and Ether Group on the Polarity of Ammonium and Imidazolium Ionic Liquids. *New. J. Chem.* **2012**, 36, 1043.

**(18)** Cláudio, A. F. M.; Swift, L.; Hallett, J. P.; Welton, T.; Coutinho, J. A. P.; Freire, M. G. Extended Scale for the Hydrogen-bond Basicity of Ionic Liquids. *Phys. Chem. Chem. Phys.* **2014**, 16, 6593–6601.

**(19)** Wang, X.; Chen, K.; Yao, J.; Li, H. *Sci. China* **2016,** 59, 517–525.

**(20)** Ab Rani M. A. et al. Recent Progress in Studies on Polarity of Ionic Liquids. *Phys. Chem. Chem. Phys.* **2011**, 13, 16831–16840.

**(21**) Smart, B. E. Fluorine Substituent Effects (on Bioactivity). *J. Fluor. Chem.* **2001**, 109, 3–11.

**(22)** He, Y.; Shang, Y.; Liu, Z.; Shao, S.; Liu, H.; Hu, Y. Interactions Between Ionic Liquid Surfactant [$C_{12}$mim]Br and DNA in Dilute Brine. *Colloids Surfaces B. Biointerfaces*. **2013**, 101, 398–404.

**(23)** Carvalho, P. J.; Regueira, T.; Santos, L. M. N. B. F.; Fernandez, J.; Coutinho, J. A. P. Effect of Water on the Viscosities and Densities of 1-Butyl-3-methylimidazolium Dicyanamide and 1-Butyl-3-methylimidazolium Tricyanomethane at Atmospheric Pressure. *J. Chem. Eng. Data.* **2010**, 55, 645–652.

**(24)** Marrucho, I. M.; Branco, L. C.; Rebelo, L. P. N. Ionic Liquids in Pharmaceutical Applications. *Annu. Rev. Chem. Biomol. Eng.* **2014**, 5, 527–546.

**(25)** Cláudio, A. F. M.; Ferreira, A. M.; Shahriari, S.; Freire, M. G.; Coutinho, J. A. P. Critical Assessment of the Formation of Ionic-Liquid-based Aqueous Two-phase Systems in Acidic Media. *J. Phys. Chem. B.* **2011**,115, 11145–11153.

**(26)** Wells, T. P.; et al. Esterification in Ionic Liquids: The Influence of Solvent Basicity. *J. Org. Chem.* **2008**, 73, 5585–5588.

**(27)** Araújo, J. M. M.; Pereiro, A. B.; Lopes, J. N. C.; Rebelo, L. P. N.; Marrucho, I. M. Hydrogen-bonding and the Dissolution Mechanism of Uracil in an AcetateIonic Liquid: New Insights from NMR Spectroscopy and Quantum Chemical Calculations. *J. Phys. Chem. B.* **2013**, 117, 4109–4120.

**(28)** Klein, R.; Zech, O.; Maurer, E.; Kellermeier, M.; Kunz, W. Oligoether Carboxylates: Task-Specific Room-Temperature Ionic Liquids. *J. Phys. Chem. B.* **2011**, 115, 8961–8969.

**(29)** Crowhurst, L.; Mawdsley, P. R.; Perez-arlandis, J. M.; Salter, P. A.; Welton, T. Solvent–Solute Interactions in Ionic Liquids. *Phys. Chem. Chem. Phys.* **2003**, 5, 2790–2794.

**(30)** Brandt, A.; Hallett, J. P.; Leak, D. J.; Murphy, R. J.; Welton, T. The Effect of the Ionic Liquid Anion in the Pretreatment of Pine Wood Chips. *Green Chem*. **2010**, 12, 672.

**(31)** Tang, B.; Bi, W.; Tian, M.; Row, K. H. Application of Ionic Liquid for Extraction and Separation of Bioactive Compounds from Plants. *J. Chrom. B: Anal. Technol. Biomed. Life Sci.* **2012**, 904:1–21.

**(32)** Hassan, F.; Babin, J.; Arnal-Herault, C.; David, L.; Jonquieres, A. Grafting of Cellulose Acetate with Ionic Liquids for Biofuel Purification by a Membrane Process: Influence of the Cation. *Carbohydr. Polym.* **2016**, 147, 313–322.

**(34)** Hu, J.; Zhu, W.; Yang, Q.; Qian, G.; Xing, H. Solvatochromic Parameters of the Binary Mixtures of Imidazolium Chloride Ionic Liquid Plus Molecular Solvent *J. Appl. Solut. Chem. Model.* **2014**, 3, 223–230

# 5.Conclusions and Perspectives

## 5.1 Conclusions

This work is an integral part of the FCT projects PTDC/QEQ-EPR/5841/2014, PTDC/QEQ-FTT/3289/2014 and IF/00210/2014/CP1244/CT0003 focused on the development of functionalized ILs, such as fluorinated ionic liquids, as novel materials for drug delivery and enhanced purification of monoclonal antibodies, respectively. The overall aim of this master thesis is to evaluate the thermophysical properties, self-aggregation and solution behavior in aqueous solutions of two novel task-specific FILs ($[C_4C_1Im][C_4F_9SO_3]$ and $[C_{10}C_1Im]$ $[C_4F_9SO_3]$). In addition, the partition coefficients octanol-water ($K_{ow}$) were also evaluated in order to understand the hydrophilicity/lipophilicity trends of general fluorinated ionic liquids. Additionally, several neat FILs and FILs aqueous solutions were tested concerning their hydrogen-bonding ability and polarizability using Kamlet-Taft parameters. This work highlights the potencial use of FILs as novel biomedical materials.

Taking into account the evaluation of the thermal properties, both $[C_4C_1Im][C_4F_9SO_3]$ and $[C_{10}C_1Im]$ $[C_4F_9SO_3]$ demonstrated good thermal stability, once they can be liquid in a large range of temperatures. In addition, the increase of the alkyl chain length of the FIL cation promotes an increase on melting and a decrease on decomposition temperatures for $[C_nC_1Im][C_4F_9SO_3]$ family with $n$= 2, 4, 6, 8, 10 and 12.

The thermophysical properties are also dependent on the chain length. Short chains, such as $[C_4C_1Im][C_4F_9SO_3]$ enhance a higher fluidity, ionic conductivity and ionicity. In contrast, $[C_{10}C_1Im]$ $[C_4F_9SO_3]$ showed the lowest density.

The aggregation behaviour in aqueous solutions was also studied. Fluorinated ionic liquids with long hydrogenated cationic chains ($[C_nC_1Im][C_4F_9SO_3]$ ($n$ = 2, 4, 6, 8, 10, 12)) have smaller CMC, as consequence of a high surfactant capacity and more stable micelles. Furthermore, the liquid-liquid equilibria phase diagrams have an unexpected behaviour of the aqueous-rich phase, indicating a delicate balance between two competing effects, the entropic contributions that decrease the solubility of FILs in water and the FILs tendency to self-aggregate in aqueous media. For the $[C_nC_1Im][C_4F_9SO_3]$ ($n$ = 2, 4, 6, 8, 10, 12) family, a "turn-over" on solution behaviour is achieved when $n$ = 8. Additionally, the neat FILs of the same series depict a similar trend for the surface tension (minimum surface tension at $n$ = 8), arising from the formation of three nanosegregated domains. The segregation behaviour together with the surfactant and solubility behaviours of these compounds lead to an unexpected behaviour of the aqueous-rich phase of the LLE phase diagram. According to the partition coefficients, $K_{ow}$, long hydrogenated and fluorinated chains influence the lipophilicity/hydrophobicity balance of FILs leading to an increase of lipophilicity. For the $[C_nC_1Im][C_4F_9SO_3]$ family, there is a shift when $n$=8 in which FIL's concentration is higher in the 1-octanol rich-phase. Regarding the fluorinated chain length, the $[C_8F_{17}SO_3]^-$ anion has a $K_{ow}$ 15 times higher than the $[C_4F_9SO_3]^-$ anion. For the $[C_4F_9SO_3]^-$ based imidazolium and pyridinium FILs, no significant differences on the $K_{ow}$ were found.

The Kamlet-Taft solvatochromic parameters showed that by a carefully selection of the FIL anion and cation, hydrogen-bonding could be managed. For neat FILs, pyridinium and imidazolium-based FILs presented similar behaviours. In addition, the increase in the cation hydrogenated alkyl chain length, for the $[C_nC_1Im][C_4F_9SO_3]$ ($n$=2, 6, 8) FILs promoted an increase on acidity and a decrease on basicity. For $[C_nC_1Im][CF_3SO_3]$ FILs with $n$=2 and 4, no significant differences where noticed. The increase of the anionic fluorinated chain length induced a more accentuated effect on the tetrabutylammonium-based FILs, increasing both acidity and basicity. However, for the imidazolium-based FILs tested the hydrogen-bonding donation increased but for the ability to accept hydrogen bonds no significant differences were found. Regarding the effect of water on the FIL basicity descriptor, it was shown that increasing the anionic perfluorinated alkyl chain length ($[CF_3SO_3]^-$ versus $[C_4F_9SO_3]^-$) promotes ILs acidity and a further stabilization of their basicity when compared to conventional ILs. No clear impact is observed in the basicity descriptor of $[C_4F_9SO_3]$-based ILs. This result address the relevance of designing functionalized (so-called task-specific) ILs that have been synthesized with a particular application in mind, e.g. dissolution of therapeutic molecules.

The overall results further stress that ILs constitutive ions, to some extent, can be tuned with several properties depending on the desired application.

## 5.2 Perspectives

During the past decades the interest in ionic liquids has increased, with applications in diverse areas such as electrochemistry, chemistry, nanotechnology, biotechnology, and in engineering processes, among others. The numerous advantages of using ionic liquids as biomaterials are unquestionable. This fact makes them very attractive mainly in the biomedical field where the use of biomaterials to enhance clinical efficacy is very challenging.

The results obtained in this work could help in the design of the most suitable FIL for application as surfactants in biomedical applications. Besides, the fluorinated domains present in emulsions can promote a higher solubility of poor soluble drug molecules and biomolecules such as enzymes, proteins and DNA. Additionally, FILs are a greener alternative to substitute armful solvents used nowadays in the pharmaceutical industry for the extraction, purification and syntheses processes of several biomolecules.

As future work, the study of the interactions between FILs and drug molecules or biomolecules is required. Also, drugs and biomolecules solubility in FILs will be needed to determine the effectiveness of these compounds as drug delivery devices. Additionally, FIL solubility should be determined in different biological fluids such as gastric and intestinal fluid. The cellular viability in different human cell lines in order to understand their behaviour in the most common routes of administration (oral, intravenous and transdermal) should be also studied. Moreover, self-aggregation properties of FILs

# 6. Scientific Communications

## 6.1 Papers

In preparation:

1. “Evaluation of Cytotoxicity and Partition Properties of Fluorinated Ionic Liquids”. Joana C. Bastos, Nicole M. Vieira, João M. M. Araújo, Sara Nunes, Ana Matias, Isabel M. Marrucho, Catarina M. M. Duarte, Ana B. Pereiro, Luís P. N. Rebelo

2. “Study of the Influence of Hydrogenated Alkyl Chain on Aggregation and Solubility of Fluorinated Ionic Liquids using the Soft-SAFT Equation” . Fèlix Llovell, Ana B. Pereiro, João M. M. Aaraújo; María J. Pastoriza -Gallego, Andreia S. S. Santos, Joana C. Bastos , Luís P. N. Rebelo, Manuel M. Piñeiro‖ and Lourdes F. Vega

3. “Fluorinated Ionic Liquids–based Aqueous Biphasic Systems: Study of Polarity and Hydrophobicity Scales” Joana C. Bastos, Sara Carvalho, Ana B. Pereiro, Luís P. N. Rebelo and João M. M. Araújo.

## 5.2 Posters in Scientific Meetings

1. Authors: Joana C. Bastos, Andreia S. S. Santos, João M. M. Araújo, Luis Paulo N. Rebelo, Ana B. Pereiro.
   Title: "Development of Fluorinated Ionic Liquids for Biomedical Applications"
   Congress: 5th Portuguese Young Chemists Meeting (5th PYCheM) and 1st European Young Chemists Meeting (1st EYCheM)
   Place: Guimarães (Portugal) Date: April, 2016

2. Authors: Joana C. Bastos, Nicole S. M. Vieira, Ana Matias, Catarina M. M. Duarte, João M. M. Araújo, Luís Paulo N. Rebelo, Ana B. Pereiro
   Title: "Evaluating Fluorinated Ionic Liquids as Novel Drug Delivery Systems"
   Congress: 5th Portuguese Young Chemists Meeting (5th PYCheM) and 1st European Young Chemists Meeting (1st EYCheM)
   Place: Guimarães (Portugal) Date: April, 2016

3. Nicole S. M. Vieira, J. C. Bastos, A. Matias, C. M. M. Duarte, João M. M. Araújo, Luís P. N. Rebelo, Ana B. Pereiro
   Title: "Fluorinated Ionic Liquids for Biomedical Application"
   Congress: 2nd EuCheMS Congress on Green and Sustainable Chemistry
   Place: Lisbon (Portugal) Date: October, 2015

4. Authors: N. S. M. Vieira, J. C. Bastos, J. M. M. Araújo, A. Matias, C. M. M. Duarte, Luís P. N. Rebelo, A. B. Pereiro
   Title: "Cytotoxicity and Partition Coefficients of Fluorinated Ionic Liquids"
   Congress: Iberoamerican Meeting on Ionic Liquids- IMIL 2015
   Place: Madrid (Spain) Date: July, 2015